Deploying Monitoring Trails for Fault Localization in All- Optical Networks and Radio-over-Fiber Passive Optical Networks

Khaled Mohamed Maamoun

Thesis submitted to the

Faculty of Graduate and Postdoctoral Studies

In partial fulfillment of the requirements

For the PhD degree in Electrical and Computer Engineering

Ottawa-Carleton Institute for Electrical and Computer Engineering

School of Electrical Engineering and Computer Science

University of Ottawa

Abstract

Fault localization is the process of realizing the true source of a failure from a set of collected failure notifications. Isolating failure recovery within the network optical domain is necessary to resolve alarm storm problems.

The introduction of the monitoring trail (m-trail) has been proven to deliver better performance by employing monitoring resources in a form of optical trails - a monitoring framework that generalizes all the previously reported counterparts.

In this dissertation, the m-trail design is explored and a focus is given to the analysis on using m-trails with established lightpaths to achieve fault localization. This process saves network resources by reducing the number of the m-trails required for fault localization and therefore the number of wavelengths used in the network.

A novel approach based on Geographic Midpoint Technique, an adapted version of the Chinese Postman's Problem (CPP) solution and an adapted version of the Traveling Salesman's Problem (TSP) solution algorithms is introduced.

The desirable features of network architectures and the enabling of innovative technologies for delivering future millimeter-waveband (mm-WB) Radio-over-Fiber (RoF) systems for wireless services integrated in a Dense Wavelength Division Multiplexing (DWDM) is proposed in this dissertation. For the conceptual illustration, a DWDM RoF system with channel spacing of 12.5 GHz is considered. The mm-WB

Radio Frequency (RF) signal is obtained at each Optical Network Unit (ONU) by simultaneously using optical heterodyning photo detection between two optical carriers. The generated RF modulated signal has a frequency of 12.5 GHz. This RoF system is easy, cost-effective, resistant to laser phase noise and also reduces maintenance needs, in principle. A revision of related RoF network proposals and experiments is also included.

A number of models for Passive Optical Networks (PON)/ RoF-PON that combine both innovative and existing ideas along with a number of solutions for m-trail design problem of these models are proposed. The comparison between these models uses the expected survivability function which proved that these models are liable to be implemented in the new and existing PON/ RoF-PON systems.

This dissertation is followed by recommendation of possible directions for future research in this area.

Acknowledgements

First, I would like to express my sincere gratitude to my supervisor, Professor Hussein T. Mouftah, for his excellent leadership and support through my graduate studies. It has been a great honor for me to be able to learn from his expertise in academic research. He has always shared his insightful entrepreneurial experiences and his perspectives on the telecommunications network industry. His constant emphasis on practical contributions has helped to shape the direction of my research which has resulted in this work.

In addition, I am also grateful for the support of my wife, Nevin, my kids, Mai and Kareem, and my beloved and encouraging daughter Maryam, who has always believed in me. Their constant encouragement and reassurance have given me the strength to complete my graduate studies.

Contents

Abstract ... ii

Acknowledgements ... iv

Contents ... v

List of Figures ... ix

List of Tables ... xiv

List of Acronyms ... xv

List of Symbols ... xxi

Chapter 1: Introduction ... 1
- 1.1 Background ... 1
- 1.2 Motivation ... 4
- 1.3 Objective ... 6
- 1.4 Contributions ... 7
- 1.5 Thesis Organization ... 8

Chapter 2: Survivability and Fault Detection/Localization in Optical Networks 9
- 2.1 Introduction ... 9
- 2.2 Optical Layer ... 9
- 2.2.1 Optical Transport Unit (OTU) ... 11
- 2.2.2 Optical Channel Data Unit (ODU) ... 12
- 2.2.3 Optical Channel Payload Unit (OPU) ... 13
- 2.3 Survivability in the Optical Layer ... 14
- 2.3.4 Protection in the Optical Layer ... 15
- 2.3.4.1 OMS Protection ... 15
- 2.3.4.2 OCh Protection ... 16
- 2.3.4.3 Dedicated and Shared Protection ... 18
- 2.3.4.3.1 Dedicated Protection ... 19
- 2.3.4.3.2 Shared Protection ... 19
- 2.3.4.4 Link and Path Protection ... 20
- 2.3.5 Restoration in the Optical Layer ... 21
- 2.3.5.1 Centralized and Distributed Restoration Control Architectures.. 22
- 2.3.5.2 Dynamic and Pre-planned Restoration Control Architectures 22

2.3.5.3 Adjacent-node, Intermediate Node and End-to-end Restoration Types 23
2.4 Fault Detection/Localization 24
2.4.1 Open Shortest Path First (OSPF) protocol 24
2.4.2 Tandem Connection Monitoring in OTN networks 26
2.4.3 LVM Fault-Localization Protocol for All-Optical Networks 29
2.5 Summary and Concluding Remarks 33

Chapter 3: Survivability and Fault Detection/Localization for Passive Optical Networks and Radio-over-Fiber Passive Optical Networks 34
3.1 Introduction 34
3.2 Radio-over-Fiber (RoF) 36
3.3 Proposed Novel RoF-PON Wireless Services System [MAA09] 40
3.4 PON Survivability 42
3.5 ONT Functions [ITU02] 48
3.5.1 1+1 model 48
3.5.2 1:1 model 49
3.6 Different Topologies to Perform PON Survivability 50
3.7 PON/ RoF-PON Topology Models 52
3.7.1 First PON/ RoF-PON Model 53
3.7.2 Second PON/ RoF-PON Model 53
3.7.3 Third PON/ RoF-PON Model 54
3.7.4 Fourth PON/ RoF-PON Model 55
3.7.5 Fifth PON/ RoF-PON Model 56
3.7.6 Sixth PON/ RoF-PON Model 57
3.7.7 Seventh PON/ RoF-PON Model 58
3.7.8 Eighth PON/ RoF-PON Model 59
3.8 Summary and Concluding Remarks 60

Chapter 4: Deploying Monitoring Trails for Fault Localization in All-Optical Networks 62
4.1 Introduction 62
4.2 An Overview on Monitoring Trails (M-Trails) 63
4.3 Deployment of M-Trails 66
4.4 Fault Localization Based on M-Trails 66
4.5 Using Monitoring Trails (M-Trails) with Established Lightpaths to Perform Fault Localization in All- Optical Networks 67
4.5.1 Manual Construction of ACT 68
4.5.2 Geographic Midpoint Technique 71
4.5.3 Chinese Postman’s Problem (CPP) Technique 73
4.5.4 The Traveling Salesman Problem (TSP) Technique 75
4.6 Summary and Concluding Remarks 78

Chapter 5: Analysis and Performance Evaluation 80
5.1 Introduction 80
5.2 M-Trails Deployment 80
5.2.1 M-Trails Deployment - Problem Definition 81
5.2.2 M-Trails Deployment - Network Topology Diversity 82

5.2.3 M-Trail Formation – Bound Analysis 82
5.2.4 M-Trail Design – ILP Formulation 84
5.2.5 M-trail Optimized Solution 89
5.2.6 M-Trail Different Solutions 91
5.3 PON Survivability Function 93
5.4 M-Trail Possible Solutions for the Proposed PON/ RoF-PON Models 96
5.5 ROF-PON Performance Evaluation 110
5.6 LVM Performance Evaluation 113
5.6.1 Network Size (Link Length) vs. Fault Localization Time 114
5.6.2 Network Traffic (Arrival Rate) vs. Blocking Probability 115
5.6.3 Network Traffic (Arrival Rate) vs. Fault Localization Time 116
5.6.4 Network Size (Number of Nodes) vs. Fault Localization Time 117
5.6.5 Similarities and differences between LVM and M-trail Fault Localization Protocols 119
5.7 Summary and Concluding Remarks 120

Chapter 6: Conclusions and Future Research 122
6.1 Conclusions 122
6.2 Future Research 125

Bibliography 127

Appendix A: Fault localization Process Difficulties 137

Appendix B: Techniques for Transporting RF Signals over Optical Fiber 141
B.1 RF Generation by Intensity Modulation and Direct Detection [MAU97] 142
B.1.1 Advantages of IM-DD 143
B.1.2 Disadvantages of IM-DD 143
B.2 The Principle of Photo detector-based Optical Heterodyning [MAU97] 145
B.2.1 Advantages of Optical Heterodyning 147
B.2.2 Disadvantages of Optical Heterodyning 148
B.3 Optical Frequency/Phase Locked-Loops (OFLL/OPLL) 148
B.3.1 Advantages of OFLL/OPLL 149
B.3.2 Disadvantages of OFLL/OPLL 150
B.4 Optical Injection Locking 151
B.4.1 Advantages of OIL 152
B.4.2 Disadvantages of OIL 152
B.5 Optical Injection Phase Locked Loop (OIPLL) 152
B.5.1 Advantages of OIPLL 155
B.5.2 Disadvantages of OIPLL 156
B.6 Dual Mode Lasers 156
B.7 Optical FM-Filter System 157
B.7.1 Advantages of FM-Filter System 159
B.7.2 Disadvantages of FM-Filter System 159
B.8 Techniques Based on Harmonics Generation 159
B.8.1 The FM - IM Conversion Technique 159

B.8.1.1 Advantages of FM - IM 161
B.8.1.2 Disadvantages of FM - IM 161
B.8.2 Modulation Sideband Techniques 161
B.8.2.1 The *2f* Method 162
B.8.2.2 *4f* Method 163
B.8.2.3 Advantages of the *2f* and *4f* methods 165
B.8.2.4 Disadvantage of the *2f* and *4f* methods 165
B.8.3 Heterodyning based on Mode-Locked Comb Generation 166
B.8.4 Interferometer based Mixing 167
B.9 Principle of Optical Frequency Multiplication 168
B.10 Sub-Carrier Multiplexing 171
B.10.1 Advantages and Disadvantages of Sub-Carrier Multiplexing ... 173
B.11 Wavelength Division Multiplexing in RoF Systems 174

Appendix C: Confidence Interval Estimation 175

List of Figures

Fig. 1.1: Classification of Fault Localization Techniques [STE04] 4

Fig. 2.1: Optical Sub-Layers 10

Fig. 2.2: Optical Sub-Layers [ITU03A] 10

Fig. 2.3: Optical Channel OCh [ITU03A] 11

Fig. 2.4: OTU Transmission [ITU03A] 11

Fig. 2.5: Optical Layer Survivability Techniques [MAL02] 15

Fig. 2.6: Possible Node for OMSP in a Ring Configuration [MAA10a] .. 16

Fig. 2.7: 1+1 OChP Ring [MAA10a] 17

Fig. 2.8: SNCP (OChP) Node in a Ring Configuration [MAA10a] 17

Fig. 2.9: Trail Protection (OChP) Node in a Ring Configuration [MAA10a] 18

Fig. 2.10: Architecture of OADM for 1+1 OCh Protection: (a) SNCP and (b) Trail Protection [MAA10a] 18

Fig. 2.11: Architecture of 1+1 Protection Schemes [ZHO00] 19

Fig. 2.12: Architecture of 1:1 Protection Schemes [ZHO00] 20

Fig. 2.13: Link-Based Protection [ZHO00] 21

Fig. 2.14: Path-Based Protection [ZHO00] 21

Fig. 2.15: Fault Detection in the Pingger-Pongger Protocol [LU04] 25

Fig. 2.16: OTN Tandem Monitoring [FUJ10] 26

Fig. 2.17: TCM Assignment 28

Fig. 2.18: Tandem Connection Monitoring [EXF09] 28

Fig. 2.19: Fault Detection and Potential Sink Formation (Potential Executive Sinks: 1 ,3 &4, Associated Path: Blue & Green) [KHA08] 30

Fig. 2.20: Executive Sink Election [KHA08] 30

Fig. 2.21: ALV Multicasting [KHA08] 31

Fig. 2.22: Matching Phase [KHA08] 32

Fig. 2.23: Failed Link Determination [KHA08] 32

Fig. 3.1: Typical PON Architecture [MAA07] 35
Fig. 3.2: The Radio over Fiber System Concept [MAA09] 37
Fig. 3.3: Different RoF System Designs: (a) EOM, RF Modulated Signal. (b) EOM, IF Modulated Signal, (c) EOM, Baseband Modulated Signal. (d) Direct Modulation [KIM05] 39
Fig. 3.4: The Proposed Novel RoF-PON Wireless Services System [MAA09] 41
Fig. 3.5: Protection Switching Architectures Suggested by ITU-T G983.1 [ITU98] 44
Fig. 3.6: WDM-PON Architecture with Self-Protection Capability against Both Feeder Fiber and Distribution Fiber Failures [SON05]. (WC: wavelength coupler; B/R: blue/red filter; M: power monitoring modules; B: port for blue-band signal only; R: port for red-band signal only; C: common port) 46
Fig. 3.7: WDM-PON Architecture with Self-Protection Capability against the Feeder Fiber Failure [SON05]. (WC: wavelength coupler; B/R: blue/red filter; M: power monitoring modules; B: port for blue-band signal only; R: port for red-band signal only; C: common port)....................................... 47
Fig. 3.8: The System's Wavelength Assignment Plan [SON05]............... 48
Fig. 3.9: G.983.6 – 1+1 Model ONT (ANI side) [ITU02]........................ 49
Fig. 3.10: G.983.6 – 1:1 Model ONT (ANI side) [ITU02]......................... 49
Fig. 3.11: PON Star/Tree Topologies with Redundant Trunk [JIN07] 50
Fig. 3.12: (a)Ring Topology with Redundant Trunk, (b) Ring-Star Topology [JIN07] 51
Fig. 3.13: Standard PON/RoF –PON Topology 52
Fig. 3.14: First PON/ RoF-PON Model.. 53
Fig. 3.15: Second PON/ RoF-PON Model 54
Fig. 3.16: Third PON/ RoF-PON Model 55
Fig. 3.17: Fourth PON/ RoF-PON Model 56
Fig. 3.18: Fifth PON/ RoF-PON Model 57
Fig. 3.19: Sixth PON/ RoF-PON Model... 58
Fig. 3.20: Seventh PON/ RoF-PON Model 59
Fig. 3.21: Eighth PON/ RoF-PON Model 60
Fig. 4.1: A Possible M-Trail Lightpath 64
Fig. 4.2: A Possible M-Trail Lightpaths... 65
Fig. 4.3: A Simple Optical Network Deploying Two Lightpaths.............. 69

Fig. 4.4: Illustration of The Two Possible Sets of M-Trails of Described in Table 4.3 70

Fig. 4.5: A Simple Optical Network Deploying Three Lightpaths............ 70

Fig. 4.6: Illustration of Possible M-Trails Described in Table 4.5 71

Fig. 4.7: An Example of a Graph of Edges to Construct a Trail 72

Fig. 4.8: Illustration Steps of M-trail formulation by GMP Algorithm..... 73

Fig. 4.9: Artificial Nodes of The Edges That Requires a Trail to Visit Them 77

Fig. 5.1: CodeWord Length vs. Number of Nodes.................................... 84

Fig. 5.2: Flow Conservation Constraint... 87

Fig. 5.3: Node Traversed Constraint.. 87

Fig. 5.4: Two Graph Voltage Rules.. 88

Fig. 5.5: Optimized Solution for the 4x4 Matrix Network 89

Fig. 5.6: Optimized Solution for the 5x5 Matrix Network 90

Fig. 5.7: Optimized Solution for the 6x6 Matrix Network 90

Fig. 5.8: M-Trail Formulation Comparison Between TSP (adapted), CCP (adapted) and GMP... 92

Fig. 5.9: Different PON/ RoF-PON Survivability Models [MAA11b] 94

Fig. 5.10: Expected Survivability Function of the Eight Models for Different Number of Faults [MAA11b] 95

Fig. 5.11: Expected Survivability Function of The Last Five Models for Different Number of Faults [MAA11b] 95

Fig. 5.12: M-Trail Possible Solution for The First PON Model.................. 96

Fig. 5.13: Another M-Trail Possible Solution for The First PON Model.... 97

Fig. 5.14: M-Trail Possible Solution for The Second PON Model 98

Fig. 5.15: Another M-Trail Possible Solution for The Second PON Model98

Fig. 5.16: M-Trail Possible Solution for The Second 1+1 PON Model 99

Fig. 5.17: M-Trail Possible Solution for The Second 1:1 PON Model 100

Fig. 5.18: M-Trail Possible Solution for The Third PON Model 101

Fig. 5.19: M-Trail Possible Solution for The Fourth PON Model 102

Fig. 5.20: Another M-Trail Possible Solution for The Fourth PON Model102

Fig. 5.21: M-Trail Possible Solution for The Fifth PON Model 103

Fig. 5.22: M-Trail Possible Solution for The Fifth PON Model That Makes Use of The Deployed Optical Paths.. 104

Fig. 5.23: M-Trail Possible Solution for The Sixth PON Model............... 105
Fig. 5.24: M-Trail Possible Solution for The Sixth PON Model That Makes Use of The Deployed Optical Paths.. 106
Fig. 5.25: M-Trail Possible Solution for The Seventh PON Model 107
Fig. 5.26: That M-Trail Possible Solution for The Eighth PON Model 108
Fig. 5.27: The Proposed Novel RoF-PON Wireless Services System [MAA09] 110
Fig. 5.28: The First Three Optical Carriers at The CS [MAA09] 111
Fig. 5.29: RF Current Generated by The Photo Detector [MAA09] 112
Fig. 5.30: The RF Signal Filtered Around 12.5 GHz Spectrum [MAA09]112
Fig. 5.31: The Eye Diagram of The Recovered User Data [MAA09]....... 113
Fig. 5.32: The Simulated Network [JAF09] 113
Fig. 5.33: Fault Localization and Network Updating Time in ms with Increasing Link Length per S-D [JAF09]... 115
Fig. 5.34: Average Blocking Probability with Increasing Arrival Rate [JAF09] 116
Fig. 5.35: Average Fault Localization Time with Increasing Arrival Rates [JAF09] 117
Fig. 5.36: Average Fault Localization Time and LOS Flooding Time with Different Size of Networks [JAF09].. 118
Fig. B.1: Generating RF Signals by Direct Intensity Modulation (a) of the Laser, (b) Using an External Modulator [MAU97] 143
Fig. B.2: Principle of Optical Frequency-/Phase-Locked Loop [LAG99]...... 149
Fig. B.3: Optical Injection Locking [WEN00] 152
Fig. B.4: The Principle of Operation of the Optical Injection Phase Locked Loop (OIPLL) Technique [ORE95].. 153
Fig. B.5: Optical Frequency Comb Generator for Carrier Generation Through Heterodyning [FUK01]... 155
Fig. B.6: Optical Coherent Mixing Based on The FM Laser [ORE95].......... 157
Fig. B.7: Remote Heterodyning by Using a Filter to Select the Mixing Sidebands [SHE03] 158
Fig. B.8: The 2f Technique for Generating Millimeter –Wave [LIM00] 164
Fig. B.9: Using the 2f Method to Remotely Deliver Baseband Data and LO For Up Conversion at The Base Station [LIM00]... 166

Fig. B.10: Optical Heterodyning Based on Optical Frequency Comb Generator (OFCG) Using Phase Modulation in an Amplified Circulation Loop [FUK01] 167

Fig. B.11: Frequency Conversion through Mixing by a Mach Zehnder Interferometer [MAU97] 168

Fig. B.12: Principle of Optical Frequency Multiplication [JOH00] 169

Fig. B.13: Illustration of Optical Frequency Multiplication - Generating the Fundamental Frequency [NGO02] 171

Fig. B.14: Sub-Carrier Multiplexing of Broadband Mixed Mode Data in RoF Systems [BRA01] 172

List of Tables

Table 2.1: Optical Sub-Layers [MAL02].. 10

Table 2.2: TCM Status Interpretation [ITU03A].. 12

Table 2.3: PM Status Interpretation [ITU03A].. 13

Table 2.4: Fault Indication Codes Interpretation [ITU03A]............................ 13

Table 2.5: Payload Type Code Points [ITU03A].. 13

Table 2.6: Optical Sub-Layers and its SONET Equivalents............................ 14

Table 2.7: Comparison of Adjacent Node, Intermediate Node, and End-to-End Restoration Types [MAA10a] 23

Table 3.1: Summary of the Main Differences between PON Technologies [MAA07] 35

Table 3.2: PON Classes [MAA07 and SHA05].. 36

Table 4.1: ACT for Network in Fig. 4.2 65

Table 4.2: ACT of Network of Fig. 4.3 With the Use of “Do not Care Terms”69

Table 4.3: Two Possible M-Trail Sets in the ACT for Network of Fig. 4.3 70

Table 4.4: ACT of Network of Fig. 4.5 With the Use of “Do not Care Terms”71

Table 4.5: A Possible M-trails in The ACT for the Network of Fig. 4.5.......... 71

Table 5.1: Ring and Fully Meshed Topologies Average Nodal Degree and Number of Links... 82

Table 5.2: Illustration of TSP (adapted), CCP (adapted) and GMP Solutions of 4x4, 5x5 and 6x6 Matrix Networks 92

Table 5.3: Summary of m-trail deployment for the different PON models.... 109

Table 5.4: Summary of m-trail deployment for the different RoF-PON models 109

Table 5.5: Processing Time to Localize Failure by LVM for Different Number of Nodes [JAF09] 118

Table 5.6: Comparison between the LVM and M-trail Algorithm................. 119

List of Acronyms

3R	Re-amplification, Re-shaping, and Re-timing Optical Regenerator
ACT	Alarm Code Table
ADM	Add-Drop Multiplexer
AIS	Alarm Indication Signal
ALV	Affected-Link-Vector
ANI	Access-Network Interface
AON	All Optical Network
APS	Automatic Protection Switching
ARPANET	Advanced Research Projects Agency Network
AS	Autonomous System
ATM	Asynchronous Transfer Mode
AWG	Arrayed Waveguide Grating
BDI	Backward Defect Indicator
BEI	Backward Error Indication
BER	Bit Error Rate
BGP	Border Gateway Protocol
BIAE	Backward Incoming Alignment Error
BLPR	Bidirectional Link Protected Ring
BPON	Broadband Passive Optical Network
CATV	Cable Television
CI	Confidence Interval
CMIP	Common Management Information Protocol
CO	Central Office

CoS	Class of Services
CPP	Chinese Postman's Problem
CS	Central Station
dB	Decibel
DCS	Digital Cross-connect System
DEMUX	De-multiplexer
DFB	Distributed Feedback
DP	Dedicated Protection
DPSK	Differential Phase-Shift Keying
DWDM	Dense Wavelength Division Multiplexing
E/O	Electrical to Optical Conversion
EAM	Electro-Absorption Modulator
EDFA	Erbium-Doped Fiber Amplifier
EGP	Exterior Gateway Protocol
EOM	Electro-Optic Modulator
EPON	Ethernet Passive Optical Network
FAS	Frame Alignment Signal
FDI	Forward Defect Indicator
FEC	Forward Error Correction
FIS	Failure Indication Signal
FSR	Free Spectral Range
FTFL	Fault Location Channel
FTTA	Fiber to the Antenna
FTTH	Fiber to the Home
GbE	Gigabit Ethernet
Gbps	Gigabits per second
GCC	General Communications Channel
GFP	Generic Framing Procedure
GMP	Geographic Midpoint Procedure
GPON	Gigabit Passive Optical Network

IAE	Incoming Alignment Error
IETF	Internet Engineering Task Force
IGP	Interior Gateway Protocol
ILP	Integer Linear programming
IP	Internet Protocol
ITU	International Telecommunications Union
LAN	Local Area Network
LCK	Locked Defect
LF	Link Failure
LH	Long-Haul
LLC	Logical Link Control
LOP	Loss Of Packet
LOS	Loss Of Signal
LS	Link State
LSP	Label Switched Path
LSR	Label Switching Router
LT	Line Terminal
LTC	Loss of Tandem Connection
LVM	Limited-perimeter Vector Matching Fault Localization Protocol
MAC	Medium Access Control
MAN	Metropolitan Area Network
Mbps	Megabits per second
mm-WB	Millimeter-Waveband
MPλS	Multi Protocol Lambda Switching
MPLS	Multi Protocol Label Switching
MSP	Multiplex Section Protection
MUX	Multiplexer
NE	Network Element
NMS	Network Management System

O/E	Optical to Electronic Conversion
OADM	Optical Add-Drop Multiplexer
OAM	Operations, Administration and Maintenance
OBS	Optical Burst Switching
OC	Optical Carrier
OCh	Optical Channel Layer
OChP	Optical Channel Layer Protection
OCI	Open Connection Indication
ODU	Optical Data Unit
OEXC	Opto-Electric Cross-Connect
OH	Over Head
OLT	Optical Line Terminator
OMS	Optical Multiplex Section
OMSP	Optical Multiplex Section Protection
ONT	Optical Network Terminal
ONU	Optical Network Units
OPU	Optical Payload Unit
OSC	Optical Supervisory Channel
OSNR	Optical Signal to Noise Ratio
OSPF	Open Shortest Path First
OTM	Optical Transport Module
OTN	Optical Transport Network
OTS	Optical Transmission Section
OTU	Optical Transport Unit
OXC	Optical Cross-Connect
PCC	Protection Communication Channel
PD	Photo Diode
PM	Path Monitoring
P-OLT	Packet Optical Line Terminal

PON	Passive Optical Network
POS	Packet Over SONET/SDH
PPP	Point-to-Point Protocol
PRBS	Pseudo Random Binary Sequence
PROB	Probe Signal
OA	Optical Amplifier
QoP	Quality of Protection
QoS	Quality of Service
QoT	Quality of Transmission
RA	Raman Amplifier
RAU	Remote Antenna Unit
RCA	Random Code Assignment
RCS	Random Code Swapping
RF	Radio Frequency
RIP	Routing Information Protocol
RN	Remote Node
ROADM	Reconfigurable Add/Drop Multiplexer
RoF	Radio-over-Fiber
RS	Remote Station
RSVP	Resource Reservation Protocol
RWA	Routing and Wavelength Assignment
SDH	Synchronous Digital Hierarchy
SHR	Self Healing Ring
SLA	Service-Level Agreement
SM	Section Monitoring
SMF	Single Mode Fiber
SNCP	Sub-Network Connection Protection
SNMP	Simple Network Management Protocol
SNR	Signal to Noise Ratio

SOA	Semiconductor Optical Amplifier
SONET	Synchronous Optical Network
SP	Shared Protection
SPRING	Shared Protection RING
SRL	Shared Risk Link Group
STM	Synchronous Transport Module
STS	Synchronous Transport Signal
TC	Tandem Connection
TCM	Tandem Connection Monitoring
TCP	Transmission Control Protocol
TDM	Time Division Multiplexing
TP	Transponder
TSP	Traveling Salesman's Problem
UFL	Unambiguous Failure Localization
UPPR	Unidirectional Path Protected Ring
VoIP	Voice over Internet Protocol
V-OLT	Video Optical Line Terminal
WAN	Wide Area Network
WC	Wavelength Coupler
WDM	Wavelength Division Multiplexing
WDM-PON	Wavelength Division Multiplexing Passive Optical Network

List of Symbols

a_j	Alarm code binary digit of the link j^{th} link
a_{uv}	A general integer variable that presents the decimal alarm code assigned to link *(u,v)*
c_m	The cost of a monitor
c_{uv}	The cost of a supervisory wavelength on link (*u,v*)
d_u^j	Binary variable. It takes 1 if node u is the sink of m-trail t_j and 0 otherwise
e_{uv}^j	Fractional variable. It is the voltage of vector $u \rightarrow v$ on m-trail t_j. It takes 0 if $u \rightarrow v$ is not in m-trail vector on t_j
E	The set of network links
f	Frequency of an optical signal
f_{uv}^{xy}	Binary variable. For two distinct links (*u,v*) and (*x,y*), it takes 1 if $a_{uv} > a_{xy}$
$G(V, E)$	Network topology with V nodes and E links
H	Eulerian graph
J	The maximum number of m-trails permitted in the solution
j	m-trail index where $j \in \{0,1,......J-1\}$
l_{uv}^j	Binary variable that takes 1 if $u \rightarrow v$ is a vector of m-trail t_j and 0 otherwise
Lj	The j^{th} link set which contains the set of links
m^j	Binary variable. It takes 1 if t_j is an m-trail and 0 otherwise
M	The graph consisting of the links contained in the optimal pair-wise matching
N_l	The largest set count of similar alarm code generated only by lightpaths
N_m	The number of m-trails needed in addition to the already establishment lightpaths)

N_u	Number of unavailable ONUs after failure
S	Survivability Function
s-d	Source-Destination
s_u^j	Binary variable. It takes 1 if node *u* is the source of m-trail t_j and 0 otherwise
S_x	A random variable over a discrete sample space
t	Optical Monitoring Trail
T	Minimum spanning tree that spans the *n* points
V	The set of network nodes
z_u^j	Binary variable. It takes 1 if node u is traversed by m-trail t_j and 0 otherwise
β	A predefined small positive value $(0 < \beta \leq 2^{-j})$
δ	A pre-assigned small positive value $((\lvert V\rvert \cdot (\lvert V\rvert - 1))/2 \leq \delta > 0)$ that presents the step of the minimum voltage increase along the m-trail
λ	Optical Wavelength

Chapter 1: Introduction

1.1 Background

There is a focused interest on the development and use of optical network technologies in the Internet world due to their almost unlimited bandwidth, which is a result of the exponential growth of Internet broadband services. The enormous traffic capacities of the optical networks have been achieved by WDM, despite ongoing development in the control plane of the optical transport system which puts some constraints in the optical networks' deployment. The goal is to have more flexible, controllable, survivable, and comprehensive traffic engineering solutions, as well as an effective optical layer. The results will carry out different capabilities, such as real time provisioning of light paths, interoperability and functionality between vendor-specific optical sub-networks, and the enabling of protection and restoration capabilities in an operational sense [MAA10a].

Fault diagnosis is the main concern of network fault management. Since one cannot prevent faults from happening, their rapid detection and isolation is required for the robustness, reliability, and accessibility of communication networks. In large and complex communication networks, automating fault diagnosis is certainly an essential task [STE04].

In the field of fault management, the following notions are introduced:

- An event is defined as an abnormal condition happening in the process of the hardware or software of a managed network; it is a key concept pertaining to fault diagnosis [JAK93, LO99, and YEM96]. In other words, an event signifies a change of state of a supervised object.
- Faults (also referred to as problems or root causes) create a class of network events that can cause, but are not caused by, other events [JAK93, LO99, and YEM96]. Faults, according to their duration time, may be classified as (1) permanent, (2) intermittent, and (3) transient [WAN89]. A permanent fault stays in a network until a repair action takes its place. Intermittent faults occur on a periodic and recurring basis causing degradation of service for small amounts of time. However, frequently re-occurring intermittent faults significantly degrade service performance. Transient faults create a temporary and minor degradation of service. They are typically repaired by error recovery procedures automatically [WAN89].
- An error is defined as a difference between an observed, measured or computed value or condition, and a real, specified, or theoretically correct value or condition [WAN89]. An error is a consequence of a fault. Faults may create one or more errors. Errors may cause the variation of a delivered service from its specified service, which is visible to the outside world. The word failure is used to identify this type of errors. Errors does not necessary get corrected. In many cases, apparently they are not observable. However, an error in a software or network device may cause faulty dependent software or network devices. Thus,

errors may propagate within the network causing failures of correct hardware or software [WAN89].

- Symptoms are exterior manifestations of failures [JAK93]. They are observed as an alarm-notification of a potential failure [JAK93, KAT97, LO99, and YEM96]. These notifications may arise from managing agents via management protocol messages (e.g. SNMP trap [CAS96] and CMIP EVENT-REPORT [ISO96]), or from management systems that monitor the network status (e.g. using command ping [STE95]), from system log-files, or character streams sent by external equipment [SCH96].

The process of fault diagnosis usually involves three steps:

- Fault detection [BOU94] is a method of capturing on-line indications of network disruption provided by malfunctioning devices in the form of alarms.
- Fault localization [BOU94, BOU95, and KAT96] (also referred to as fault isolation, alarm/event correlation, and root cause analysis) is a procedure in which a group of observed fault indications is analyzed to find an explanation of the alarms.
- Testing [BOU95 and KAT96] is a process that determines the actual faults given a number of possible hypotheses.

This thesis focuses on fault localization, the second part of fault diagnosis.

In the past, several paradigms were proposed upon which fault localization techniques were based. These paradigms stem from different areas of computer science, including graph theory, information theory, artificial intelligence, neural networks, and automata theory. In Fig. 1.1, a classification of the known solutions is presented. These solutions include techniques derived from the field of artificial intelligence (rule-, model- and case-based analysis tools, decision trees, and neural networks), graph-theoretic techniques, model-traversing techniques, and the codebook approach [STE04].

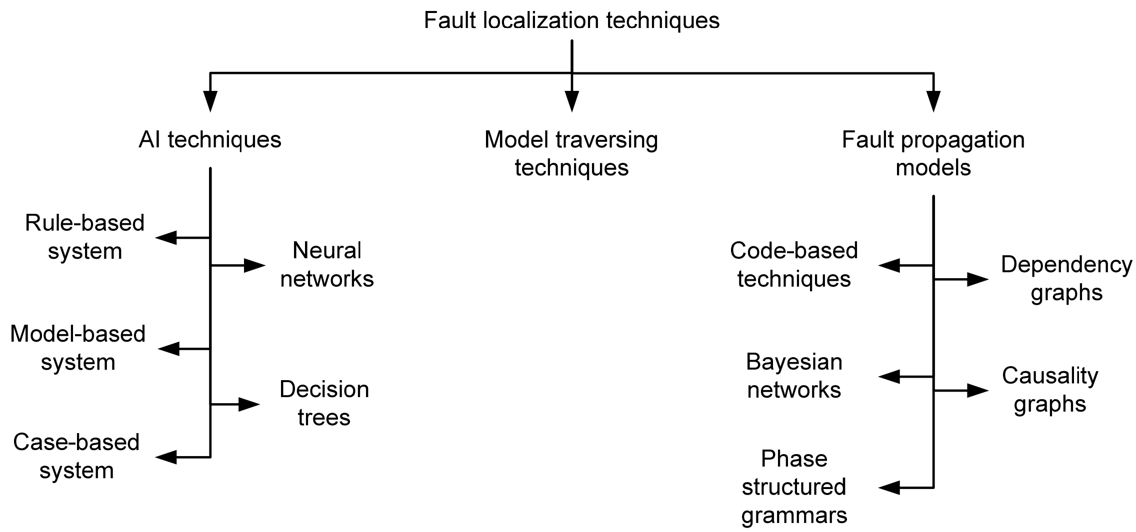

Fig. 1.1: Classification of Fault Localization Techniques [STE04]

However, as the modern communication systems are getting more complicated and presenting new capabilities, the requirements imposed on fault localization techniques have changed. It is reasonable to assume that, despite the research efforts done so far in this area, fault localization in the modern communication systems remains an open research issue [STE04].

1.2 Motivation

In wavelength-routed WDM networks, a fiber provides a number of wavelengths or optical channels that carry data traffic, each operating at the extremely high rate of several hundred gigabits per second. In an event of a single network failure such as a fiber cut, it may be a reason for an interruption of all the lightpaths that traverse the failed fiber link. This can, therefore, lead to a great amount of data loss in the network. That would typically degrade and disrupt the network services. For this reason, survivability is of particular importance in such networks. In order to ensure network services, the network must provide efficient survivability capabilities to overcome different types of network failures (e.g. a fiber cut or a node fault). In general, there are two basic survivability paradigms for the optical layer: predetermined protection and dynamic restoration. The fault localization function is used to locate rapidly link failures. It can also be used to support some local protection and restoration mechanisms. Logically, fault localization occurs only after a fault is detected [ZHE04].

In today's all-optical networks, signals remain in the optical domain from the source to the destination thereby eliminating any O/E and E/O conversions at each intermediate node. In the incident of a link failure on the lightpath, only the destination node can discover the power loss or signal degradation. This presents a considerable challenge in fault localization.

Isolating failure recovery within the network optical domain is necessary to resolve an alarm storm problem. That happens when a failure event at the optical layer (such as a fiber-cut) triggers alarms in other higher protocol layers [DEM99], which will be enabled by an intelligent and cost-effective failure monitoring and localization mechanism dedicated to the network optical layer. In addition, a single failure can trigger many redundant alarms [DEM99 and MAE98].

One of the most commonly adopted approaches is to utilize optical monitors responsible for generating alarms when a failure is detected. The alarm signals will then flood in the control plane of the optical network. Any routing entity uses these alarm signals to localize the failure and implement traffic restoration in a timely manner. Minimizing the number of alarm signals while achieving unambiguous failure localization (UFL) serves as the main target in the design of a failure localization scheme. In addition, reducing the bandwidth consumption for fault monitoring also should be jointly considered [TAP09].

A typical link-based monitoring scheme requires one monitor at each link. This requires $O(|E|)$ optical monitors and a length of alarm code as $|E|$, where $|E|$ is the number of network links. To make the solution more scalable, the studies in [ZEN06, ZEN07, TAL12, WU06, and WU07] investigated the monitoring-cycle (m-cycle). It is a pre-configured optical loop-back connection that is terminated by a monitor and launched with supervisory optical signals. When cut is occurred to any link along the cycle, the failure will be detected by the monitor and the monitor will issue an alarm to the rest of the network [TAP09].

A study in [ANG12] presented a monitoring system that utilizes partial physical layer information generated by a small number of monitors in a mesh optical network. That is to assess the quality of transmission (QoT) of all the established connections. The proposed method focuses on the placement of the monitors and the minimization of required monitoring equipment.

1.3 Objective

Since the advent of modern communication systems, there is a focus of research activities that produced numerous fault localization techniques. However, as communication systems evolved becoming more complex and offering new capabilities, the requirements imposed on fault localization techniques have changed as well.

The objectives of this thesis are:

(1) To explore different techniques used for fault localization in all-optical networks.

(2) To study m-trail design concepts for the fault localization process and to explore new techniques for deploying them along with established lightpaths to reserve network resources.

(3) To investigate RoF and PON systems and their corresponding applications.

(4) To analyze different PON/ RoF-PON structure models, make a comparison between them compare them, and provide a solution for their m-trail design problems.

1.4 Contributions

This dissertation proposes new techniques for deploying m-trails on networks along with its established lightpaths to perform fault localization in all-optical networks.

The main contributions of this thesis can be summarized as follows:

(1) A novel technique based on Geographic Midpoint Technique, as well as an adapted version of the Chinese Postman's Problem (CPP) solution and an adapted version of the Traveling Salesman's Problem (TSP) solution algorithms is introduced.

(2) A novel system for delivering future mm-WB RoF systems for wireless services integrated in DWDM architecture is proposed. This system made use of the PON technology and is denoted as RoF-PON. A complete design and simulation of such a system has been carried out along with an overview of related RoF network proposals and experiments.

(3) An investigation of a number of suggested innovative models for PON/ RoF-PON with a number of solutions for its m-trail design problem. The comparison between these models has been carried out by using the expected survivability function. That verifies that these models are reasonably suitable to be implemented in the new and existing PON/ RoF-PON systems.

1.5 Thesis Organization

The thesis is organized as follows: Chapter 2 presents a detailed study on the optical layer and the survivability techniques that have been used according to the existing and new technology trends. Chapter 3 gives an overview of survivability and fault detection/localization in the PON and RoF-PON. In Chapter 4, the context of the m-trails is presented and a straightforward method for establishing them. Innovative techniques for establishing m-trails and using them along with established lightpaths to perform fault localization is also offered. Chapter 5 demonstrates the performance evaluation done for the proposed techniques in comparison with other introduced techniques. The performance evaluation is based on numerical results from analytical models and/or by studying simulation outcomes. Finally, Chapter 6 concludes with remarks on this research and recommends further research work.

Chapter 2: Survivability and Fault Detection/Localization in Optical Networks

2.1 Introduction

In this chapter, the results of a survey on the detection and localization protocols for survivable optical networks, that guarantee service connectivity in a presence of a failure, will be described. This study also investigates tandem connection monitoring (TCM) in OTN networks.

2.2 Optical Layer

The optical layer can be divided into three sub-layers. These sections are described in the ITU-T G.872 recommendation. The three sub-layers are:

- The Optical Channel sub-layer (OCh),
- The Optical Multiplex Section sub-layer (OMS), and
- The Optical Transmission Section sub-layer (OTS).

These layers are shown in Fig. 2.1 and Table 2.1.

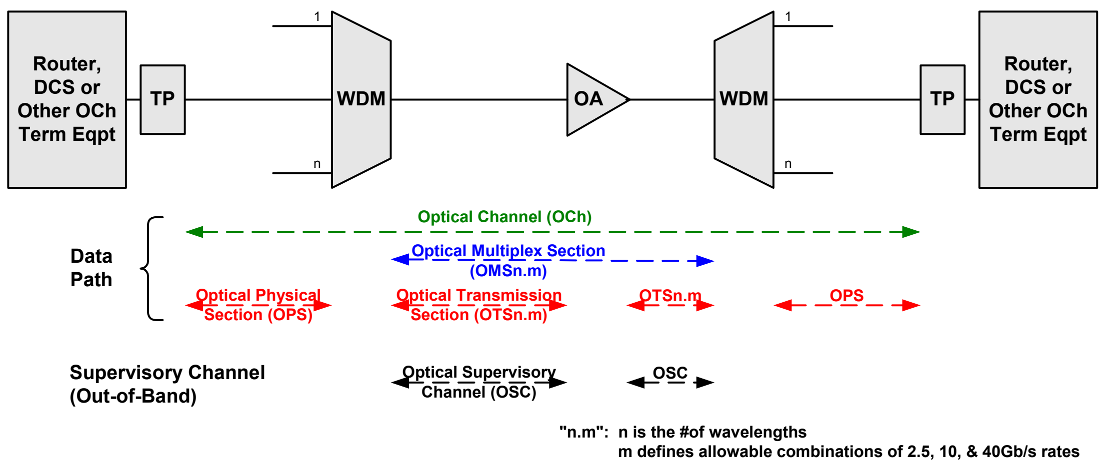

Fig. 2.1: Optical Sub-Layers

Table 2.1: Optical Sub-Layers [MAL02]

Electronic Layers	
OTN	OCh-Optical Channel
	OMS-Optical Multiplex Section
	OTS-Optical Transmission Section
	Physical media (optical fiber)

The Optical Transport Module (OTM) according to ITU-T G709 is illustrated in Fig. 2.2.

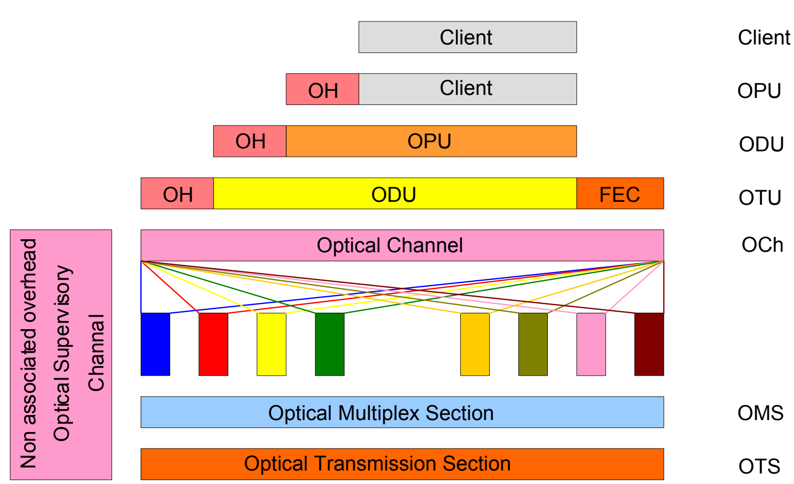

Fig. 2.2: Optical Sub-Layers [ITU03A]

To achieve management functionality, overhead is added to the client signal that, together with the FEC, forms the Optical Transport Unit (OTU).

2.2.1 Optical Transport Unit (OTU)

The OTU is carried by a single wavelength as an Optical Channel (OCh) (as shown in Fig. 2.3) and is transmitted as illustrated in Fig. 2.4.

Adding OH via the Optical Supervisory Channel (OSC) forms the OMS and the OTS.

Fig. 2.3: Optical Channel OCh [ITU03A]

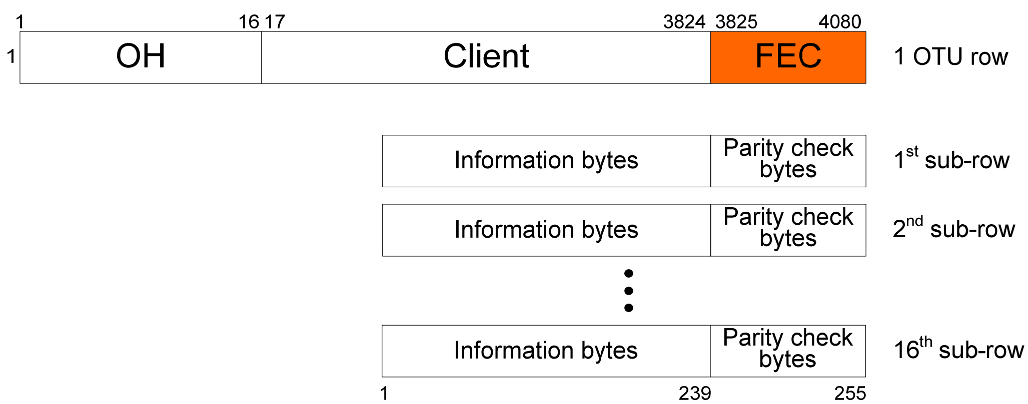

Fig. 2.4: OTU Transmission [ITU03A]

The OTU row is split into 16 sub-rows (code words) each consisting of 255 bytes. The sub-rows are formed from interleaved bytes. 239 bytes of the sub-row are used to calculate the FEC parity check, the result of which is transmitted in bytes (symbols) 240 to 255 of the same sub-row.

The Frame Alignment Signal (FAS) is used for synchronization.

The Optical Channel Transport Unit (OTU) overhead consists of sub-fields for the path monitoring OH (with the exception of the Incoming Alignment Error (IAE) bit); Section Monitoring (SM) provides monitoring functions and supports transport between 3R regenerators and General Communication Channels (GCC). These two fields allow communication between section end points.

2.2.2 Optical Channel Data Unit (ODU)

The Optical Channel Data Unit (ODU) overhead allows the user to support Tandem Connection Monitoring (TCM) (as shown in Table 2.2) which enables signal management across multiple networks, Path Monitoring (PM) (as shown in Table 2.3) which enables the monitoring of particular sections within the network and fault location, Automatic Protection Switching and Protection Communication Channel (APS/PCC) which provides APS switching on one or more levels, however these four bytes are currently undefined, Fault Type and Fault Location Channel (FTFL) (as shown in Table 2.4), and a 256 byte multi-frame signal providing fault status information regarding type and location of the fault.

Table 2.2: TCM Status Interpretation [ITU03A]

TCM byte 3, bits 6,7&8	Status
000	No source TC
001	In use without IAE
010	In use with IAE
011	Reserved
100	Reserved
101	Locked Defect LCK maintenance signal
110	Open Connection Identification OCI maintenance signal
111	Alarm Indication Signal AIS maintenance signal

Table 2.3: PM Status Interpretation [ITU03A]

PM byte 3, bits 6,7&8	Status
000	Reserved
001	Normal path signal
010	Reserved
011	Reserved
100	Reserved
101	Locked Defect LCK maintenance signal
110	Open Connection Identification OCI maintenance signal
111	Alarm Indication Signal AIS maintenance signal

Table 2.4: Fault Indication Codes Interpretation [ITU03A]

Fault Indication Codes	Definition
0000 0000	No Fault
0000 0001	Signal Fail
0000 0010	Signal Degrade
0000 0011	Reserved
.	
.	
.	
1111 1111	

2.2.3 Optical Channel Payload Unit (OPU)

The Optical Channel Payload Unit (OPU) overhead regulates the mapping and concatenation of the client data and provides information on the type of data transported (as shown in Table 2.5).

Table 2.5: Payload Type Code Points [ITU03A]

Hex code	Interpretation
01	Experimental mapping
02	Asynchronous STS-N mapping

03	Bit synchronous STS-N mapping
04	ATM mapping
05	GFP mapping
06	Virtual Concatenated signal
10	Bit stream with octet timing mapping
11	Bit stream without octet timing mapping
20	ODU multiplex structure
55	Not available
66	Not available
80-8F	Reserved codes for proprietary use
FD	NULL test signal mapping
FE	PRBS test signal mapping
FF	Not available

The optical sub-layers and its SONET equivalents are illustrated in table 2.6.

Table 2.6: Optical Sub-Layers and its SONET Equivalents

OTN (ITU Terms)	SONET (rough equivalent)
OCh	Path
OMS	Line
OTS	Section

2.3 Survivability in the Optical Layer

Fig. 2.1 illustrates the different survivability techniques that can be implemented in optical networks with different topologies [FUM00].

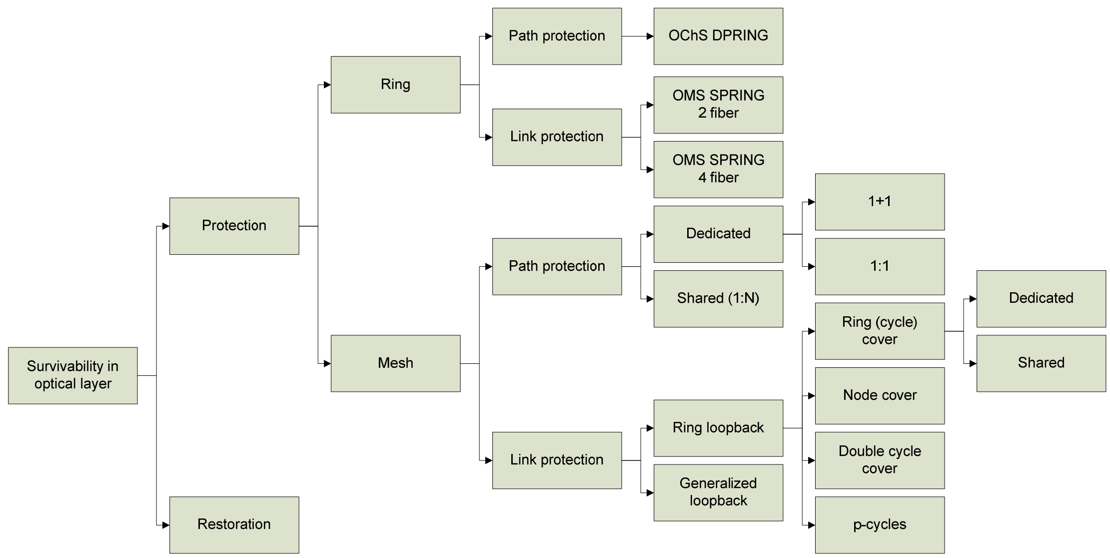

Fig. 2.5:   Optical Layer Survivability Techniques [MAL02]

2.3.4 Protection in the Optical Layer

According to ITU-T G709 specifications automatic protection can be performed only at the OMS and OCh sub-layers which will be described in detail later on.

2.3.4.1 OMS Protection

OMS protection can be viewed as a bulk protection in which the protection is done for all wavelengths carried by the fiber. That type of protection is at the fiber level. The advantages of using this type of protection are that it is fast, simple, and robust. On the other hand, the disadvantages of using this type of protection are its coarse granularity and the low efficiency of utilization. Fig. 2.6 shows one of the possible configurations of the OMSP. This configuration can provide protection for the possible failures of fiber cables and optical amplifiers. On the other hand, it cannot provide protection for the possible failures of transponders, OTN MUX and DEMUX, and IP router interface cards.

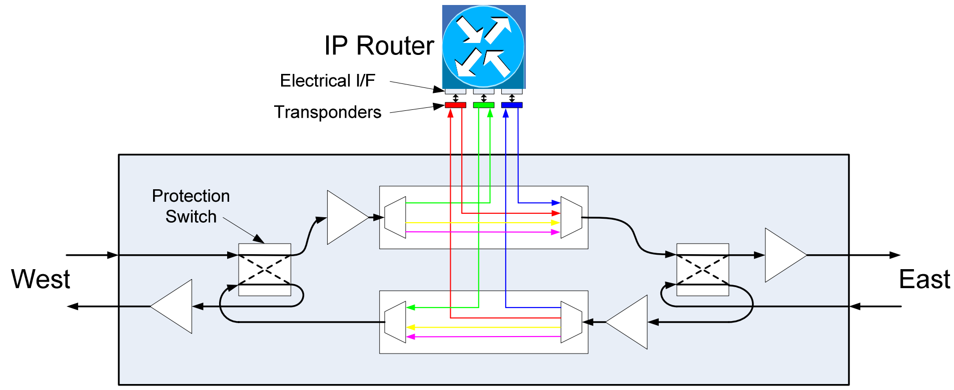

Fig. 2.6: Possible Node for OMSP in a Ring Configuration [MAA10a]

2.3.4.2 OCh Protection

OCh protection differs from OMS protection. OCh protection covers only selected wavelengths carried by the fiber. In case of failure, the protection is automatic; it switches these selected wavelengths (channels) to the pre-assigned wavelengths. The advantages of using this type of protection are effective use of the network capacity, that is, a high efficiency of network utilization and fine granularity. On the other hand, the disadvantages of using this type of protection are that it is complicated and provides low network utilization efficiency.

Fig. 2.7 and Fig. 2.8 show one of the possible configurations for the 1+1 OChP or a Sub Network Connection Protection (SNCP). This is the primary protection system used in today's OTN networks. This configuration can provide protection for the following possible failures: OTN MUX and DEMUX, optical amplifiers, and IP router interface cards. On the other hand, it cannot provide protection for the possible failures of transponders and IP routers.

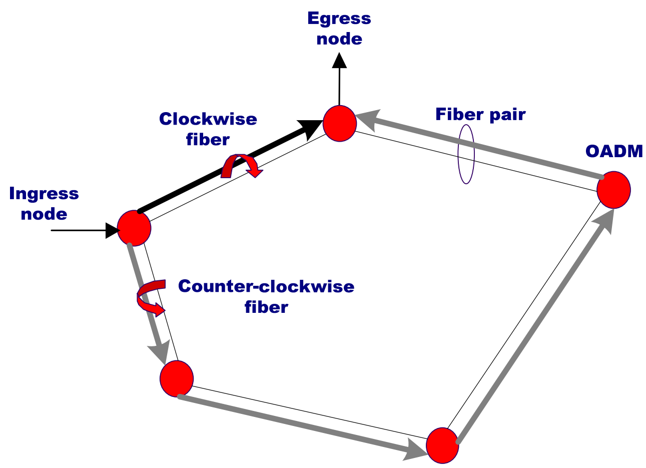

Fig. 2.7: 1+1 OChP Ring [MAA10a]

The second possible configuration of the OChP (as shown in Fig. 2.9) is Trail Protection. This configuration can provide protection for the following possible failures: transponders, OTN MUX and DEMUX, optical amplifiers, and IP router interface cards. On the other hand, it cannot provide protection for the possible failure of IP routers.

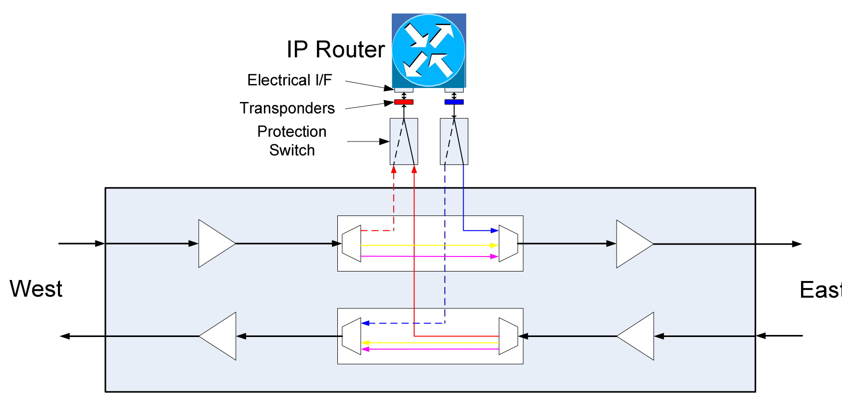

Fig. 2.8: SNCP (OChP) Node in a Ring Configuration [MAA10a]

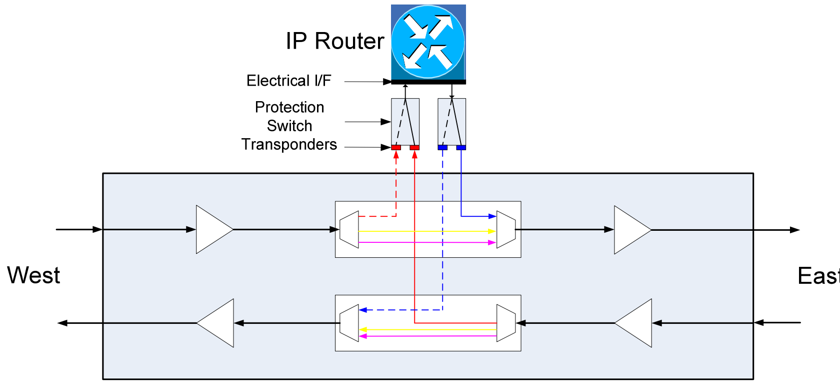

Fig. 2.9: Trail Protection (OChP) Node in a Ring Configuration [MAA10a]

There is a difference between these two types of protection. In the OCh trail, the protection is done by duplicating the transponder cards (as shown in Fig. 2.10b). In the SNCP, the optical switches are placed between the transponder and the OTN filters; this splits/combines the wavelengths (Fig. 2.10a).

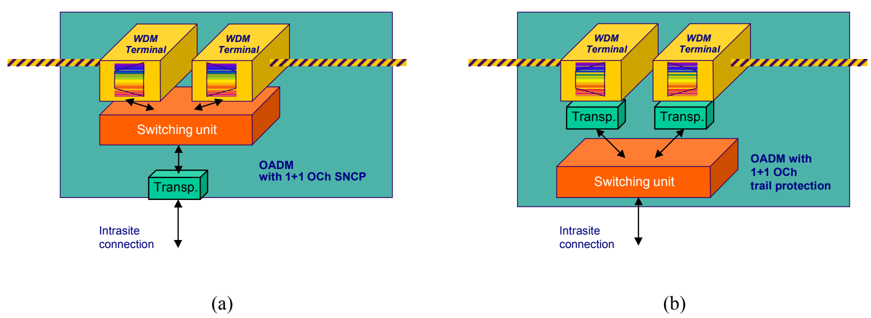

Fig. 2.10: Architecture of OADM for 1+1 OCh Protection: (a) SNCP and (b) Trail Protection [MAA10a]

Trail Protection provides superior performance from the survivability point of view, however, it increases the cost because it requires more hardware.

2.3.4.3 Dedicated and Shared Protection

The protection in the optical sub-layer is either OMSP or OChP. Each of them can be either dedicated (DP) or shared (SP).

2.3.4.3.1 Dedicated Protection

DP is in the form of 1+1 (as shown in Fig. 2.11) where the working traffic is copied to another route. The route that provides lower error rate to the receiver is selected. That means this protection plan uses the protected route all the time (100%). In other words, the network protection capacity is equal to the network transmission capacity, and each of them is half of the network total capacity [ZHO00]. The advantages of using this type of protection are that it is fast, simple, and has high QoP utilization. On the other hand, the disadvantage of using this type of protection is its poor utilization of the network capacity.

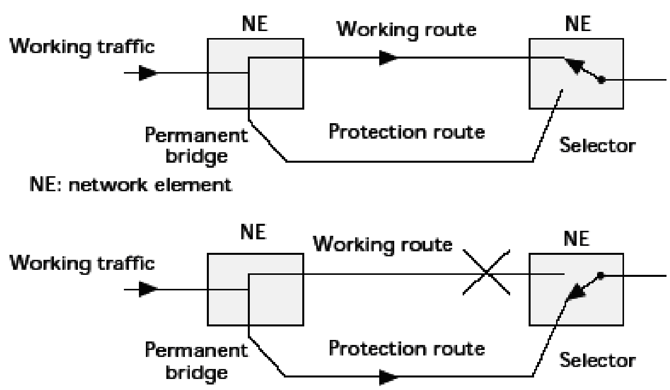

Fig. 2.11: Architecture of 1+1 Protection Schemes [ZHO00]

2.3.4.3.2 Shared Protection

Shared protection can be in the form of 1:1 (as shown in Fig. 2.12), 1:N, or k:N. One or more traffic routes are used to protect the working traffic. The shared protection routes may be used to carry extra traffic of less importance [ZHO00].

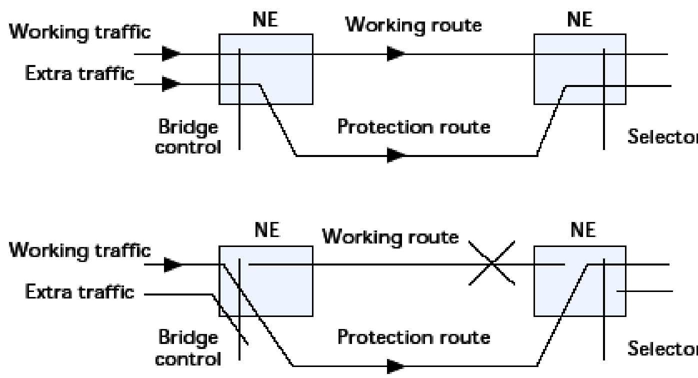

Fig. 2.12: Architecture of 1:1 Protection Schemes [ZHO00]

The advantage of using this type of protection is its efficient utilization usage of network capacity. On the other hand, the disadvantage of using this type of protection is its complications.

Both dedicated and shared OChP methods are implemented in OTN in both peer-to-peer and OADM ring networks. However, only the dedicated OMSP method is implemented in the existing peer-to-peer networks. The existing OADMs usually implements only 1+1 OCh protection. This means that these networks either support this type of protection or do not provide any protection at all.

2.3.4.4 Link and Path Protection

In OTN, protection can be done either on the link (the connection between any adjacent nodes that may be OADMs) as shown in Fig. 2.13, or on the path (the complete route from the source node to the destination node) as shown in Fig. 2.14. The different protection schemes described above (OCh and OMS, either dedicated or shared) are generally link-based types of protection. The protected link (or path) must be disjointed with the working link (or path). Also, any two working paths having one or more links sharing the same risk of failure, must have disjointed protected paths (this is known as SRLG constraints).

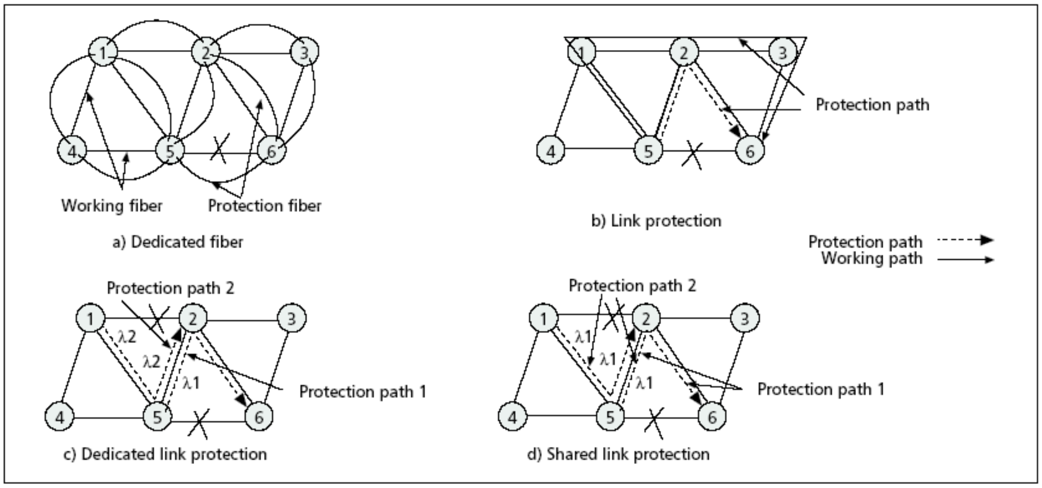

Link-based protection.

Fig. 2.13: Link-Based Protection [ZHO00]

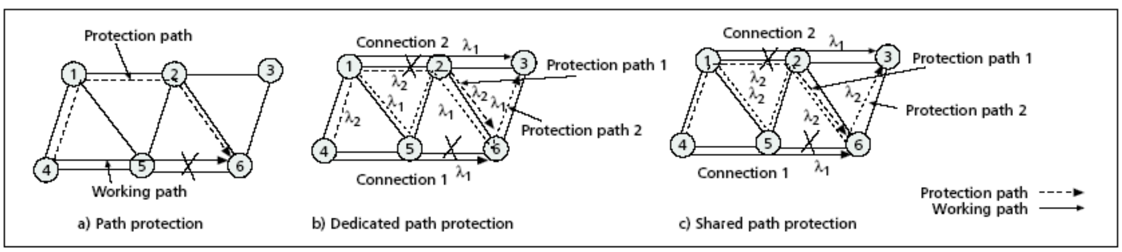

Path-based protection.

Fig. 2.14: Path-Based Protection [ZHO00]

2.3.5 Restoration in the Optical Layer

Restoration can use any capacity available between nodes in order to get a transport entity that can replace the failed one. Restoration is based on re-routing algorithms that to get a new path to recover failed network entities at the time of failure. The algorithms are those operating in levels higher than the network layer where the actions are applied. In general, the restoration process follows the following steps:

1. Detection of the failure,

2. Dissemination of alarms and control messages,
3. Re-routing,
4. Network updates,
5. Return to normal.

2.3.5.1 Centralized and Distributed Restoration Control Architectures

Restoration architecture can be classified according to the locations of its control act to either centralized or distributed. Restoration process control in the centralized architecture operates from one unit that is integrated within the network management. On the other hand, the control of the restoration process in distributed architecture, operates from a number of units spread throughout the network and is integrated within a number of network elements. The advantages of distributed restoration are that it is faster and more flexible while the advantages of centralized restoration are that it has better network management and a lower complexity of network elements.

2.3.5.2 Dynamic and Pre-planned Restoration Control Architectures

In dynamic restoration, re-routing activities are performed after the receipt of a restoration request that is based on the current network status. In pre-planned restoration the re-routing activities are performed after receiving a restoration request according to a pre-determined route determined by the network restoration management. The advantages of pre-planned restoration are that it is faster and has better network management, while the advantages of dynamic restoration are that it does not require continuous network management activities to update re-routing tables, and it demonstrates better use of network resources [ALB06].

2.3.5.3 Adjacent-node, Intermediate Node and End-to-end Restoration Types

In end-to-end restoration, re-routing is done by finding an entirely different path between end nodes of the affected traffic. In adjacent-node restoration, re-routing is done by finding another link between the nodes for the affected link traffic. In intermediate-node restoration, re-routing is done by finding another link/path between any intermediate nodes to re-route the affected traffic between the two end nods.

A comparison between adjacent node, intermediate node, and end-to-end restoration types is presented in Table 2.7.

Table 2.7: Comparison of Adjacent Node, Intermediate Node, and End-to-End Restoration Types [MAA10a]

Restoration Type	End-to-End	Adjacent-Node	Intermediate-Node
Network resources needed	Few	More	Moderate
Resource sharing offered	High	Low	Moderate
Restoration speed	Slower	Faster	Moderate
Capacity reserved	~60%	~80%	~70%

In today's optical networks, restoration techniques that have been applied at each node (including an Optical Cross-Connect (OXC)) can be implemented at the OCh layer in these networks. Some restoration techniques can also be implemented using O-E-O cross-connects designed to establish fast restoration. The use of OCh restoration allows us to define a priority classes.

2.4 Fault Detection/Localization

In this section, an investigation of signaling protocols including failure localization, protection, and restoration mechanisms, is carried out. This survey comprises those signaling techniques that are related to the context of this dissertation.

2.4.1 Open Shortest Path First (OSPF) protocol

The most basic fault detection procedure is the Open Shortest Path First (OSPF) protocol [MAC00]. Fault detection in OSPF is achieved by sending/receiving packet signals called “hello messages". The hello signals are traveling between neighboring routers to obtain the link/node status. These signals are transmitted on a pre-programmed short interval namely, the hello interval. A smaller hello interval allows faster connectivity detection. However, smaller Hello intervals consume much more bandwidth than longer ones. Furthermore, using a long hello interval for extended multi-domain networks will delay the network response in determining the connectivity status. As a result, network partitions and the partition size are factors in the design of the hello interval. In addition, a hello interval should be chosen in correspondence to another parameter known as the router dead interval [WOL95]. Normally, the default router dead interval is four times the chosen Hello interval. By default, the hello signals are transferred every 10 seconds. After four missing Hello messages, a failure is detected. It takes at least 40 seconds for the OSPF hello protocol to detect the failure occurrence. Although this method is practical, its speed is far below the required speed of fault detection in high speed networks especially in the optical networks.

A technique similar to the OSPF hello protocol is implemented in the Voice over Internet Protocol (VoIP). In this network, short- and low-speed control packets, called keep-alive packets, monitor the network periodically to help quick switchover of calls [KAR04]. Fault detection is achieved by means of a master node called the dispatcher. This process monitors the network nodes and associated links by means of parallel centralized signaling as illustrated in Fig. 2.15. A known protocol from this category is ping-pong protocol, which is typically used in submarines. This technique is also called master-slave or pingger-pongger [LU04]. This method is neither scalable nor efficient because of its use of a centralized dispatcher. Furthermore, returned low power signals are sometimes misinterpreted as faults. The process of fault detection is applied to large quantities of data to discover implicit knowledge hidden in these data information. Various machine-intelligence and information techniques including pattern analysis, induction decision trees, clustering, and time series analysis are used to facilitate data processing [TSO04]. These methods are usually applied to power systems that are subject to interruption. However, they are significantly time-consuming and not always reliable. As a result, they cannot be tuned into extremely high bandwidth networks.

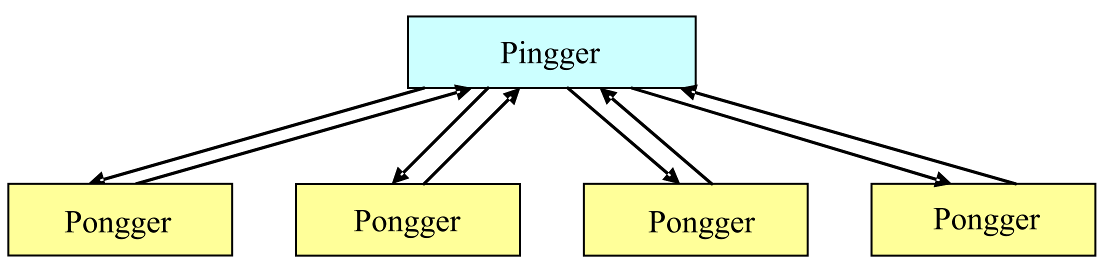

Fig. 2.15: Fault Detection in the Pingger-Pongger Protocol [LU04]

Over the last two decades, several probabilistic analysis frameworks have also been introduced, however, their background is out of the scope of this thesis. Interested readers can find a comprehensive study on them in [LAZ92]. Although the introduced protocols have been put in operation for decades, they are not compatible with optical networks and they do not meet the desired speed and reliability levels. Thus, specific survivable signaling protocols were devised during the past decades for rapid fault localization in optical networks [SIC06].

2.4.2 Tandem Connection Monitoring in OTN networks

Within the OTN overhead, the path monitoring bytes provide an essential role in monitoring end-to-end signal quality. They allow carriers to guarantee customer Service Level Agreements (SLAs). In large, interconnected networks such as those shown in Fig. 2.16, it is particularly useful to have multiple path monitoring points [FUJ10].

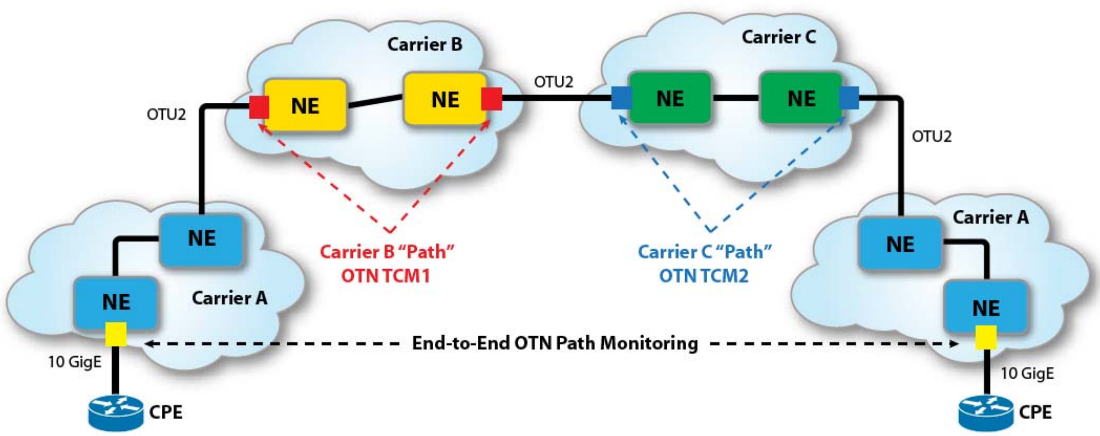

Fig. 2.16: OTN Tandem Monitoring [FUJ10]

The traditional OTN path monitoring bytes allow carriers to implement end-to-end signal monitoring across the overall network as shown in Fig. 2.16. In large networks that constructed over wide geographical areas, it is common for multiple carriers to transport a single signal, each providing transport services across their respective geographical area or "cloud." These other carriers have requirements for monitoring the path layer as the signal enters and exits their "cloud" to provide service commitment to the end-to-end carrier [FUJ10].

OTN enables path layer monitoring at multiple user defined endpoints which is one of its more powerful features. TCM bytes support this user-defined path monitoring function. SONET/SDH allows a single level of TCM to be configured, while ITU G.709 allows six levels of tandem connection monitoring to be configured. The TCM bytes are available in the OTN overhead, labeled TCM1 through TCM6. These bytes allow carriers to define their own path layers. For example, Carrier B could use TCM1 to perform path monitoring at the entry and exit points of its network. Likewise, Carrier C could use TCM2 to perform path monitoring on the signal as it enters and exits the Carrier C cloud [FUJ10].

TCM monitoring capabilities include: TCM-bit interleave parity-8 (TCM-PIB-8) and TCM backward error indication (TCM-BEI) error monitoring as well as TCM-alarm indication signal (TCM-AIS), TCM-loss of tandem connection (TCM-LTC), TCM-open connection indication (TCM-OCI), TCM-locked (TCM-LCK), TCM-trace identifier mismatch (TCM-TIM), TCM-backward defect indication (TCM-BDI), TCM-incoming alignment error (TCM-IAE), and TCM-backward incoming alignment error (TCM-BIAE) alarms. By using TCM errors and alarms, operators can monitor the performance of their networks in details or as an overview.

Fig. 2.17 illustrates TCM1 being used by the customer to monitor the connection's end-to-end path, where TCM2 is used by network operator A, B and C separately to monitor the connection through their own sub-network [EXF09].

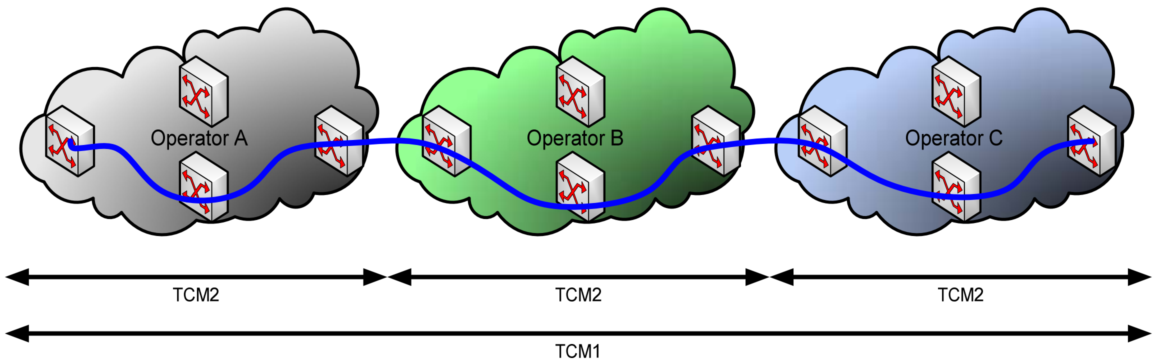

Fig. 2.17: TCM Assignment

There are different types of monitored connection topologies: cascaded, nested, and overlapping. Examples of these topologies are provided in Fig. 2.18.

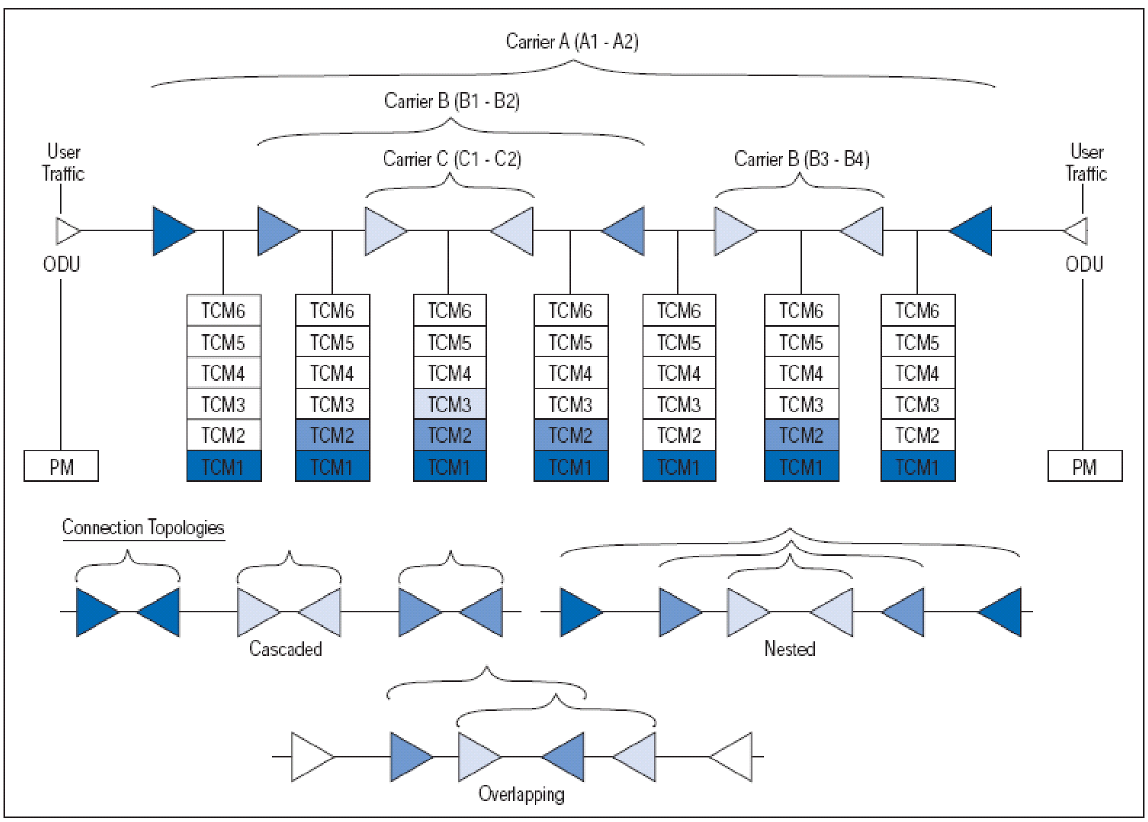

Fig. 2.18: Tandem Connection Monitoring [EXF09]

Each of the six TCMi fields in the ODU overhead is assigned to a monitored connection. It can be between zero and six levels or connections that can be configured for each ODU trail. An example is presented in Fig. 2.18. There are three different levels that are actually monitored. The location of Carrier C allows it to monitor three TCM levels as the ODU passes through its portion of the network. The other carriers also monitor the levels according to their agreement and position [EXF09].

In addition to the monitoring maintenance signals, using the STAT sub-field associated with each TCM level, the TCM connection also monitors the BIP-8 and BEI errors for each connection level. Maintenance signals are used to advertise upstream service conditions that affect the traffic. Errors provide an indication of the quality of service offered at each segment of the network. This information is a valuable tool for the user and carrier to isolate faulty sections of the network [EXF09].

2.4.3 LVM Fault-Localization Protocol for All-Optical Networks

The LVM protocol is a fault-localization protocol proposed for localizing single-link failures in all-optical networks [ZHE04]. It is based on a distributed control concept. Unlike existing fault-localization protocols, it provides the maximum-level of transparency by skipping any power monitoring or spectrum analysis at the intermediate nodes on an established lightpath. The fault localization process of the LVM protocol can be divided into five phases which are described briefly:

1. Pausing: In this phase, the potential executive sinks (all sinks affected by the failure) and the corresponding path (the shortest affected path) of each potential executive sink is specified as illustrated in Fig. 2.19.

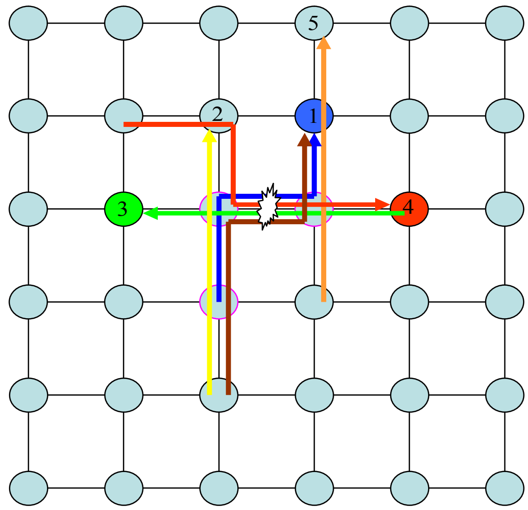

Fig. 2.19: Fault Detection and Potential Sink Formation (Potential Executive Sinks: 1 ,3 &4, Associated Path: Blue & Green) [KHA08]

2. Flooding: In this phase, all potential executive sinks flood alarms containing their IDs and associated paths to all nodes in the network in order to determine the executive link, as shown in Fig. 2.20. The executive link is the one with the shortest associated path or in case of equal path lengths the one with the smallest ID.

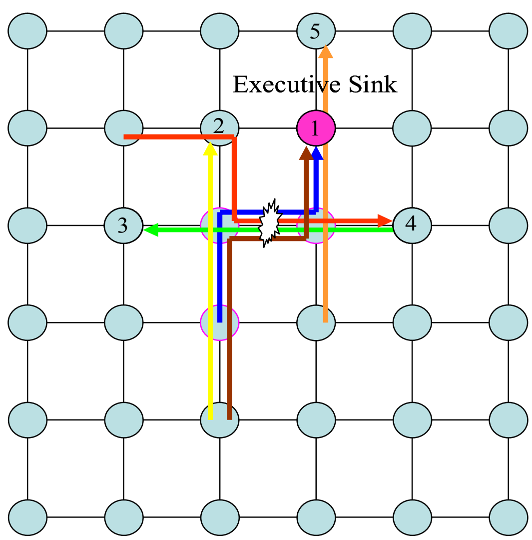

Fig. 2.20: Executive Sink Election [KHA08]

3. Multicasting: In this phase, the executive sink multicasts a vector contains its associated path links, called the Affected-Link-Vector (ALV), to the nodes within its limited perimeter. Fig. 2.21 illustrates the ALV message and its contents.

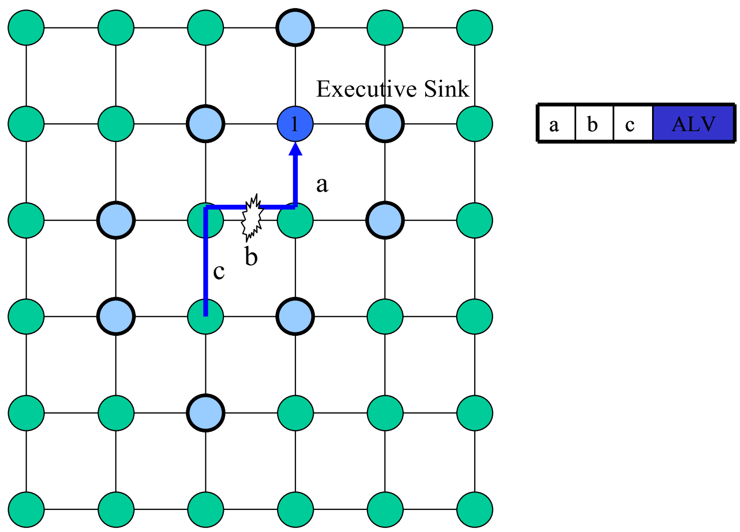

Fig. 2.21: ALV Multicasting [KHA08]

4. Matching: Fig. 2.22 illustrates this phase. Each node that receives an ALV creates its own link vector and compares its elements with the ALV. If its link vector has a matching link, it sends back a binary vector consisting of the matching vector and the status of the lightpath (1 = working, 0 = not working).

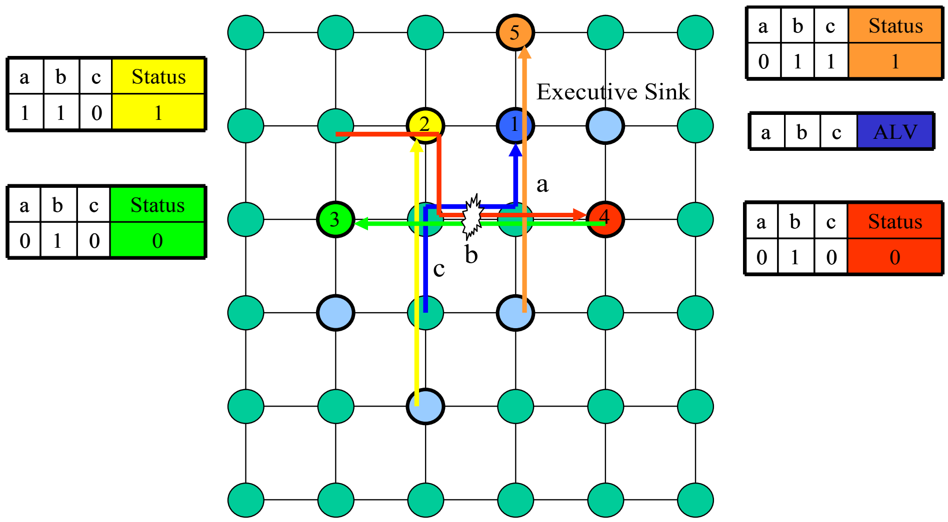

Fig. 2.22: Matching Phase [KHA08]

5. Determining: In this phase, the executive sink performs logical "AND" on all received binary vectors to determine the location of the failure. The link corresponding to "1" in the resultant binary vector is determined to be a failed link as shown in Fig. 2.23.

Once the failed link is localized, the executive sink broadcasts the location of the failure to all nodes in the network. The end nodes of the failed link can then start a link restoration process, readers are referred to [SIC07] for more information.

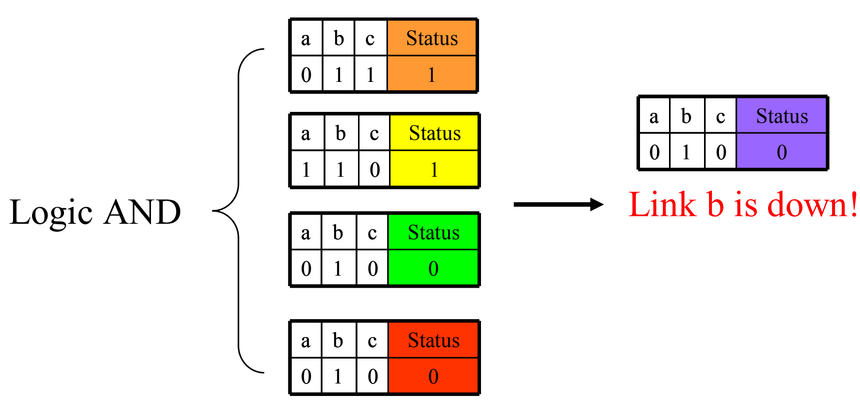

Fig. 2.23: Failed Link Determination [KHA08]

2.5 Summary and Concluding Remarks

In this chapter, a survey on the detection and localization protocols for survivable optical networks is provided. Survivability methods, protection, and restoration are investigated at the optical layer with their pros and cons.

Although OSPF is considered to be an effective protocol, its speed is far below the required speed of fault detection in high speed networks especially in the optical networks.

The pingger-pongger protocol is neither scalable nor efficient because of the use of a centralized dispatcher. Furthermore, returned low power signals are sometimes misinterpreted as faults.

Within the OTN overhead, the path monitoring bytes provide an essential role in monitoring end-to-end signal quality. They allow carriers to guarantee customer Service Level Agreements (SLAs). SONET/SDH allows a single level of TCM to be configured while ITU G.709 allows six levels of tandem connection monitoring to be configured. Maintenance signals are used to advertise upstream service conditions affecting the traffic. Errors provide an indication of the quality of service offered at each segment of the network. This information is a valuable tool for the user and carrier to isolate faulty sections of the network.

The LVM protocol is a fault-localization protocol used for localizing single-link failures in all-optical networks. It is based on a distributed control concept. Unlike existing fault-localization protocols, it provides the maximum-level of transparency by skipping any power monitoring or spectrum analysis at the intermediate nodes on an established lightpath.

Chapter 3: Survivability and Fault Detection/Localization for Passive Optical Networks and Radio-over-Fiber Passive Optical Networks

3.1 Introduction

A PON is a point-to-multipoint optical network. It consists of an Optical Line Terminator (OLT) located at the Central Office (CO) and a set of Optical Network Units (ONUs) in remote nodes at the customer's location. The connection between the OLT and ONUs is realized by a single fiber and the use of one or more optical splitters.

The network between the OLT and the ONUs is passive, meaning that it does not require any power supply. The exclusive presence of passive elements in the network makes the network more tolerant to faults and decreases the operational and maintenance costs once the infrastructure has been laid down. A typical PON, as illustrated in Fig. 3.1, uses a single wavelength for all downstream transmissions (from OLT to ONUs) and another wavelength for all upstream transmissions (from ONUs to OLT). These two wavelengths are multiplexed on a single fiber through coarse wavelength-division multiplexing CWDM [MAA07].

Four main PON technologies are considered, namely, Broadband PON (BPON), Ethernet PON (EPON), Gigabit PON (GPON), and Wavelength Division Multiplexing

PON (WDM PON). Table 3.1 summarizes the main differences between these four technologies.

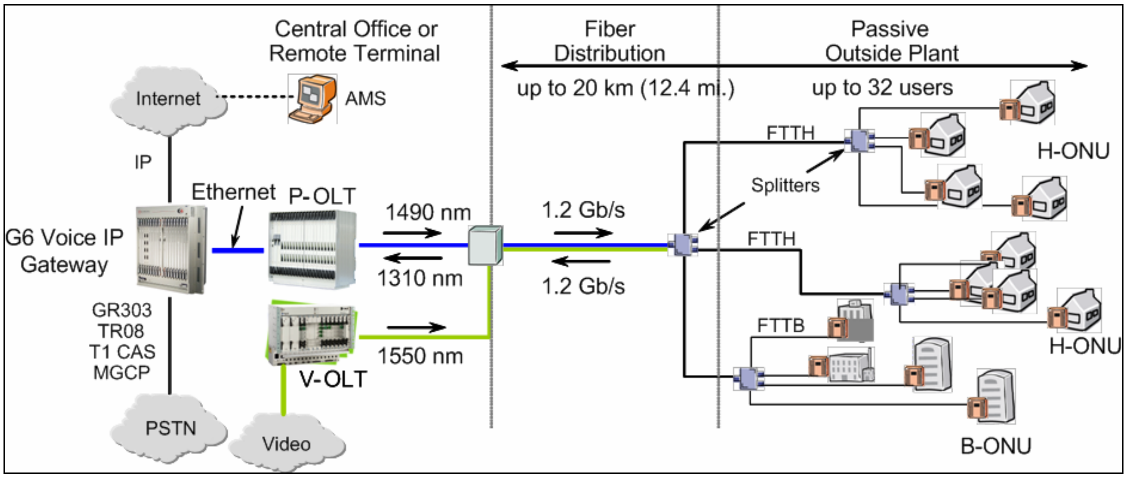

Fig. 3.1: Typical PON Architecture [MAA07]

Table 3.1: Summary of the Main Differences between PON Technologies [MAA07]

	A/BPON	EPON (GEPON)	GPON	10 GEPON	WDM PON
Standard	ITU G.983	IEEE802ah	ITU G.984	IEEE P802.3av	ITU G.983
Data Packet Cell Size	53 bytes	1518 bytes	53 to 1518 bytes	1518 bytes	Independent
Maximum Downstream Line Rate	622 Mbps	1.2 Gbps	2.4 Gbps	IP; 2.4 Gbps, Broadcast; 5 Gbps On-demand; 2.5 Gbps	1-10 Gbit/s per channel
Maximum Upstream Line Rate	155/622 Mbps	1.2 Gbps	1.2 Gbps	2.5 Gbps	1-10 Gbit/s per channel
Downstream wavelength	1490 and 1550 nm	1550 nm	1490 and 1550 nm	1550 nm	Individual wavelength/channel
Upstream wavelength	1310 nm	1310 nm	1310 nm	1310 nm	Individual wavelength/channel
Traffic Modes	ATM	Ethernet	ATM Ethernet or TDM	Ethernet	Protocol Independent
Voice	ATM	VoIP	TDM	VoIP	Independent
Video	1550 nm overlay	1550 nm overlay/IP	1550 nm overlay/ IP	IP	1550 nm overlay/ IP
Max PON Splits	32	32	64	128	16/100's
Max Distance	20 Km	20 Km	60 Km	10 Km	20 Km
Average Bandwidth per User	20 Mbit/s	60 Mbit/s	40 Mbit/s	20 Mbit/s	Up to 10 Gbit/s

From the four main types of PON networks, the commonly used today are EPON and GPON system. The maximum distance from the OLT to the ONUs should not exceed

20 km and 60 km, respectively. The promising WDM-PON and hybrid TDM/WDM-PON are considered the future enabled technologies for the optical access networks [KAT12].

Table 3.2 lists PON classes as per ITU-T recommendation G.983.1 [MAA07 and SHA05].

Table 3.2: PON Classes [MAA07 and SHA05]

	Class A (622 Mbps only)	Class B	Class C
Minimum loss	5 dB	10 dB	15 dB
Maximum loss	20 dB	25 dB	30 dB
ONUs Max. No.	Up to 8	Up to 16	Up to 32

3.2 Radio-over-Fiber (RoF)

RoF is generated by modulating a light beam by radio frequency signal traversing in an optical fiber link. This type of technology is used for wireless access networks where the word RoF is normally referred to it in spite of its other applications like cable television (CATV) networks and satellite base stations feed.

RoF makes it possible to combine the RF signal processing utilities in one common area (head-end). The use of optical fiber offers low signal loss (0.2 dB/km at 1550 nm wavelength) to distribute the RF signals to the Remote Antenna Units (RAUs) as shown in Fig. 3.2.

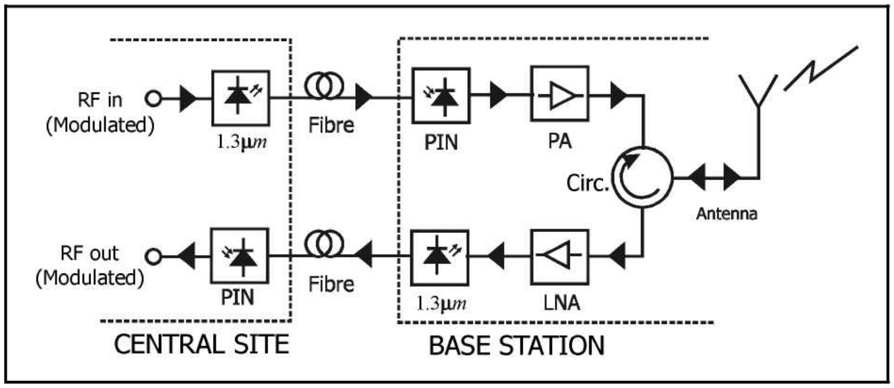

Fig. 3.2: The Radio over Fiber System Concept [MAA09]

Fiber to the Antenna (FTTA) is another RoF application where an optical fiber is directly connected to the antenna base with the use of a small simple Optical-to-Electrical (O/E) device. The advantages of this configuration are the reduction of the signal losses due to the small fiber losses, system protection against electrical discharges and lightning strikes, and cost reduction in the devices used at the antenna base station.

RoF systems, such as the one showed in Fig. 3.2, were commonly used to transport microwave signals and to obtain mobility functions in the CS.

The modulated microwave signals at the input end of the RoF system are transported to the RS in the form of optical signals. At the RS, the microwave signals are restored and radiated by antennas. The advantage of using such a system lies in the ability to dynamically allocate capacity based on traffic demands. In addition to transport and mobility tasks that RoF systems provide, there are others like data modulation, signal processing, and up/down frequency conversion. [OPA09].

The RoF system design layout varies according to its electrical signal at the input side. Every system, according to its deployed technology, specifies the design configuration and the input type. Fig. 3.3 shows four different designs: (a) The RF modulated signal is generated by two stage mixers and externally modulated the Laser Diode (LD). The RF modulated optical signal is then transmitted to the Base Station (BS), detected by the Photo Detector (PD), and eventually goes to the antenna unit. (b) The IF modulated signal is generated by an IF mixer and externally modulated by the LD. The IF modulated optical signal is then transmitted to the BS, detected by the PD, then up converted to RF by RF mixer, and eventually goes to the antenna unit. (c) The baseband signal is externally modulated by the LD. The modulated optical signal is then transmitted to the BS, detected by the PD, and up converted to RF by two stage mixers. Finally, it goes to the antenna unit. (d) The baseband signal is directly modulated by the LD. The modulated optical signal is then transmitted to the BS, detected by the PD, and up converted to RF by two stage mixers. Finally, it goes to the antenna unit.

The delivery of the RF signal directly to the antenna site and the need for complicated and expensive devices there, is eliminated and kept it at the CO side. That simplifies the remote side and adds mobility features to it. Macro-diversity for seamless handover is one advantage of this feature [KIM05].

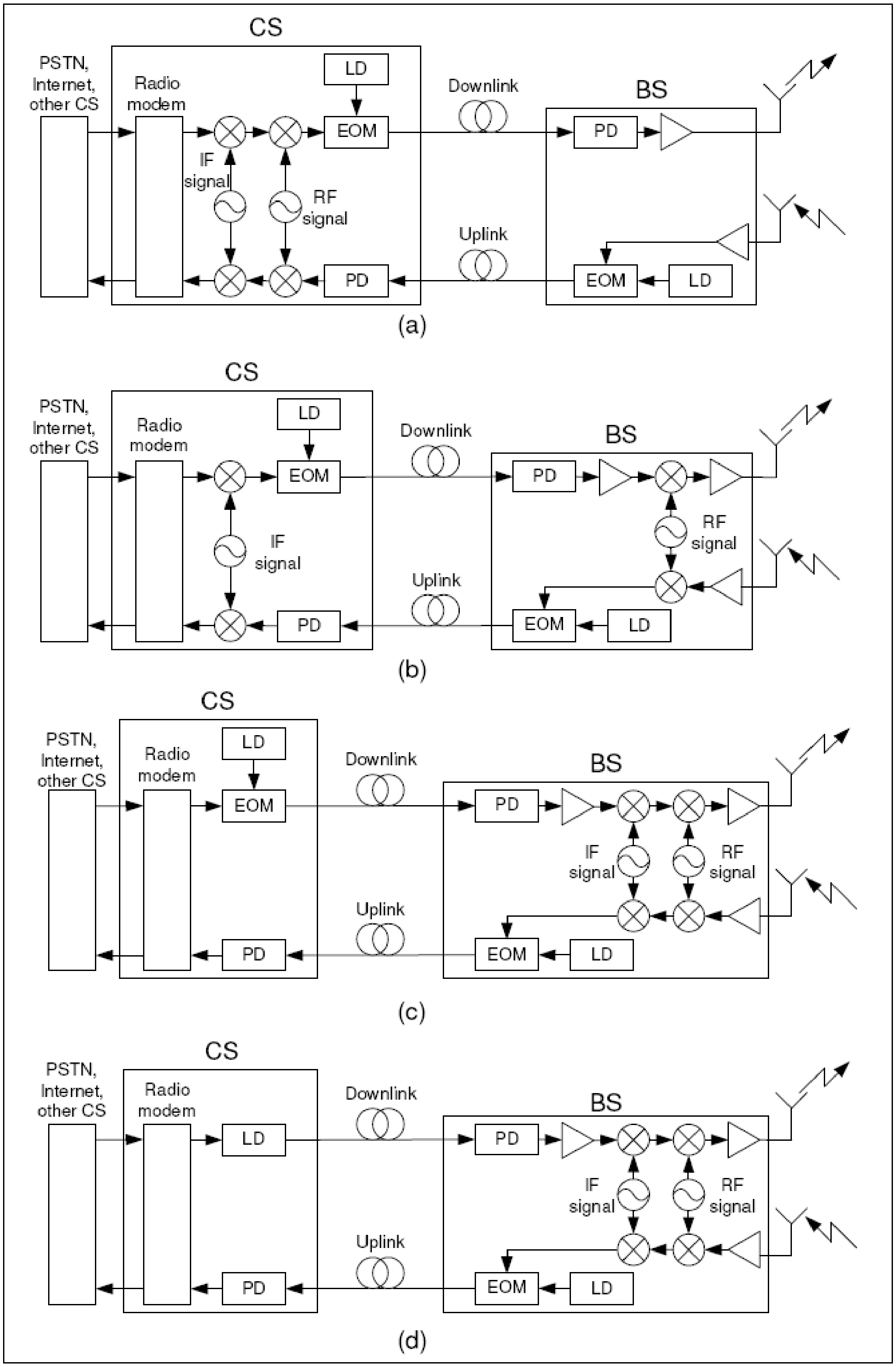

Fig. 3.3: Different RoF System Designs: (a) EOM, RF Modulated Signal. (b) EOM, IF Modulated Signal, (c) EOM, Baseband Modulated Signal. (d) Direct Modulation [KIM05]

A proposed system to deliver radio signals from a bank of base stations located in the central office (CO) to the RAU, by means of optical channels that using active routing optical access network, is demonstrated in [TRA12]. Another system for high-speed full-duplex indoor optical wireless communication, for both down-link and up-link, is experimentally demonstrated in [WAN12].

3.3 Proposed Novel RoF-PON Wireless Services System [MAA09]

The proposed novel RoF-PON wireless services system is illustrated in Fig. 3.4.

The Central Station (CS) contains the optical mm-wave source, customers' uploading data, direct detection Photo-diodes (PDs) associated with its amplification circuitries, Dense Wavelength Division Multiplexing (DWDM MUX), externally modulated Distributed-Feedback Laser (DFBs) using an Electro-optic Modulator (Mach Zehnder Modulator) EOM, and Arrayed Waveguide Grating AWG. While the RAU contains heterodyne PDs, EOM, DFBs and AWG.

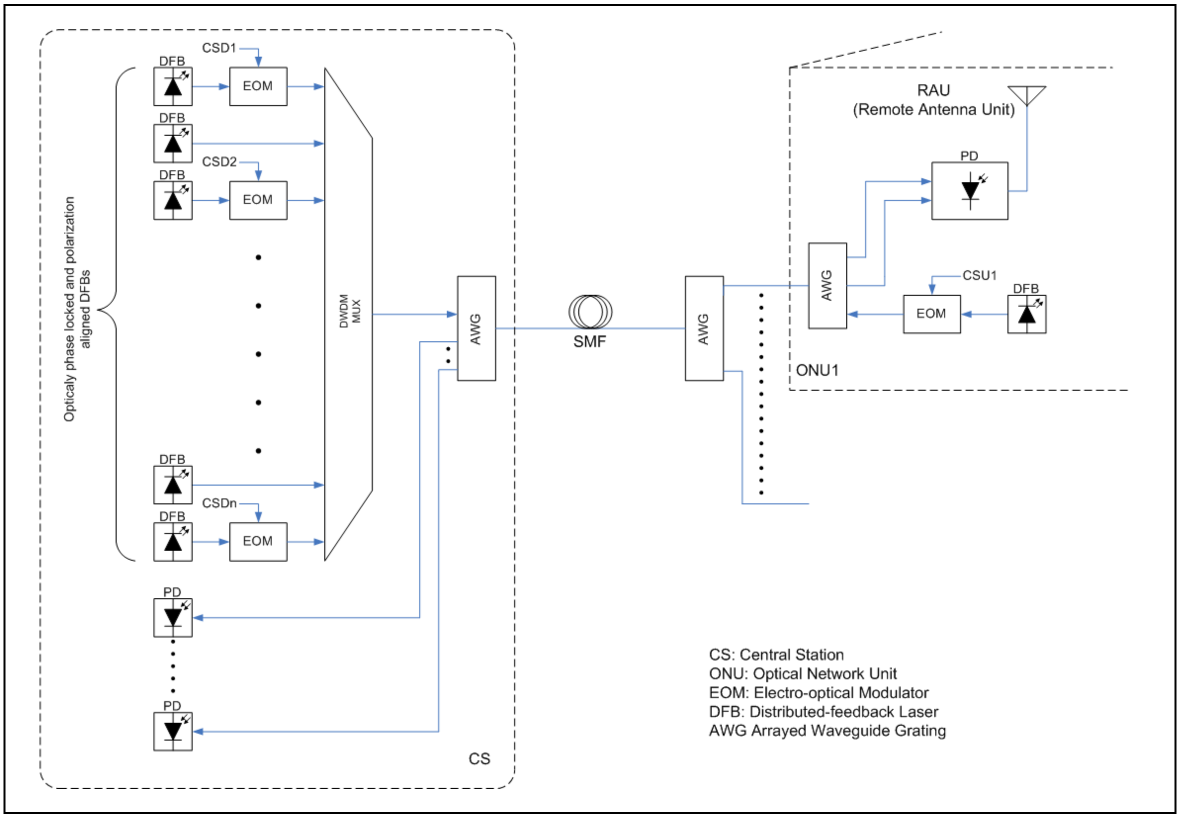

Fig. 3.4: The Proposed Novel RoF-PON Wireless Services System [MAA09]

Optical mm-wave source: The realization of the optical mm-wave source is based on a novel idea which relies on a heterodyne technique for the remote generation of mm-wave signals. The optical phase-locked and polarization-aligned-source provides two carriers (for each RAU) separated by the desired mm-wave frequency *f*. The total number of required wavelengths for *N* RAU is *2N-1*. For the conceptual illustration, a DWDM RoF system with channel spacing of 12.5 GHz is considered. Other frequency spacing may be considered e.g. 25 GHz or 50 GHz. These frequency spacing is according to ITU-T G.696.1 spectral grid recommendation. Reducing the frequency spacing can cause undesirable effects like Four Wave Mixing (FWM) and Cross Phase Modulation (XPM). 12.5 GHz (KU band) may be considered as a future extension to the current 5.8 GHz frequency for home wireless communication.

RAU mm-wave receiver: The RAU demodulates the coherent optical signals generated by the mm-wave optical source through a high speed, high responsivity photodiode.

The RF signal is obtained at each Optical Network Unit (ONU) by using optical heterodyning photo detection between two optical carriers simultaneously; one optical carrier is modulated with the downloading customer data while the second is an un-modulated carrier. The generated RF-modulated signal has a frequency of 12.5 GHz. The resulting RF signal is then amplified and transmitted by the antennae. In the uplink system, direct photo detection is used.

Such a RoF system is simple, cost-effective, and reduces the maintenance operations at the BS. In principle, this system is immune to laser phase noise provided that it affects both optical lightpaths that transmitted to the RAU.

3.4 PON Survivability

In chapter two, a study on the network survivability is conducted. The two common survivability types are: network protection and network restoration. The protection is a pre-planed scheme which reserves a network capacity in the form of another path/link to switch over in case of the working path/link failure in a remarkably short time. Alternatively, the restoration is a dynamic process which uses any available capacity to restore the traffic at the failed link. Restoration uses re-routing algorithms to find the recovery path/link which starts after the occurrence of a failure. The processing time is quite large, ranges from tens of seconds to several minutes.

In PON system where the topology is usually pretty easy, the pre-planned protection schemes are often deployed to perform network survivability [LAM07 and WAN09].

There is a trade-off between achieving PON network survivability and expenses as well as the complexity of the system that produced by adding additional fibers, and/or installing duplicate components. That is in addition to the extra operation and maintenance costs.

PON is exposed to the failure due to its tree topology as it is the topology specified in ITU-T G.983. In the case of the segment failure, which may occur due to a failure of the feeder fiber or all transportation fibers, all ONUs in the segment lose their connections with the OLT [LIU12]. It is necessary to use either protection or restoration schemes to provide network survivability.

Fig. 3.5 shows the four ITU-T G.983.1 suggested protection architectures [ITU98]. In (a), the protection is done by duplicating the trunk fiber which provides survivability for the system against trunk fiber cut only. Another enhancement is added in (b) by duplicating the LT. That structure provides survivability for the system against either trunk fiber cut or LT failures. In (c), further enhancement is achieved by duplicating the optical splitter. That structure provides survivability for the system against a certain set of simultaneous two failures in trunk fiber cut, feeder fiber cut, and LT. Adding 2:1 optical splitters before N:2 optical splitters in (d) increase the number in the set of simultaneous two failures which provides better system survivability.

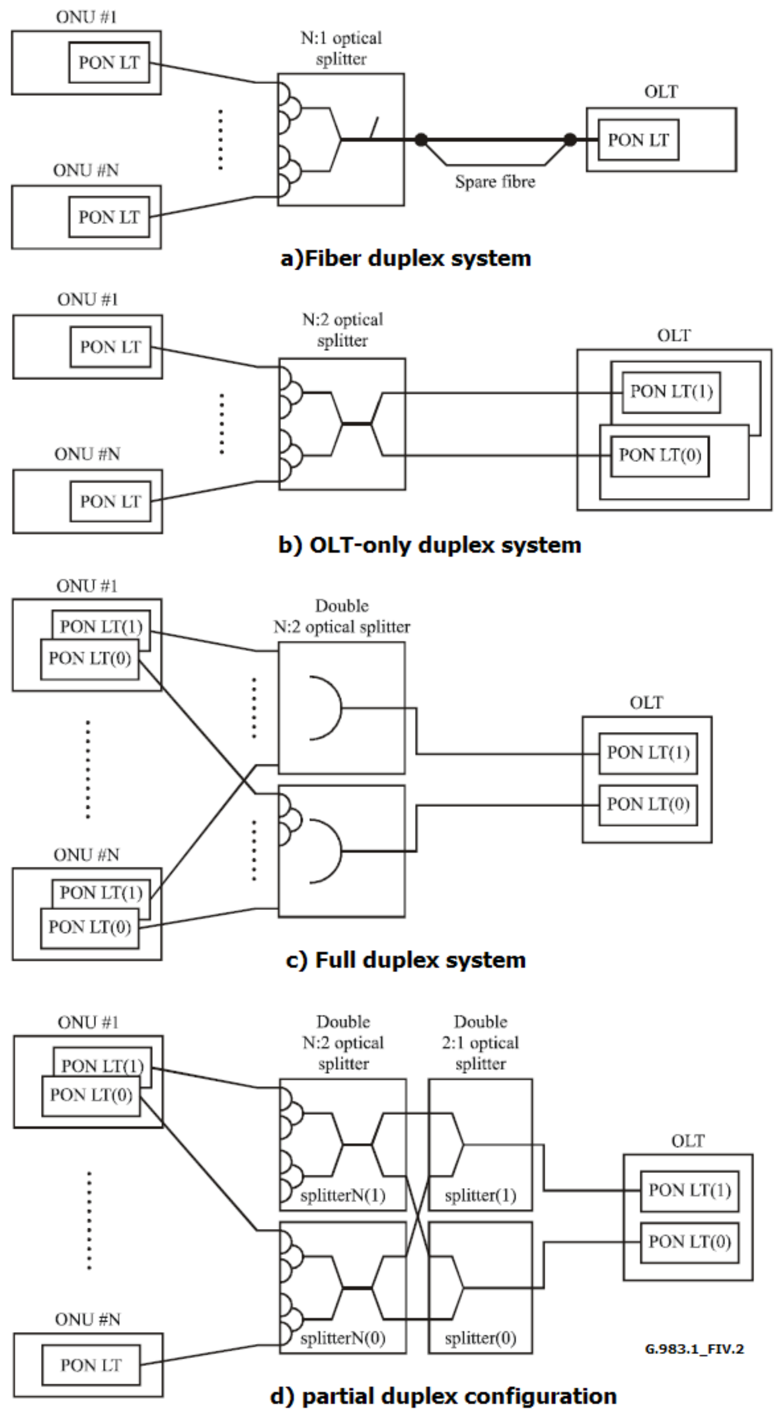

Fig. 3.5: Protection Switching Architectures Suggested by ITU-T G983.1 [ITU98]

In the previously described architectures, protection is done by duplicating either or both the fiber links and the device components. Accordingly, many WDM-PON protection schemes are proposed as shown in Fig. 3.6 [LAM07 and SON05] and Fig. 3.7 [SON05]. In the configuration of Fig. 3.6, the layout is protected against any failure in either the feeder or distribution fiber, while the architecture in Fig. 3.7 provides a protection only towards a failure in the feeder fiber.

In those illustrations, the optical signal inside the CO, which feeds each Remote Node (RN), is split into working and protection paths by a 3 dB splitter/combiner passing by the B/R wavelength splitter/combiner. The blue presents the working path while the red presents the protection path. At the RN side, there is a 1xN cyclic AWG and B/R wavelength splitter/combiner [WAN09].

The Group 1 ONUs receives the working blue signals while Group 2 ONUs receives the protecting red signals.

The wavelength channel, which is assigned for each ONU, is split into two; one traversed through the working route while the other traversed through the protecting path.

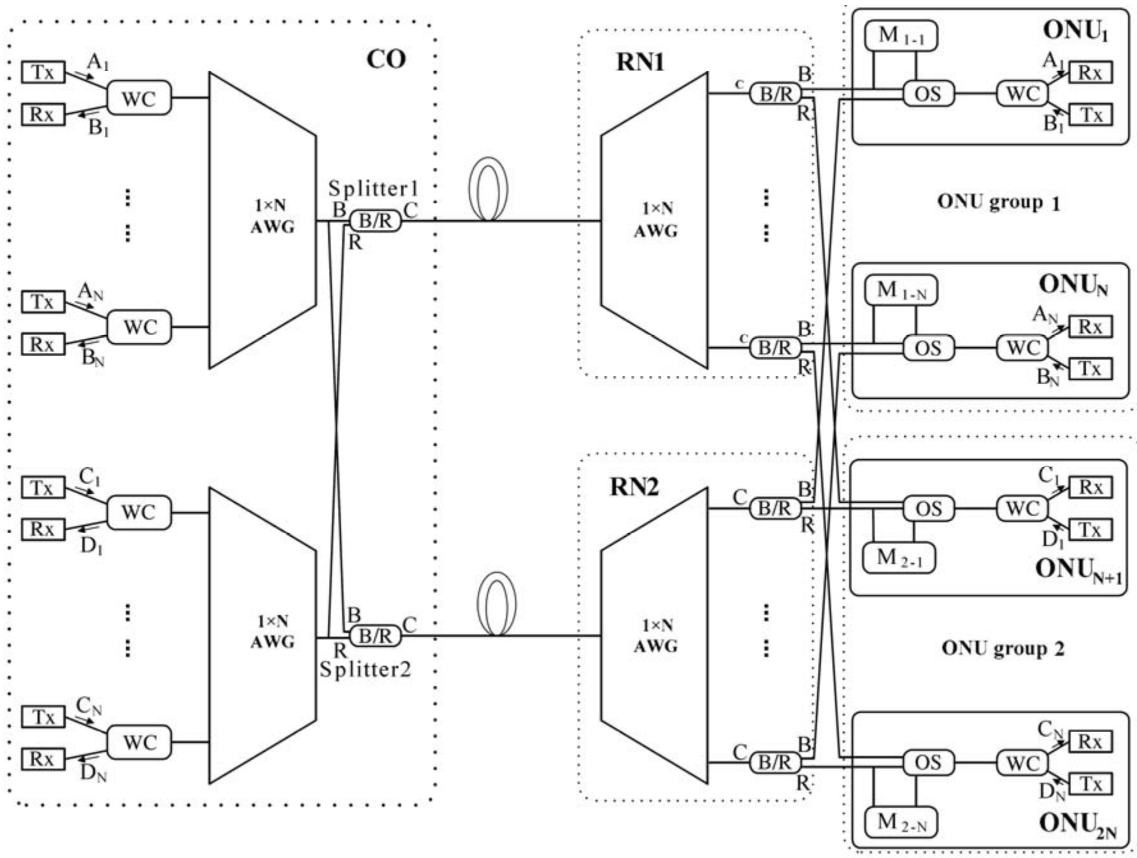

Fig. 3.6: WDM-PON Architecture with Self-Protection Capability against Both Feeder Fiber and Distribution Fiber Failures [SON05]. (WC: wavelength coupler; B/R: blue/red filter; M: power monitoring modules; B: port for blue-band signal only; R: port for red-band signal only; C: common port)

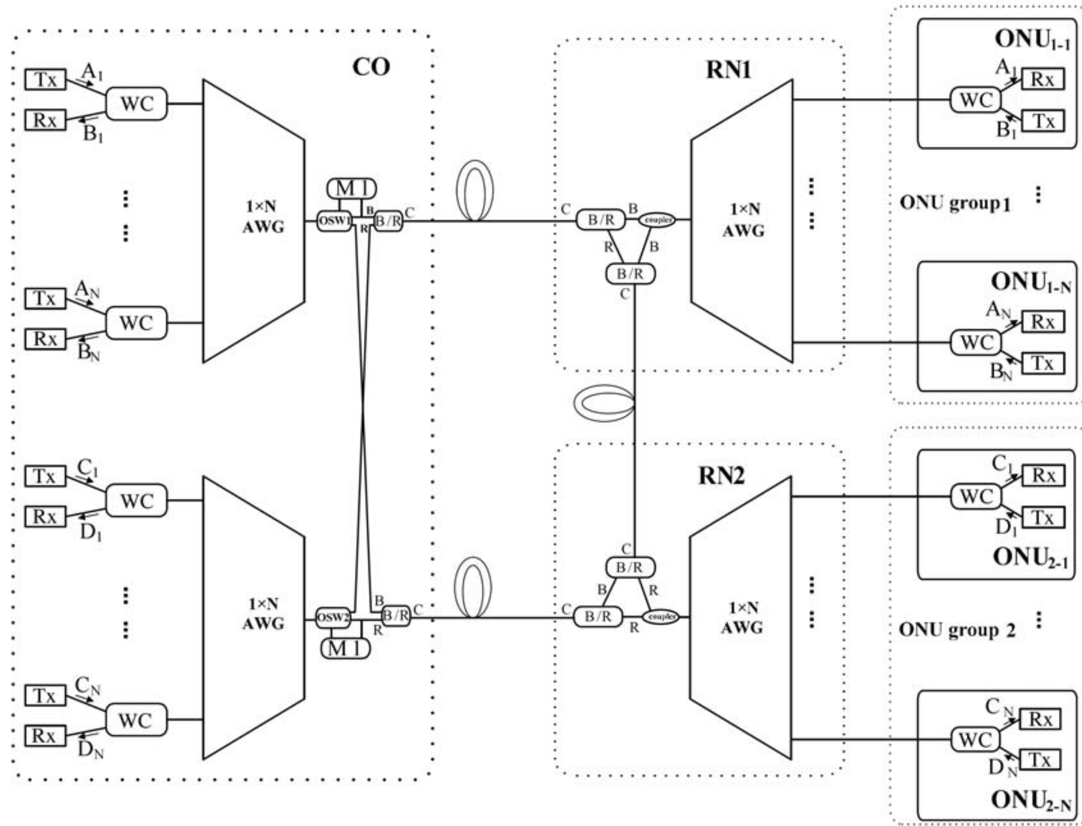

Fig. 3.7: WDM-PON Architecture with Self-Protection Capability against the Feeder Fiber Failure [SON05].
(WC: wavelength coupler; B/R: blue/red filter; M: power monitoring modules; B: port for blue-band signal only; R: port for red-band signal only; C: common port)

At each ONU, there is an optical monitor which detects the optical power loss at the working path and sends out an alarm signal that triggers an optical switch forcing the receiver side of that ONU to receive the signal from the protection path. That process is done automatically as soon as the failure is detected. An opposite process will happen as soon as the failure is repaired that revert the system to its working structure.

The wavelength assignment diagram is shown in Fig. 3.8 [SON05]. To perform bidirectional WDM-PON feature in these architectures, each AWG in the system compromises two AWGs; one for downstream and the other for upstream. Both AWGs are from the same band spaced by Free Spectral Range (FSR) of the each AWG. That design increases the cost of the overall WDM-PON system [WAN09].

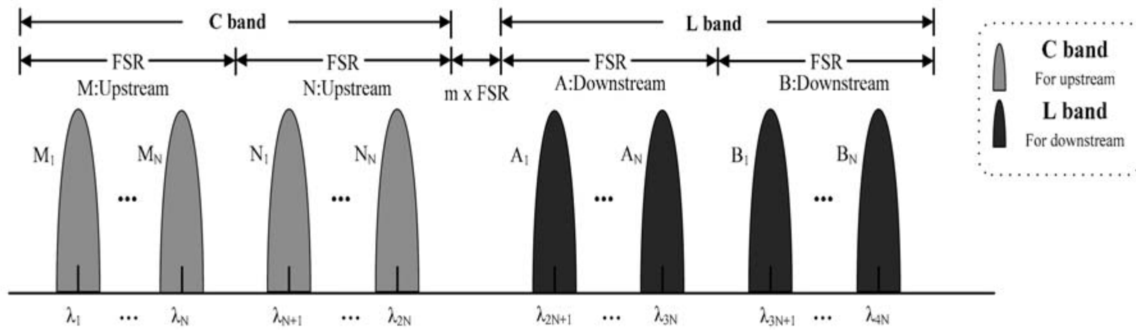

Fig. 3.8: The System's Wavelength Assignment Plan [SON05]

3.5 ONT Functions [ITU02]

The Optical Network Terminal (ONT) functions are described in section 4.2 of the G.983.2. This clause gives the spotlight on the ONT at its Access Node Interface (ANI) region. ITU-T Rec. G.983.5 specifies two types of protection structural design: 1+1 configuration and 1:1 configuration. Accordingly, there are two models that can be taken into consideration which include protection effect on ONT capabilities.

3.5.1 1+1 model

Fig. 3.9 shows an ONT model with a 1+1 protection architectural design. Both the working and protection path are receiving the same traffic. Inside the Transmission Convergence (TC) Adaptor, the same traffic is supplied via Physical Path Termination Point (PPTP) to both the working and the protection PON-LTs.

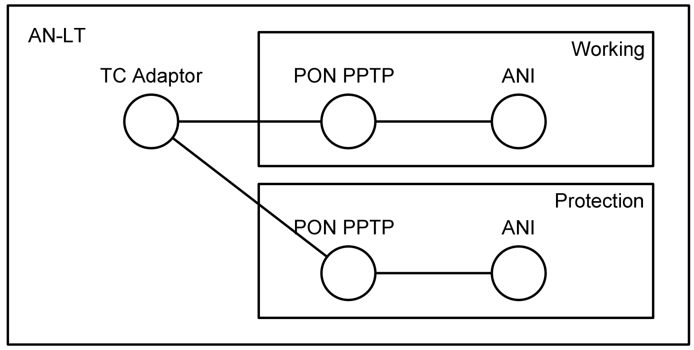

Fig. 3.9: G.983.6 – 1+1 Model ONT (ANI side) [ITU02]

3.5.2 1:1 model

Fig. 3.10 shows an ONT model with a 1:1 protection. In this configuration, the working path is carrying the traffic load while the protection path may take an extra, less important traffic. If a failure happens to the working path, the traffic will be switched automatic/manually to the protecting path. That will drop any traffic it may be carried at this moment. In normal operation mode, the TC adapter forwards the main traffic to the working PON-LT and the additional traffic to the protecting PON-LT. While in protection mode, TC adapter forwards the main traffic only to the protecting PON-LT.

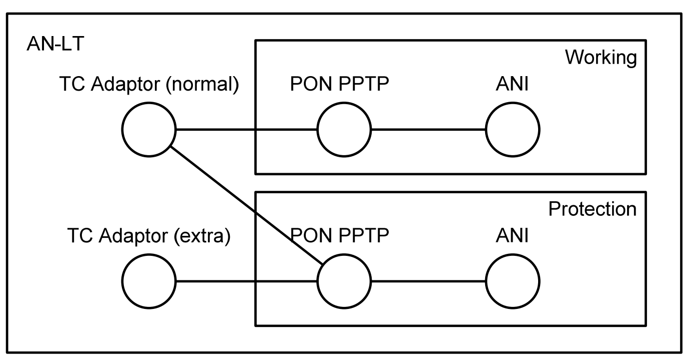

Fig. 3.10: G.983.6 – 1:1 Model ONT (ANI side) [ITU02]

3.6 Different Topologies to Perform PON Survivability

Different PON topologies are proposed in [HON03] to provide network survivability protection. In this section, a number of those topologies in addition to another number of proposed topologies are described.

According to the topology study done for the PON systems, the trunk fiber has the main impact on the system sustainability. To improve the system survivability, any kind of protection to this trunk fiber needs to be done. Duplicating the trunk fiber may be an excellent choice [JIN07].

Fig. 3.11 shows some PON tree topologies for the same ONU numbers and locations.

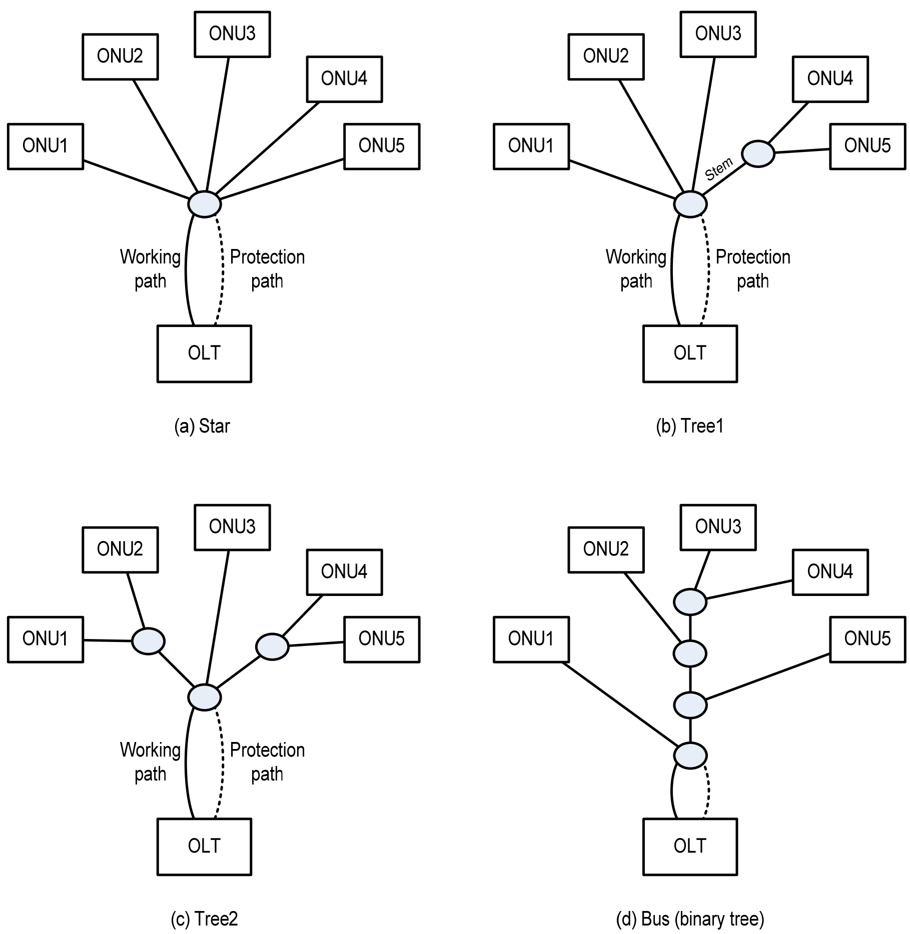

Fig. 3.11: PON Star/Tree Topologies with Redundant Trunk [JIN07]

Fig. 3.11(a) presents a star topology; a topology with one splitter in the middle. Fig. 3.11(b) shows another topology having two splitters connected by a stem. In Fig. 3.11(c), a topology is showing a system having three splitters and two stems. The tree topology complexity increases with the increase of the ONU number as this requires adding more splitters and stems. Adding stems may be required if splitting number is increased and/or the location of the ONUs are apart from each other. The most complex topology is shown in Fig. 3.11(d). This topology is a binary tree. It is also known as a bus topology. Both star and bus topologies are considered as two special cases of the tree [JIN07].

A ring topology is known by its survivability characteristics. Using it as a special topology for PON system is considered for this fact. A PON in a ring topology is shown in Fig. 3.12(a).

From the survivability point of view, a ring topology is considered to have better survivability features than both star and tree topologies. In comparison between star and tree topologies, the first shows better survivability capability than the later. The main disadvantage of the ring topology is its lack of flexibility as well as updating complexity.

A combination between a ring and a star topologies forming ring-star topology is shown in Fig. 3.12(b) in order to get better performance.

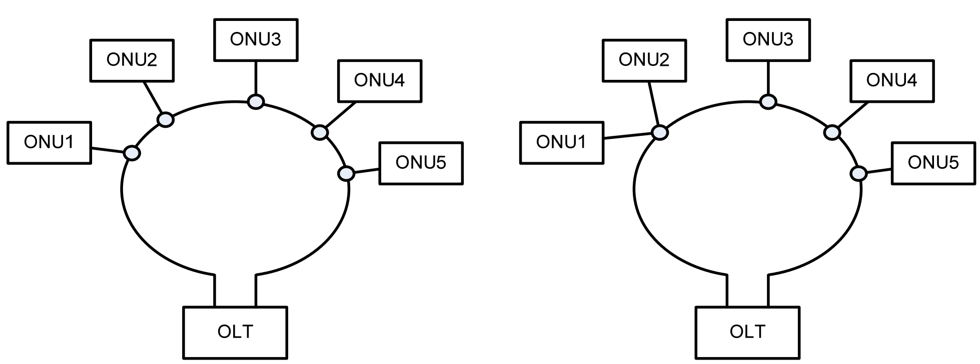

Fig. 3.12: (a)Ring Topology with Redundant Trunk, (b) Ring-Star Topology [JIN07]

3.7 PON/ RoF-PON Topology Models

The following topology models are based on the ITU-T Rec. G.983 standards. The RN consists of a number of AWGs and does not contain any optical monitors or active devices used for this function, so, it is considered as passive optical splitters. On the other side, OLT and ONUs are equipped with those optical monitors who detect any optical power loss due to fiber cuts or optical transmitters' failures. The number of these optical monitors depends on the number of wavelengths deployed on the fiber which terminated at that monitor. Fig. 3.13 illustrates the standard PON/RoF-PON topology that was considered the basis of the models designed to achieve desired survivability.

The survivability models discussed in this dissertation aim the failure related to fiber cuts and not the other source of failures.

In Chapter 4, an analysis base on a defined survivability function which compares these different models is provided. Also, a presentation of the most excellent m-trail designs for those models to achieve the desired survivability using this method is done.

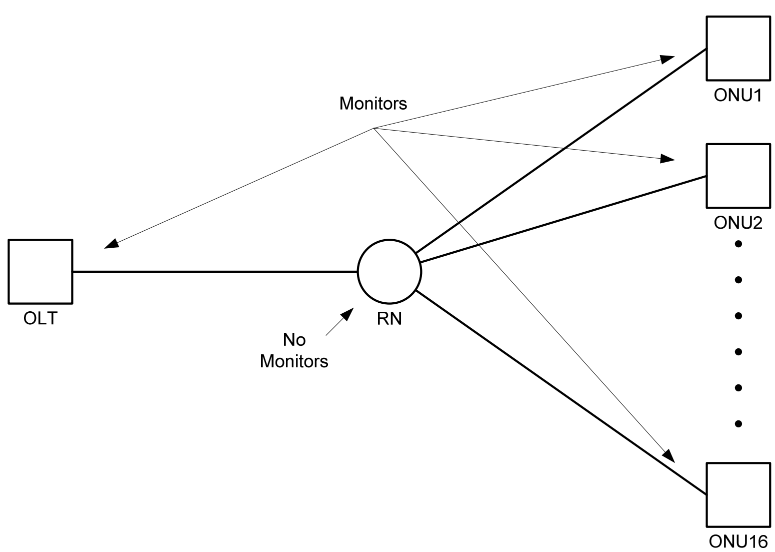

Fig. 3.13: Standard PON/RoF –PON Topology

3.7.1 First PON/ RoF-PON Model

The first PON/ RoF-PON model is the standard topology based on the ITU-T Rec. G.983 as shown in Fig. 3.14.

This model does not provide any kind of protection or restoration against fiber cuts. It should be noted that a fiber cut in the trunk fiber will affect the operation of the entire network while a fiber cut in the branch fiber will affect only the ONU fed by that fiber.

This model was chosen as a benchmark for the analytical survivability function used for the comparison between the different models selected.

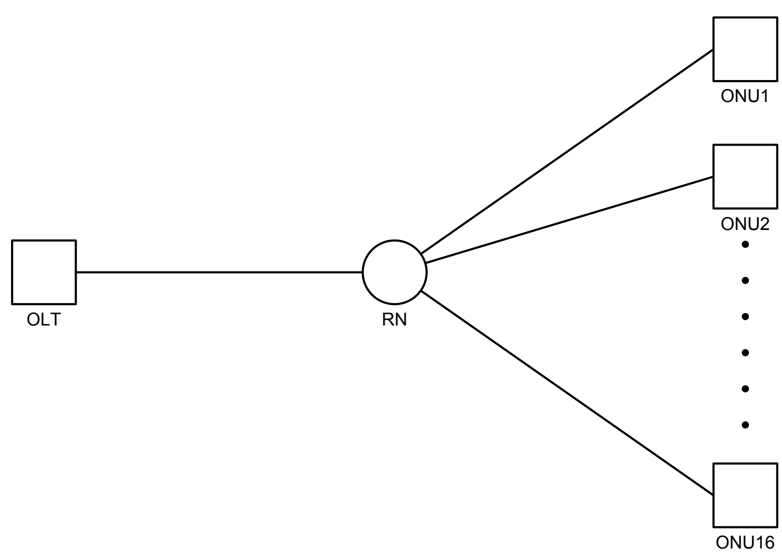

Fig. 3.14: First PON/ RoF-PON Model

3.7.2 Second PON/ RoF-PON Model

Fig. 3.15 shows the second PON/ RoF-PON Model. The trunk fiber is protected by deploying a parallel fiber. This model provides protection for the trunk fiber. By this way, the network can overcome a trunk fiber cut by routing the traffic to the protecting trunk fiber. This model does not provide any protection for any cuts that may happen to the branch fibers. Thus, in the case of any branch fiber cut, the services at the ONU fed by this fiber are disturbed.

This model presents protection by switching architectures suggested by ITU-T G983.1 as discussed earlier.

The protection enhancement of this model over the previous model significantly improved the survivability measures which can be considered as an essential issue in the architecture design.

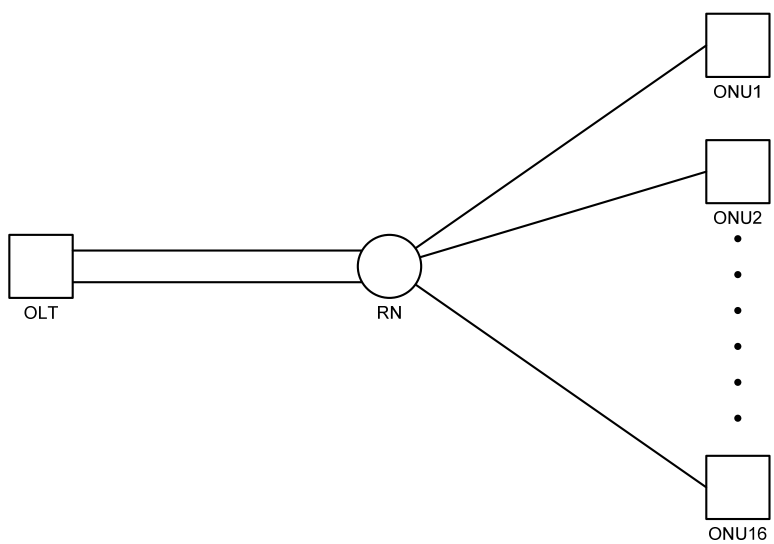

Fig. 3.15: Second PON/ RoF-PON Model

3.7.3 Third PON/ RoF-PON Model

Protecting the trunk fiber has a significant impact on network survivability as discussed previously. This survivability improvement can be enhanced further by replicating the RN.

Fig. 3.16 illustrates the new modification to the network associated with the addition of the other RN.

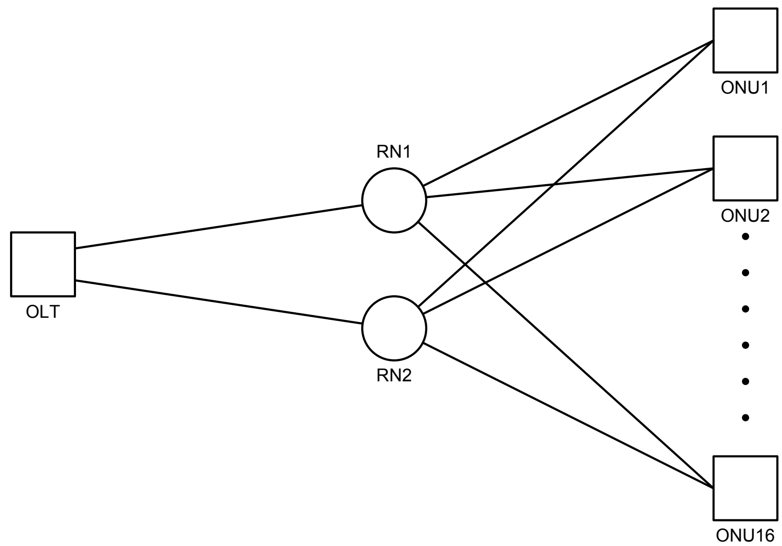

Fig. 3.16: Third PON/ RoF-PON Model

As stated previously, survivability issues are related to the fibers. A group of fiber connections can be deployed in the network to create two parallel architectures between the OLT and ONUs.

3.7.4 Fourth PON/ RoF-PON Model

The architecture in this model adds another layer of survivability. To illustrate that, one may assume that there are multiple fibers cuts; one affects a trunk fiber and another affects a branch fiber. The previously discussed models cannot provide this level of survivability. Only the structure of this model provides this level of survivability.

Fig. 3.17 illustrates the fourth model topology showing the fiber connection between the RNs.

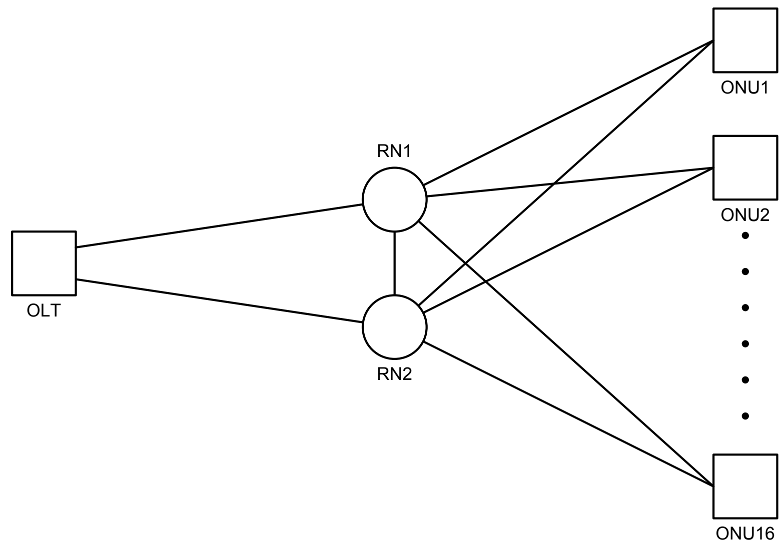

Fig. 3.17: Fourth PON/ RoF-PON Model

Models three and four demonstrate survivability solutions to a branch fiber cut in a situation where ONUs are apart from each other or the connections between them are complicated.

3.7.5 Fifth PON/ RoF-PON Model

This model provides another survivability technique similar to models three and four regarding branch fiber cut. It differs in that it; deals with a case where the ONUs are close to each other. Some examples are high-rise buildings or business centers.

Fig. 3.18 illustrates the fifth PON/ RoF-PON model with protecting fibers connecting the ONUs in a ring configuration.

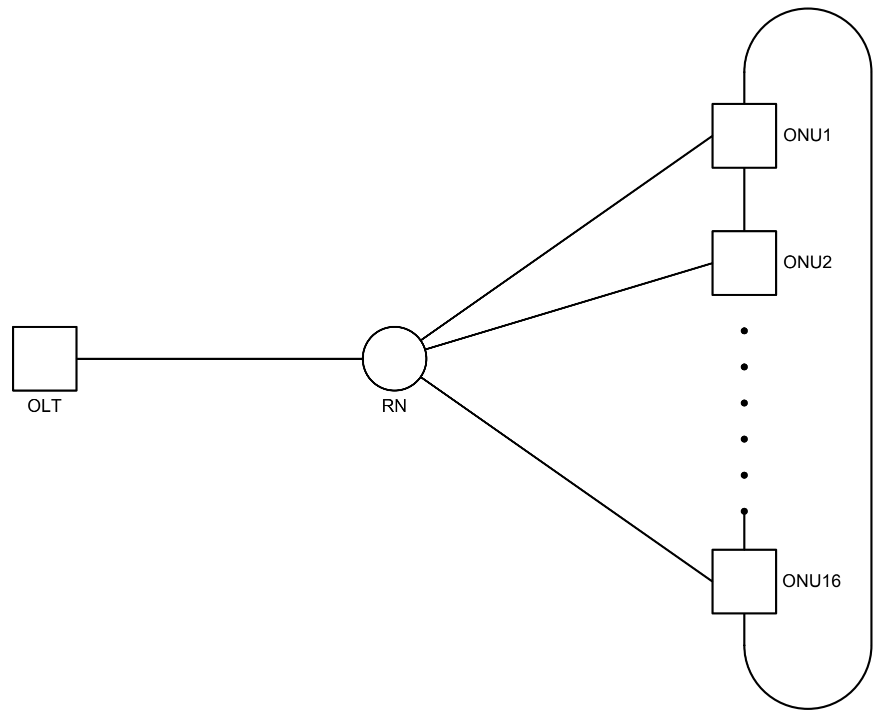

Fig. 3.18: Fifth PON/ RoF-PON Model

3.7.6 Sixth PON/ RoF-PON Model

This model combines the survivability techniques used in the second and fifth models; it provides protection for the trunk fiber so the network can overcome a trunk fiber cut. It does this by routing the traffic to the protecting trunk fiber. That ensures its survivability for a number of branch fiber cuts.

Fig. 3.19 illustrates the sixth PON/ RoF-PON model with protecting fibers connecting the ONUs in a ring configuration. The trunk fiber is protected by deploying a parallel fiber.

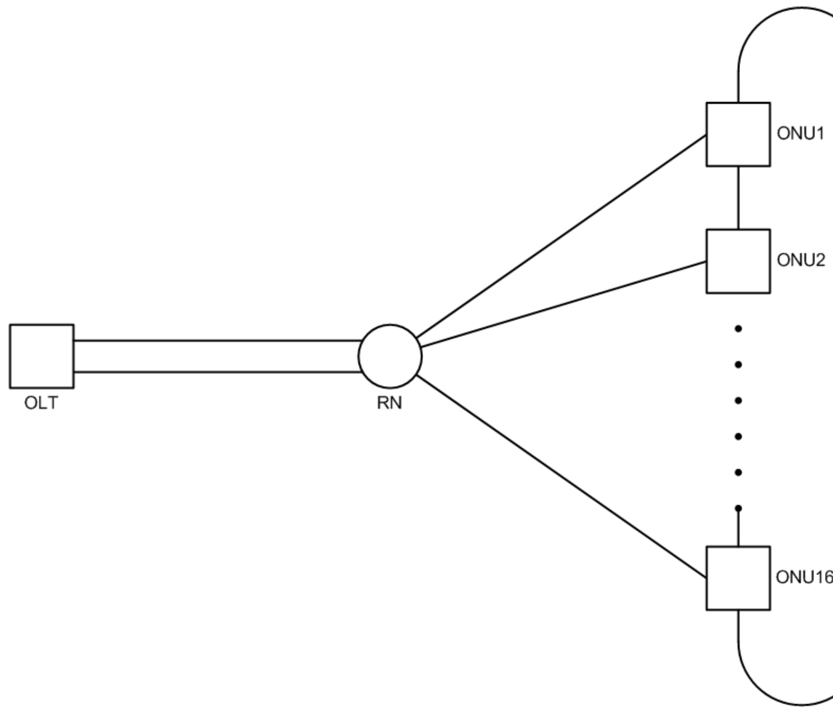

Fig. 3.19: Sixth PON/ RoF-PON Model

3.7.7 Seventh PON/ RoF-PON Model

This model combines the survivability techniques used in the third and fifth models; it provides protection for the trunk fiber and the feeders by replicating the RN. This ensures its survivability for a number of branch fiber cuts.

Fig. 3.20 illustrates the seventh PON/ RoF-PON model with a replicated RN and protecting fibers connecting the ONUs in a ring configuration.

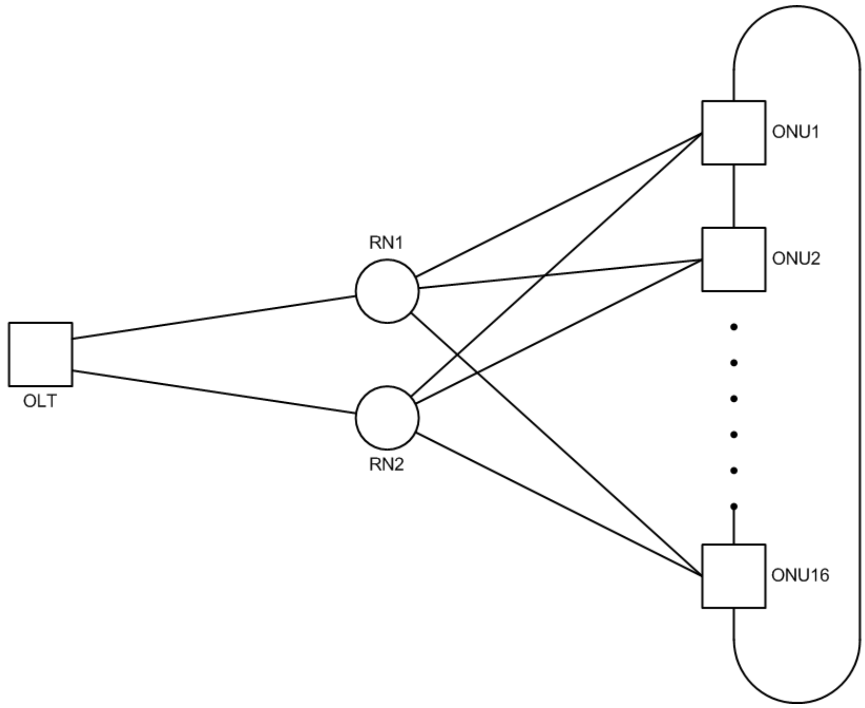

Fig. 3.20: Seventh PON/ RoF-PON Model

3.7.8 Eighth PON/ RoF-PON Model

The architecture in this model provides the ultimate layer of survivability; it gives protection against multiple fibers cuts simultaneously; a cut that affects a trunks fiber, another affects the feeder fibers, and a third cut that affects a branch fiber.

This model combines both survivability techniques used in the fourth and fifth models.

Fig. 3.21 illustrates the seventh PON/ RoF-PON model with a replicated RN, a fiber connection between the RNs, and protecting fibers connecting the ONUs in a ring configuration.

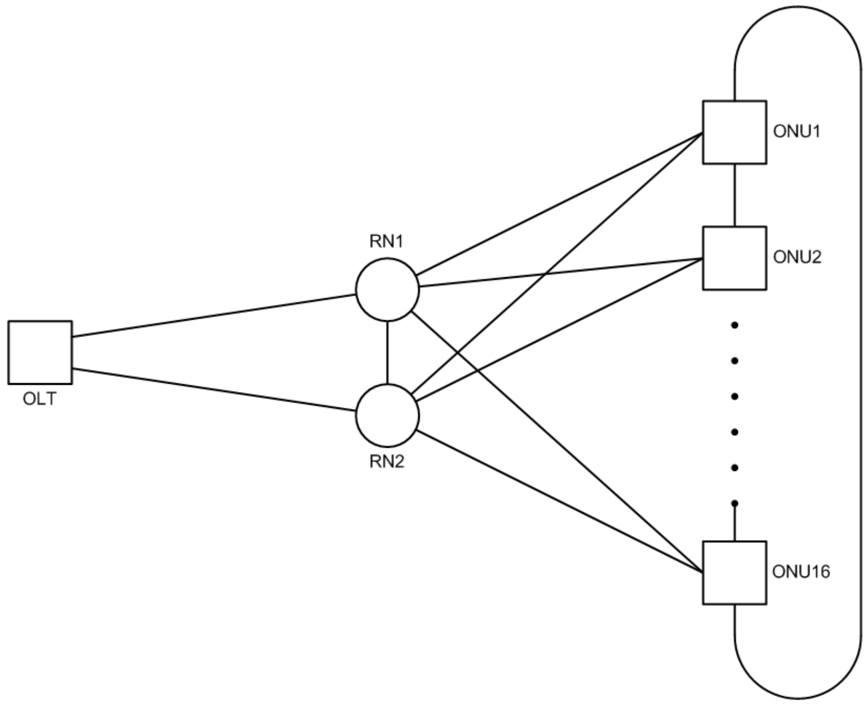

Fig. 3.21: Eighth PON/ RoF-PON Model

3.8 Summary and Concluding Remarks

Fiber to the Antenna (FTTA) is another RoF application where an optical fiber is directly connected to the antenna base with the use of a small simple Optical-to-Electrical (O/E) device. The advantages of this configuration are the reduction of the signal losses due to the small fiber losses, system protection against electrical discharges and lightning strikes, and cost reduction in the devices used at the antenna base station.

The generated RF modulated signal in our proposed RoF-PON model has a frequency of 12.5 GHz at the receiver which is then amplified and transmitted by the antennae. Such a RoF system has simple, cost-effective, and maintenance-reduced BS. In principle, this system is immune to laser phase noise. For the conceptual illustration, a DWDM RoF system with channel spacing of 12.5 GHz is considered. Other frequency spacing may be considered e.g. 25 GHz or 50 GHz. These frequency spacing is according to ITU-T

G.696.1 spectral grid recommendation. Reducing the frequency spacing can cause undesirable effects like Four Wave Mixing (FWM) and Cross Phase Modulation (XPM). 12.5 GHz (KU band) may be considered as a future extension to the current 5.8 GHz frequency for home wireless communication.

PON is exposed to the failure due to its tree topology. In the case of the segment failure, which may occur due to a failure of the feeder fiber or all transportation fibers, all ONUs in the segment lose their connections with the OLT. It is essential to use either protection or restoration schemes to provide network survivability.

ITU-T Rec. G.983.5 specifies two types of protection structural design: 1+1 configuration and 1:1 configuration. Accordingly, there are two models that can be taken into consideration that include protection effect on ONT performance.

A ring topology is known by its survivability characteristics. Using it as a special topology for PON system is considered for this fact.

From the survivability point of view, a ring topology is considered to have better survivability features than both a star and tree topologies. In comparison between a star and tree topologies, the first shows better survivability capability than the later. The main disadvantage of the ring topology is its lack of flexibility as well as updating complexity.

The proposed models for PON/ RoF-PON combine some known designs as well as some just proposed. The pros and cons of each model are described with a comparison between them.

Chapter 4: Deploying Monitoring Trails for Fault Localization in All-Optical Networks

4.1 Introduction

In today's all-optical networks, signals remain in the optical domain from the source to the destination thereby eliminating any O/E and E/O conversion at each intermediate node. In the event of a link failure on the lightpath, only the destination node can detect the power loss or signal degradation. This presents a significant challenge in fault localization.

Optical monitors are an appropriate approach to achieve fault localization in optical networks. As soon as it detects a failure, an alarm signal is generated and disseminated in the control plan. A NMS or any routing entity can make use of this alarm signal to produce fault localization and thus restore the affected traffic in a timely manner. There is a tradeoff between the large number of the alarm signals that provide better fault localization but consumes the bandwidth, and few alarm number but does not give unambiguous failure localization (UFL). UFL for all-optical networks is defined as how quickly and accurately the fault can be localized. The big challenge to achieve a perfect fault localization scheme is to reduce the alarm signal number and to obtain unambiguous failure localization (UFL) [TAP09 and TAP12].

The network provider will benefit from that reduction requirement in the alarm signal number. That reduction leads to an equal reduction in the installed optical monitors and does not overwhelm the NMS engine which makes it faster in performing the fault localization. As stated earlier, that should not be on the expense on the performance of the fault localization algorithm or its accuracy [BAB11].

In general, deploying fault localization by using alarm monitors requires an alarm monitor to be installed in every link. For an optical network having $|E|$ number of links, $O(|E|)$ optical monitors are required. The alarm code length as a result is $|E|$.

As the network link number increases, the number of the required alarm monitors increases. That produces a scalability issues. [ZEN06] and [WU07] in their studies investigates an optical loop-backed route called monitoring-cycle (m-cycle). The pre-configured route launched at the optical supervisory channel (OSC). Each of these m-cycles terminates with an optical monitor that generates an alarm signal in case of a fiber-cut happen to the route [TAP09].

Another brilliant solution to the scalability issues is to establish monitoring-trail (m-trail). Studies conducted in [WEI11a and TAP11] demonstrated that m-trail technique is a generalized form of m-cycle and other monitoring routes that were introduced before. Moreover, m-trails method proves its assurance and accuracy in localizing a single fault in the optical networks [HAD10].

In this chapter, the m-trail design is explored and focusing this research on using m-trails with established lightpaths to achieve fault localization.

4.2 An Overview on Monitoring Trails (M-Trails)

M-trail is a trail-shape optical route that can cross any node several times while it cannot traverse a link more than one time. It is more complicated than a regular optical-path and simpler that an optical-walk [ZEN06].

M-trail is launched in the OSC in a uni-directional route from a transmitting node T to a receiving node D. Fig. 4.1 shows two possible m-trails from T to R. The first possible m-trail is $T \rightarrow a \rightarrow c \rightarrow b \rightarrow a \rightarrow d \rightarrow e \rightarrow R$, and the second is $T \rightarrow a \rightarrow b \rightarrow c \rightarrow a \rightarrow d \rightarrow e \rightarrow R$ [TAP09 and BAB11].

The fault localization solution by deploying m-trails compromises the realization of the m-trails in the OSC.

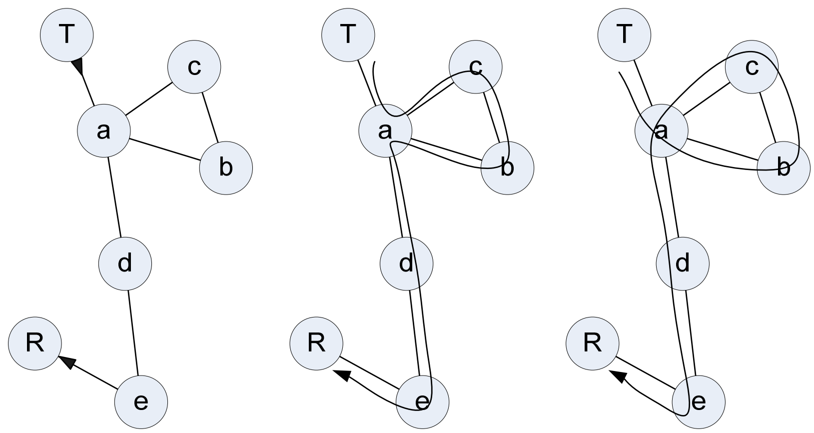

Fig. 4.1: A Possible M-Trail Lightpath

In case of a fiber cut happens to a link in an optical system that deploys m-trail, the optical signals including the m-trails that traverse through OSCs will be disturbed. The monitors that are responsible for those m-trails will trigger alarm signals that disseminate through the control domain and be collected by the NMS [TAP09].

For a set of *J* m-trails, t_1, t_2... t_J, an alarm code [a_1, a_2... a_J] will be produced by the monitors of the m-trail for a fiber cut at that link. The value of a_j = 1 if the monitor of the m-trail t_j generate an alarm signal and a_j = 0 otherwise.

An example of an optical system that deployed m-trails is shown in Fig. 4.2. If a fiber cut is happened at link (2 - 4), the monitors on the m-trails t_1 and t_2 will cause alarm signals. The corresponding alarm code is [1 1 0]. Similarly, if a fiber cut happens at link

(3 - 4), an alarm code [1 1 1] is generated. An alarm code table (ACT) as shown in Table 4.1 can be constructed and provided to the NMS or any routing entity in the network. By correlating an alarm code generated at any given time by the network monitors to the ACT, the failed link can be unambiguously located [TAP09].

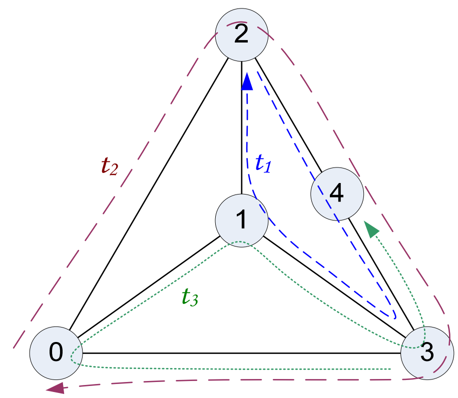

Fig. 4.2: A Possible M-Trail Lightpaths

A simple method of generating m-trails is illustrated in Table 4.1. The different binary combinations from 001 to 111 can construct the m-trails as shown in Fig. 4.2.

Table 4.1: ACT for Network in Fig. 4.2

		Trail		
		t_1	t_2	t_3
Link	0 – 1	0	0	1
	0 – 2	0	1	0
	0 – 3	0	1	1
	1 – 2	1	0	0
	1 – 3	1	0	1
	2 – 4	1	1	0
	3 – 4	1	1	1

In monitoring-trails (m-trails) [TAP09, WU08], optical loop back switching is not allowed. Both m-walk and m-trail can traverse a node multiple times. A simplified variant of m-trail, called monitoring path (m-path), has been suggested in [ALS90] which does not allow loops. The simplicity is at the expense of less flexibility and impaired performance. As the ILP solutions for m-trail allocation problem in [WU10a, WU10b, and WEI11b] are not suitable for large-size networks, [ZHA10] proposed a heuristic which achieves an efficient trade-off between monitor cost and bandwidth cost.

4.3 Deployment of M-Trails

There are two main factors in the m-trail design problem: monitoring expenses and bandwidth usage expenses. Monitoring expenses is categorized under OPEX which reflects the additional NMS functionality needed. It is proportional to the number of m-trail deployed in the network or to the alarm code length. Other charges that add to the monitoring expenses are related to the network down-time which is proportional to the recovery-time. Larger the alarm code is, larger the time the NMS needs to receive and process the entire required alarm signal. Bandwidth consumption expenses are categorized under CAPEX which is the cost of deploying additional wavelengths for the m-trails [TAP09].

[TAP09] presented an m-trail deployment algorithm for a general topology. That algorithm uses random code assignment (RCA), and random code swapping (RCS) to deal with network diversity issues.

4.4 Fault Localization Based on M-Trails

In this and the following sections, an analytical study on the design issues of m-trail deployment in all-optical networks to achieve fault localization is conducted.

Lemma 1: An optical network is said to be fault locatable iff it has a unique error code for every link in it [MAA10b].

Proof: Let us assume that the optical network can locate the faulty link while there are similar alarm codes. As an example, a situation of having two similar alarm codes for two different links. In the case of a failure in one of those links, the NMS receives an alarm code which points to the two links, one is the failed link while the other is the working one (The NMS does not distinguish between the two). As a result, the NMS cannot locate the faulty link. That proves lemma 1 by contradiction.

Lemma 2: An error code of zeros is not to be considered an alarm code as it does not allow monitoring on the corresponding link. There is no detriment if it fails as it does not hold any traffic [MAA10b].

Proof: For an optical network with a graph *G (N, A)*, each of its links has a unique alarm code according to lemma 1. A modified optical network with a graph *G' (N, A')* is formed by adding artificial links to the original graph. The added links have an error code of zeros as there are no wavelengths traversing through them. According to lemma 1, this should not happen as they all have the same alarm code (zeros). To agree with lemma 1, all of these links should be removed from the graph leaving only links that have non-zero alarm codes. That proves lemma 2.

The following section describes a method for establishing m-trails and using them along with established lightpaths to achieve fault localization.

4.5 Using Monitoring Trails (M-Trails) with Established Lightpaths to Perform Fault Localization in All- Optical Networks

Using m-trails with established lightpaths to achieve fault localization in all-optical networks is a superb method as it saves network resources; it reduces the number of the m-trails required for fault localization and accordingly it reduces the number of wavelengths used in the network [MAA10c]. The matrix network is chosen in the following sections as the topology model because it has the following identities:

1. It has a large number of nodes.
2. It is heavily connected.
3. It has high nodal degree (up to four).

4.5.1 Manual Construction of ACT

Provisioning m-trails to perform fault localization is a challenging task. Manual construction of the ACT is the primitive method to do that. Following are the steps of performing that exercise:

STEP 1 *Construct a truth-table with the established network lightpaths N_λ.This is the list of partially assigned alarm codes.*

STEP 2 *Calculate the largest set count of similar alarm code generated in the table N_l.*

STEP 3 *Calculate the number of m-trails needed in addition to the already established lightpaths to have distinct alarm codes N_m by knowing N_l from step 2*

STEP 4 *For the unique partially assigned binary codes, assign "X" to the corresponding N_m bits to complete their alarm codes.*

STEP 5 *From the top of the table, start to assign 1's and 0's to the N_m bits in a binary increasing order.*

STEP 6 *In order to have distinct alarm codes, try to swap between the 1's and 0's of the N_m bits that were assigned in step 5.*

STEP 7 *If step 6 is not enough to produce distinct alarm codes, try to assign 1's to some of the "X" bits to get that.*

STEP 8 *Ensure that the m-trail formed by steps 6 and 7 are continuous and not disconnected routes otherwise repeat them again.*

STEP 9 *Repeat steps 6, 7 and 8 till you have distinct alarm codes then assign 0's to the rest "X" bits.*

Fig. 4.3 shows an example of a simple optical network deploying two lightpaths: λ_1 and λ_2.

Table 4.2 illustrates how to construct an ACT respecting lemmata 1 and 2. "X" denotes the "do not care" term which it can be either 0 or 1 depending on the need to establish the m-trail.

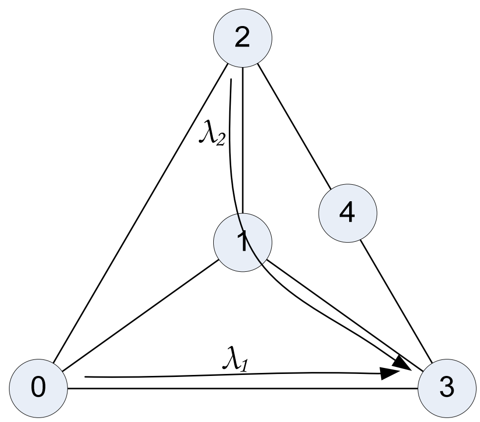

Fig. 4.3: A Simple Optical Network Deploying Two Lightpaths

Table 4.2: ACT of Network of Fig. 4.3 With the Use of "Do not Care Terms"

		Wavelength		Trail			
		λ_1	λ_2	t_1	t_2	t_3	
Link	0 – 1	0	0	0	0	1	
	0 – 2	0	0	0	1	0	
	0 – 3	1	0	X	X	X	
	1 – 2	0	1	X	X	0	
	1 – 3	0	1	X	X	1	
	2 – 4	0	0	0	1	1	
	3 – 4	0	0	1	0	X	→ 1

Table 4.2 helps us to make t_1 and t_2 in its present form while t_3 requires further development. Two possible solutions can be achieved: one by swapping the entry value of link 1-2 and link 1-3, and the other by using the "do not care term" in link 3-4 with a value of 1.

The two sets of m-trails are described in Table 4.3 and illustrated in Fig. 4.4.

Table 4.3: Two Possible M-Trail Sets in the ACT for Network of Fig. 4.3

		Wavelength		Trail Set 1			Trail Set 2		
		λ_1	λ_2	t_1	t_2	t_3	t_1	t_2	t_3
Link	0 – 1	0	0	0	0	1	0	0	1
	0 – 2	0	0	0	1	0	0	1	0
	0 – 3	1	0	0	0	0	0	0	0
	1 – 2	0	1	0	0	1	0	0	0
	1 – 3	0	1	0	0	0	0	0	1
	2 – 4	0	0	0	1	1	0	1	1
	3 – 4	0	0	1	0	0	1	0	1

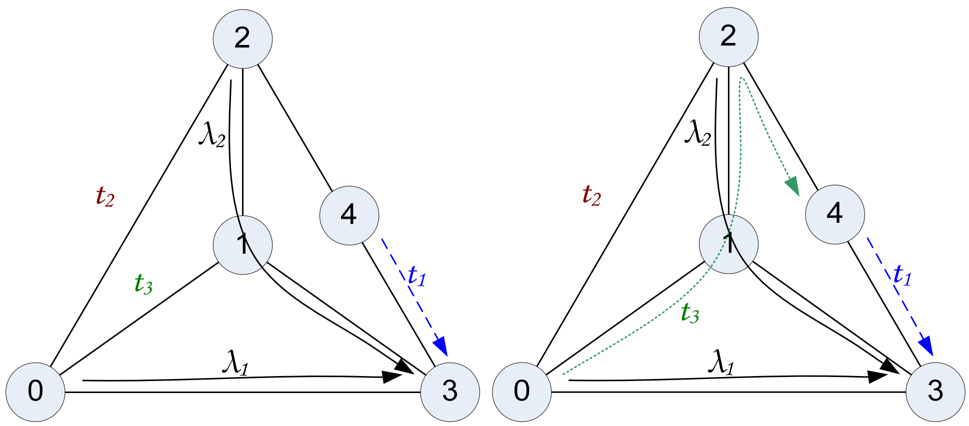

Fig. 4.4: Illustration of The Two Possible Sets of M-Trails of Described in Table 4.3

Another example of a network that deployed three lightpaths is illustrated in Fig. 4.5.

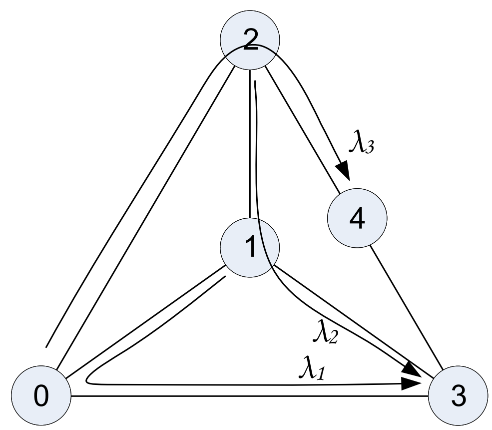

Fig. 4.5: A Simple Optical Network Deploying Three Lightpaths

Table 4.4 illustrates the process of creation of the m-trails with the use of an ACT and the requisite choice of the "do not care term" of t_1 with a value of 1.

Table 4.4: ACT of Network of Fig. 4.5 With the Use of "Do not Care Terms"

		Wavelength			Trail	
		λ_1	λ_2	λ_3	t_1	t_3
Link	0 – 1	1	0	0	0	1
	0 – 2	0	0	1	0	1
	0 – 3	1	0	0	0	0
	1 – 2	0	1	0	0	1
	1 – 3	0	1	0	0	0
	2 – 4	0	0	1	0	0
	3 – 4	0	0	0	X	X

1

A possible selection of m-trails are described in Table 4.5 and illustrated in Fig. 4.6.

Table 4.5: A Possible M-trails in The ACT for the Network of Fig. 4.5

		Wavelength			Trail	
		λ_1	λ_2	λ_3	t_1	t_2
Link	0 – 1	1	0	0	0	1
	0 – 2	0	0	1	0	1
	0 – 3	1	0	0	0	0
	1 – 2	0	1	0	0	1
	1 – 3	0	1	0	0	0
	2 – 4	0	0	1	0	0
	3 – 4	0	0	0	1	0

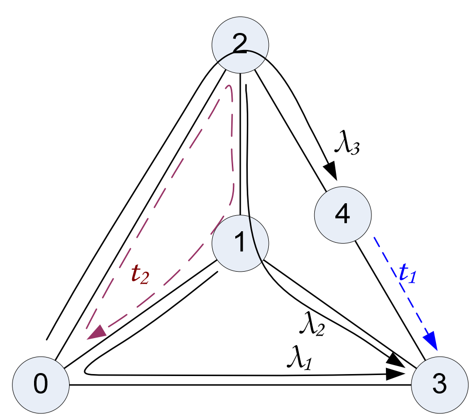

Fig. 4.6: Illustration of Possible M-Trails Described in Table 4.5

4.5.2 Geographic Midpoint Technique

This novel method is based on a method that is used to calculate the geographic midpoint (also known as the geographic center, center of gravity, or center of mass) for two or more points that constitute the graph of the edges requiring construction of a trail to route [MAA11a].

Fig. 4.7 shows an example of that graph of edges. The solid edges represent edges that the trail must pass through and have a value of “1” in the ACT. Those which have a “0” value are truncated so they cannot be used. Those with an “X” value are used by the algorithm if needed.

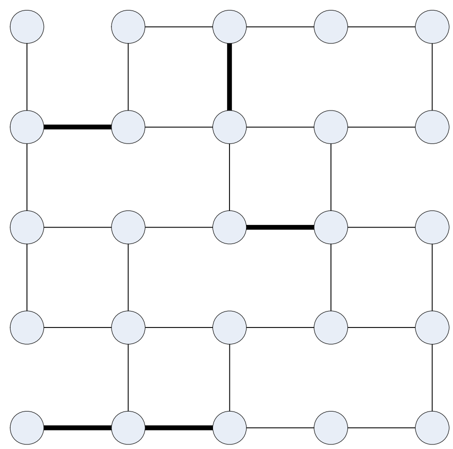

Fig. 4.7: An Example of a Graph of Edges to Construct a Trail

Geographic Midpoint Algorithm can be summarized as follows:

STEP 1	*Identify all n nodes that represent arc ends of the nodes that constitutes the solid edges in G (N, A).*
STEP 2	*Calculate the Geographic Midpoint for these n nodes.*
STEP 3	*Select the two arcs which are the closest to the calculated midpoint*
STEP 4	*Find the pair-wise shortest-paths between the two arc-nodes, that are selected in Step 3, in the graph by using the standard Dijkstra algorithm.*
STEP 5	*Connect the two arcs with the shortest path between their end nodes to form a new arc in the graph.*
STEP 6	*Remove the intermediate nodes of the newly formed arc from the n nodes (calculated in step 1) so that there are n^1 nodes.*
STEP 7	*Repeat steps 2 to 6 until all of the arcs that form the trail are connected.*

An illustration in steps for m-trail formulation is shown in Fig. 4.8.

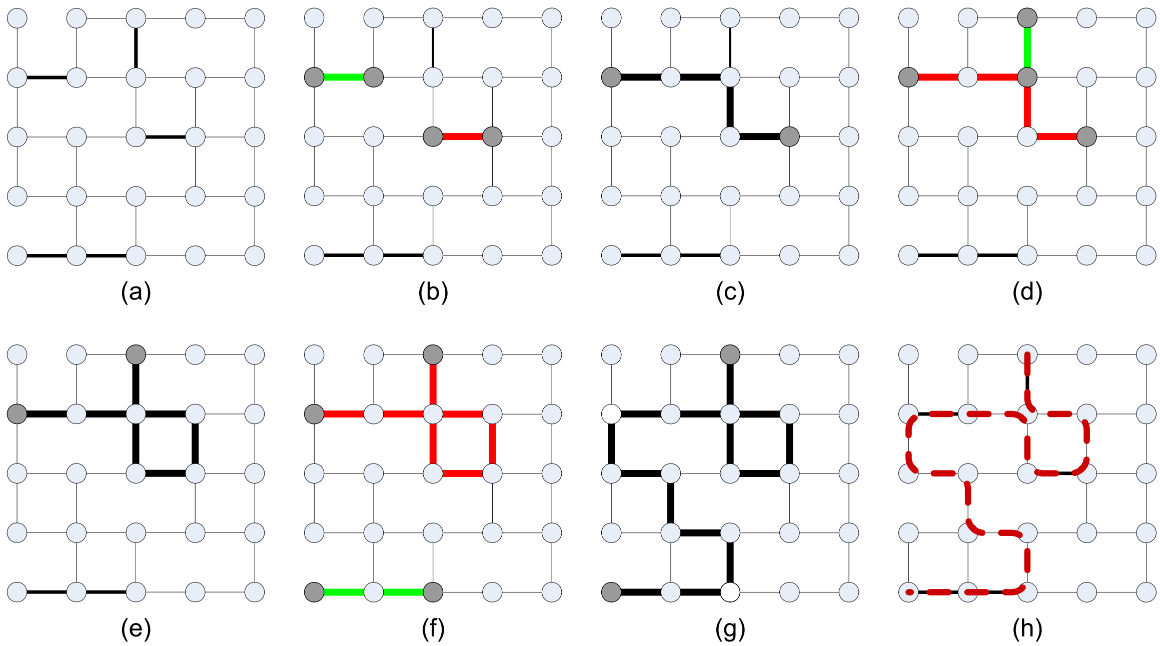

Fig. 4.8: Illustration Steps of M-trail formulation by GMP Algorithm

After the construction of the first trail, the ACT is edited and a new graph is formed ready for the second trail. This process continues until all the required number of trails has been constructed.

4.5.3 Chinese Postman's Problem (CPP) Technique

Chinese postman's problem is the shortest, edge-covering tour-finding problem for a graph *G (N, A)* such that the tour should be connected and undirected. [PAP76] showed that this problem related to the NP-complete category such as it is extremely difficult to find a polynomial-time algorithm to solve it.

The CPP solution is to develop a route that will cover every edge of *G* at least once and for which the sum:

$$\sum_{all(i,j)\in A} n(i,j)l(i,j) \text{ is minimum} \quad \ldots \quad (4.2)$$

as *n(i, j)* is the number of times edge *(i, j)* is traversed and *l(i, j)* is the distance length of the edge *(i, j)*. An algorithm to solve the Chinese Postman Problem for an undirected graph is described in [LAR81] as follows:

STEP 1	*Identify all odd-degree nodes in G (N, A). Say there is m number of them, where m is an even number.*
STEP 2	*Find a shortest pair-wise matching of the m odd-degree nodes and identify the m/2 shortest paths between the two nodes composing each of the m/2 pairs.*
STEP 3	*For each of the pairs of odd-degree nodes in the minimum-length pair-wise matching found in Step 2, add to the graph G(N, A) the edges of the shortest path between the two nodes in the pair. The graph G^1 (N, A^1) thus obtained contains no nodes of odd degree.*
STEP 4	*Find an Euler tour on G^1 (N, A^1). This Euler tour is an optimal solution to the Chinese Postman's Problem on the original graph G (N, A). The length of the optimal tour is equal to the total length of the edges in G (N, A) plus the total length of the edges in the minimum-length matching.*

The algorithm adds carefully artificial edges parallel to the existing ones in the original graph *G* to create a new graph G^1 *(N, A^1)*. The purpose of this addition is to convert all odd-degree nodes that exist on *G* into even-degree nodes on the new G^1. Consequently, an Euler tour can be found on the new graph. The desired shortest tour will be exercised on the modified graph which compromises the added artificial edges and the original graph edges. The resulting solution, therefore, may involve visiting some nodes twice [LAR81].

For the new graph G^1, since a pair-wise matching for a set N^1 is a subset of another set *N* in the original graph *G* ($N^1 \subset N$), the set *N* a pairing of all the nodes in the original graph *G*. Consequently, the shortest pair-wise matching of the nodes in the new graph G^1 is then a shortest pair-wise matching in the original graph *G*. That proves that the shortest-paths total distance between the paired nodes is the smallest. Since this algorithm finds the optimal matching, is it considered as an “exact” solution that could be implemented by an efficient computer in a time proportional to n^3 or $O(n^3)$, where n is the graph node number. Another observation to the algorithm is that it also recognizes the shortest path for each pair [LAR81].

The artificial parallel edges are the shortest pair of node-disjoint or vertex-disjoint paths between those two nodes. The determination of optimal pairs of disjoint paths is described in detail in [BHA99] using either the modified Dijkstra algorithm or the Breath First Search (BPS) shortest path algorithm. Another algorithm developed by Suurballe [SUU74 and SUU84] for disjoint paths construction is realized by using an unusual graph transformation that permits the use of the standard Dijkstra algorithm.

Due to the fact that the algorithm described above requires the postman to start and end on the same depot, an artificial depot may be added to the graph and connected to all nodes. This depot must be very far from the network graph for the following reasons:

- To be equidistant from all nodes,
- To prevent the algorithm from using the new generated edges from this artificial depot to the graph nodes as part of the targeted route and,
- To allow the solution be unbiased toward any node if it is chosen as the depot.

4.5.4 The Traveling Salesman Problem (TSP) Technique

TSP is the most primitive node-covering problem. It has been studied and analyzed for decades. The original statement of the problem is: “start from a specific node, which is called depot, visit all the network nodes at least once, and return to the starting node (depot)”. The most commonly used statement differs from the original in that: the network nodes should be visited only once which produce more restrictions on the solution.

TSP is related to a NP-complete category such as it is extremely difficult to find a polynomial-time algorithm to solve it [LAR81].

Although this problem is particularly important in graph routing applications, there are two variants having the same or more importance: vehicle routing and machine scheduling problems.

TSP is considered to be the benchmark in any evaluation/ comparison of a new combinatorial optimization for routing algorithms.

[GOL76] reviews several heuristic algorithms for TSP with a comparison between their performances.

Following is a heuristic algorithm described in [CHR76] for Euclidean TSP[1] (TSP's with Euclidean tour metrics). Consider n points that must be traversed by a TSP[1] tour (symmetric distances, complete connectivity, and triangular inequality). Then we have:

STEP 1	*Find the minimum spanning tree that spans the n points. Call this minimum spanning tree T.*
STEP 2	*Let No. of the n nodes of T be odd-degree nodes (n is always an even number). Find a minimum-length pair-wise matching of these nodes, using a matching algorithm. Let the graph consisting of the links contained in the optimal pair-wise matching be denoted as M. Create a graph H consisting of the union of M and T ($H = M \cup T$). Note that if one or more links are contained in both M and T. these links will appear twice in H.*
STEP 3	*The graph H is an Eulerian graph, since it contains no odd-degree nodes. Draw an Eulerian circuit on H (beginning and ending at the starting node of the sought-after TSP tour, if such a starting node has already been specified). This Eulerian circuit is the (approximate) solution to the TSP.*
STEP 4	*(Optional): Check for nodes of H (points) that are visited more than once in the Eulerian tour and improve the traveling salesman tour of Step 3 by taking advantage of the triangular inequality.*

The route produced by the above heuristic algorithm guarantees that it is less than 50 percent longer than the optimal *O (1+0.5)*. This is the best "worst-case performance" that can be got from any TSP efficient algorithm developed so far [LAR81]. Typical implementations of a variety of algorithms verified the difficulties of getting a solution that goes above 10 percent worse than the optimal route [LAR81].

In order to use the algorithm mentioned above, which is a node-covering in the problem, we must create artificial nodes should be created and located at the middle of each edge in the graph. In order to establish a trail, a route should traverse the edges as illustrated in Fig. 4.9.

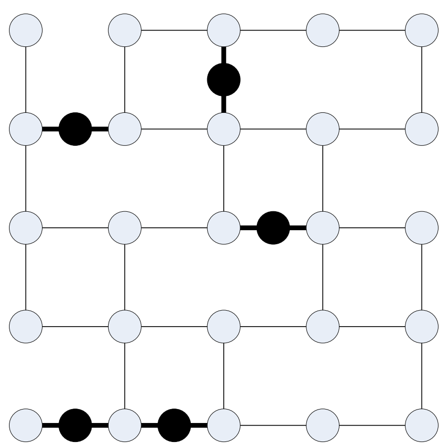

Fig. 4.9: Artificial Nodes of The Edges That Requires a Trail to Visit Them

As the algorithm described above requires that the salesman starts and ends at the same depot, an artificial depot may be added to the graph and connected to all nodes. This depot needs to be very far from the network graph for the following reasons:

- To be equidistant from all nodes,
- To prevent the algorithm from going back to the artificial depot nodes as part of the targeted route and,
- To allow the solution be unbiased to any node if any is select as the depot.

4.6 Summary and Concluding Remarks

M-trail design problem intended to reduce monitoring expenses and bandwidth usage expenses. Monitoring expenses is categorized under OPEX which reflects the additional NMS functionality needed. It is proportional to the number of m-trail deployed in the network or to the alarm code length. Other charges that add to the monitoring expenses are related to the network down-time which is proportional to the recovery-time. Larger the alarm code is, larger the time the NMS needs to receive and process the entire required alarm signal. Bandwidth consumption cost is categorized under CAPEX which is the cost of deploying additional wavelengths for the m-trails

Using m-trails with established lightpaths saves network resources. It reduces the number of the m-trails required for fault localization and therefore the number of wavelengths used in the network.

Manual construction of ACT is a simple and a straight-forward method of determining the m-trail and it can lead to satisfactory results, but it is time-consuming and requires a lot of skill.

The GMP novel method is based on a technique used to calculate the geographic midpoint for two or more points that constitute the graph of the edges requiring the production of a trail to route.

A modification is introduced to the original Chinese Postman's problem because the original algorithm requires the postman to start and end at the same depot. It is done by adding an artificial depot may be added to the graph and connected to all nodes.

As the original Traveling Salesman Problem is node-covering while the m-trail design problem is edge-covering, a modification to the TSP is done by creating artificial nodes that will be located at the middle of each edge in the graph. Another modification to the original Traveling Salesman Problem (which is node-covering) to use it in the m-trail design problem, this is done by creating artificial nodes that will be located at the middle of each edge in the graph.

Chapter 5: Analysis and Performance Evaluation

5.1 Introduction

In this chapter, analysis and the performance evaluation of the deployment of the m-trail fault localization survivability concept in all-optical networks, as well as PON networks, is presented. The proposed RF-PON system design is also investigated.

5.2 M-Trails Deployment

In the design of all-optical networks, one of the main targets is to minimize the CAPEX and OPEX. Costs may be considered as the total of bandwidth costs (CAPEX) and survivability costs (OPEX). Survivability costs, in the case of the deployment of m-trails as a survivability technique, are related to the alarm monitoring and m-trail bandwidth costs. The monitoring costs are mainly due to the fault management difficulties in terms of alarm code length. It can also be viewed as the additional monitoring deployment cost. Other than the increase in fault management cost, a longer alarm code could cause a longer failure recovery time as the network node has to collect all the required alarm signals to make an accurate failure localization decision. The bandwidth cost is due to the extra bandwidth used for monitoring, for which the total length of each m-trail is considered.

5.2.1 M-Trails Deployment - Problem Definition

The goal of m-trail design is to reduce the linear combination of both monitoring cost and bandwidth cost. The target function can be written as follows [WU09]:

Total Cost = *monitoring cost* + *bandwidth cost*.. *(5.1)*

Lemma 1: An optical network is said to be fault-locatable iff it has a unique error code for every link in it.

Lemma 1 states that each link must have a unique binary alarm code [a_1, a_2,..., a_J], where J is the length of the alarm code, and a_j is a binary digit, which is 1 if the j_{th} m-trail passes through this link and 0 otherwise.

Lemma 2: An error code of zeros is not to be considered an alarm code as it does not allow monitoring on the corresponding link. There is no detriment if it fails as it does not carry any traffic [MAA10b].

The m-trail t_j should traverse through all the links that have $a_j = 1$ and should not do that if $a_j = 0$. Let Lj denote the j^{th} link set which contains the set of links with $a_j = 1$; thus, to form t_j, one must find a trail that traverses only through all the links in Lj and not any others.

The m-trail design problem seeks to find a set of m-trails in the network with minimized cost as in Equation (5.1), such that a network element can unambiguously localize any single failure event by reading the alarm code collected from the monitors. The alarm code assignment on each link and m-trail formation is an extremely important task that should be subject to a joint design. A valid m-trail design can only be achieved through a manipulative interplay of the two tasks, which makes the m-trail design problem challenging, yet interesting [TAP09].

5.2.2 M-Trails Deployment - Network Topology Diversity

Network topology diversity has a significant impact on the design, development, and deployment of various network algorithms and protocols. Without exception, m-trail solutions are significantly affected by network topologies [TAP09].

The connectivity of a network topology is defined in terms of average nodal degree. While the ring topology is the most sparsely connected, the fully meshed topology is the most densely connected. Table 5.1 summarizes the average values of the nodal degree and the number of links for ring and fully meshed topologies.

Table 5.1: Ring and Fully Meshed Topologies Average Nodal Degree and Number of Links

	Ring topology	Fully meshed topology
Nodal Degree	*2*	$\|V\|-1$
Number of links $\|E\|$	$\|V\|$	$\frac{\|V\|(\|V\|-1)}{2}$

5.2.3 M-Trail Formation – Bound Analysis

The bounds on the minimum number of m-trails required to meet the UFL requirement are of interest because they can give us a clear picture of the overhead of network fault management for failure localization. An m-trail solution is significantly affected by network topology diversity and connectivity [TAP09].

Theorem 1: In any two-connected network (e.g. A ring network of more than 4 nodes), the UFL requirement can always be achieved with no more than $\lceil |E|/2 \rceil$ *m-trails for UFL* [TAP09].

Minimum CodeWord $J = \lceil |E|/2 \rceil$ ………………………………………………………………. *(5.2)*

Theorem 2: A fully meshed topology needs no more than $6 + \lceil \log_2(|E|+1) \rceil$ *m-trails to achieve UFL* [TAP09 and WU11b].

Minimum CodeWord $J = 6 + \lceil \log_2(|E|+1) \rceil$ ……………………………………………… *(5.3)*

Theorem 2 gives an upper bound on the minimum number of m-trails required for UFL in a fully meshed topology. The theorem is proved by means of a deterministic polynomial time construction that generates a valid m-trail solution for a fully mesh topology with $6 + \lceil \log_2(|E|+1) \rceil$ m-trails.

Theorem 3: The number of m-trails N_m needed, in addition to the already established lightpaths, to achieve fault localization in optical networks is given by [MAA10b]:

$$N_m = \lceil \log_2(N_l) \rceil = \lfloor \log_2(N_l) \rfloor + 1 \quad (5.4)$$

as N_l is the largest set count of similar alarm code generated only by lightpaths.

Proof: In an optical network that has N_l similar alarm codes generated by the network wavelengths which are carrying customer traffics, to distinguish between these alarm codes according to lemma 1, one need to add more bits to them with different binary combination values. The number of bit represents the number of m-trails N_m needed, in addition to the already established lightpaths, to achieve fault localization which is equivalent to the RHS of Equation (5.4).

Minimum CodeWord $J = N_m\big|_{\min} + N_\lambda$ ……………………………………………… *(5.5)*

as N_λ is number of wavelength used before establishing the m-trails and

$$N_l\big|_{\min} = |E| - 2^{(N_\lambda - 1)} \quad (5.6)$$

Fig. 5.1 shows CodeWord Length vs. number of nodes with and without the use of the network traffic-carried wavelengths in the m-trail survivability solution.

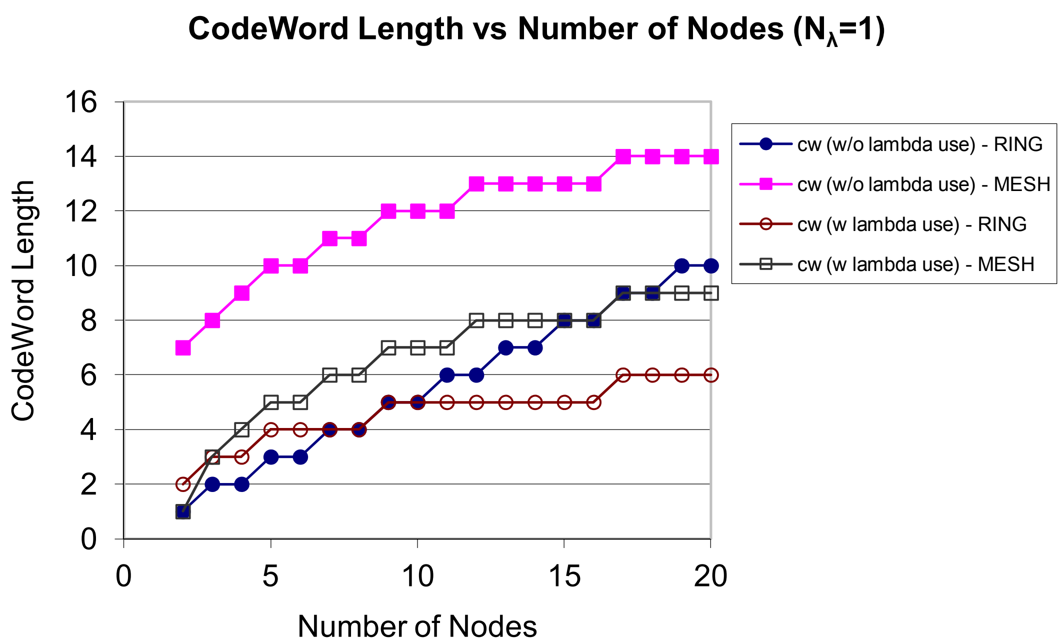

Fig. 5.1: CodeWord Length vs. Number of Nodes

5.2.4 M-Trail Design – ILP Formulation

In this section, the ILP formulation for the m-trail design problem is presented. The analysis is based on the work done by [WU08]. Following is the modified analysis that reflects the design needs.

The following notations are used in the ILP formulation:

E: The set of network links

V: The set of network nodes

N_l : The largest set count of similar alarm code generated only by lightpaths

N_m: The number of m-trails needed in addition to the already established lightpaths)

J: The maximum number of m-trails permitted in the solution

j: m-trail index where $j \in \{1,....., J\}$

c_{uv}: The expenditure of a supervisory wavelength on link (u,v)

c_m: The expenditure of a monitor

δ : A pre - assigned small positive value $((|V| \cdot (|V|-1))/2 \le \delta > 0)$ that presents the step of the minimum voltage increase along the m-trail.

β : A predefined small positive value $(0 < \beta \le 2^{-j})$

l_{uv}^{j} : Binary variable that takes 1 if $u \rightarrow v$ is a vector of m-trail t_j and 0 otherwise

m^j : Binary variable that takes 1 if t_j is a m-trail monitor and 0 otherwise

s_u^j : Binary variable that takes 1 if node u is the source of m-trail t_j and 0 otherwise

d_u^j : Binary variable that takes 1 if node u is the sink of m-trail t_j and 0 otherwise

z_u^j : Binary variable that takes 1 if node u is traversed by m-trail t_j and 0 otherwise

e_{uv}^{j} : A fractional variable that presents the vector voltage $u \rightarrow v$ on m-trail t_j and 0 otherwise.

a_{uv}: A general integer variable that presents the decimal alarm code assigned to link *(u,v)*.

f_{uv}^{xy} : Binary variable such that: for two distinct links (u,v) and (x,y), it takes 1 if $a_{uv} > a_{xy}$ and 0 otherwise.

The target function in Equation (5.1), for a given a topology *G (V, E)* with the parameters c_{uv}, c_{vu} , c_m *J*, δ and β, may create the following ILP which produce at most *J* m-trails:

Objective:

$$\text{Minimize}\left\{c_m \sum_j m^j + \sum_j \sum_{(u,v)\in E} \left(c_{uv} \cdot l_{uv}^{j} + c_{vu} \cdot l_{vu}^{j}\right)\right\} \quad \text{..} \quad (5.7)$$

Subject to:

$$\sum_{u \in V} s_u^j = 1, \qquad \forall j \;\ldots\ldots\ldots\ldots\ldots\ldots\ldots\ldots\ldots\ldots \quad (5.8)$$

$$\sum_{u \in V} d_u^j = 1, \qquad \forall j \;\ldots\ldots\ldots\ldots\ldots\ldots\ldots\ldots\ldots\ldots \quad (5.9)$$

$$\sum_{v \in E} \left(l_{uv}^j - l_{vu}^j \right) = s_u^j - d_u^j, \qquad \forall u \in V, \forall j \;\ldots\ldots\ldots\ldots\ldots\ldots \quad (5.10)$$

$$l_{uv}^j + l_{vu}^j = 1, \qquad \forall (u,v) \in E, \forall j \;\ldots\ldots\ldots\ldots\ldots \quad (5.11)$$

$$z_u^j = \left(l_{uv}^j + l_{vu}^j + s_u^j + d_u^j \right) / 2, \qquad \forall u \in V : (u,v) \in E, \forall j \;\ldots\ldots\ldots \quad (5.12)$$

$$\delta \le e_{uv}^j \le l_{uv}^j, \; \delta \le e_{vu}^j \le l_{vu}^j \qquad \forall (u,v) \in E, \forall j \;\ldots\ldots\ldots\ldots\ldots \quad (5.13)$$

$$d_u^j + \sum_{(u,v) \in E} \left(l_{uv}^j - l_{vu}^j \right) \ge \delta \times z_u^j, \qquad \forall u \in V, \forall j \;\ldots\ldots\ldots\ldots \quad (5.14)$$

$$\sum_j m^j \ge \left\lfloor \log_2 \|E\| \right\rfloor + 1 \;\ldots\ldots\ldots\ldots\ldots\ldots\ldots\ldots\ldots\ldots \quad (5.15)$$

$$c_m \sum_j m^j + \sum_j \sum_{(u,v) \in E} \left(c_{uv} \cdot l_{uv}^j + c_{vu} \cdot l_{vu}^j \right) \ge \left(N_m \big|_{\min} + N_\lambda \right) \cdot \left(c_m + \sum_{(u,v) \in E} \left(c_{uv} + c_{vu} \right) \right). \quad (5.16)$$

$$m^j = \sum_j d_u^j, \qquad \forall j \;\ldots\ldots\ldots\ldots\ldots\ldots\ldots\ldots\ldots\ldots \quad (5.17)$$

$$\alpha_{uv} = \sum_j 2^j \left(l_{uv}^j + l_{vu}^j \right), \quad \forall (u,v) \in E \;\ldots\ldots\ldots\ldots\ldots\ldots\ldots\ldots \quad (5.18)$$

$$\alpha_{uv} \ge 1, \qquad \forall (u,v) \in E \;\ldots\ldots\ldots\ldots\ldots\ldots\ldots\ldots\ldots\ldots \quad (5.19)$$

$$\beta + \beta \left(\alpha_{uv} - \alpha_{xy} \right) \le f_{uv}^{xy}, \quad \forall (u,v),(x,y) \in E : (u,v) \ne (x,y) \;\ldots\ldots\ldots\ldots \quad (5.20)$$

$$\beta + \beta \left(\alpha_{xy} - \alpha_{uv} \right) \le 1 - f_{uv}^{xy}, \quad \forall (u,v),(x,y) \in E : (u,v) \ne (x,y) \;\ldots\ldots\ldots\ldots \quad (5.21)$$

The objective function in Equation (5.7) minimizes both the monitoring and the bandwidth costs.

The constraints in Equations (5.8) and (5.9) allow only one source and one destination for every m-trail t_j.

The constraint in Equation (5.10) formulates flow conservation. Fig. 5.2 illustrates that the number of inbound vectors must equal to the number of outbound vectors unless the node is a source or a destination.

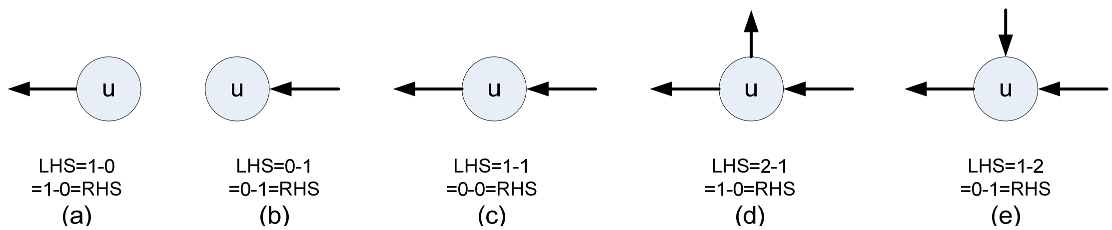

Fig. 5.2: Flow Conservation Constraint

The constraint in Equation (5.11) allows only one vector of the m-trail t_j on each link (u, v). This constraint agrees with the principle definition of the m-trail.

The constraint in Equation (5.12) verifies that if a node has an inbound or outbound vector on t_j, the m-trail t_j must traverse this node as shown in Fig 5.3.

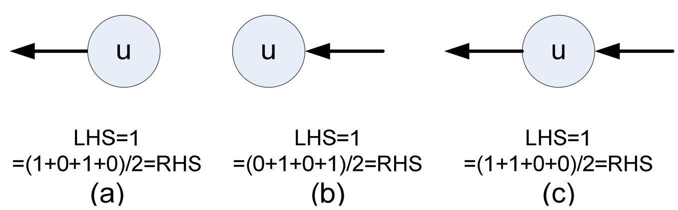

Fig. 5.3: Node Traversed Constraint

The constraint in Equation 5.13 presents the directed graph voltage rules. It states that every vector should have a unique non-zero voltage value. Fig. 5.4 illustrates two graph voltage rules: (a) a route has a step increase along its vectors; (b) a cycle, which is a route with both the source and destination in one node.

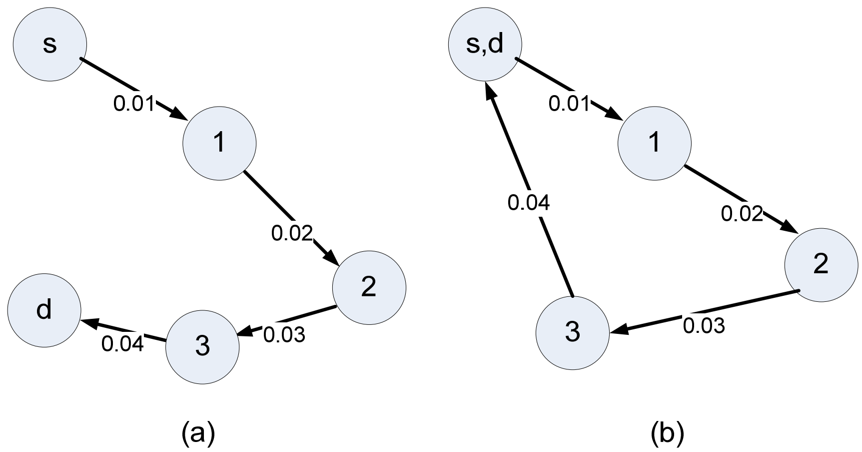

Fig. 5.4: Two Graph Voltage Rules

The voltage constraint is governed by the constraint in Equation 5.14. The outbound vector voltage value is one step more than the inbound vector voltage value. The only exception to that is the destination node that has inbound vector but no outbound.

The constraint in Equation (5.15) gives the lower bound for the required number of m-trails.

The constraint in Equation (5.16) gives the lower bound for both the monitoring and bandwidth costs.

The constraint in Equation (5.17) correlates the monitor of a m-trail t_j to the destination node.

The constraint in Equation (5.19) does binary to decimal conversion to the alarm codes.

The constraint in Equation (5.20) prevents zero alarm codes.

The constraints in Equations (5.21) and (5.22) ensure unique alarm codes provided by the solution which guarantees unambiguous link failure localization.

5.2.5 M-trail Optimized Solution

The optimized solution for the m-trail construction of a network with already established lightpaths is carried out by the student version of FICO Xpress Mosel optimizer version 3.2.3 with the following run data:

- Gap to optimality is 1.43%
- Number of constraints is 143799

Fig. 5.5 show the optimized solution for the 4x4 matrix networks given earlier. The trail solution has 9 hops.

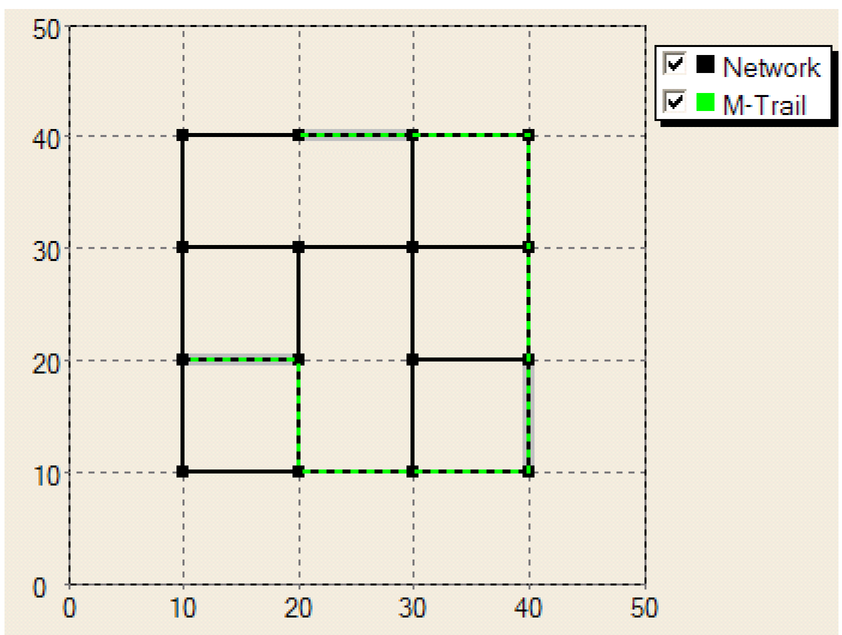

Fig. 5.5: Optimized Solution for the 4x4 Matrix Network

Fig. 5.6 shows the optimized solution for the 5x5 matrix networks given earlier. The trail solution has 11 hops.

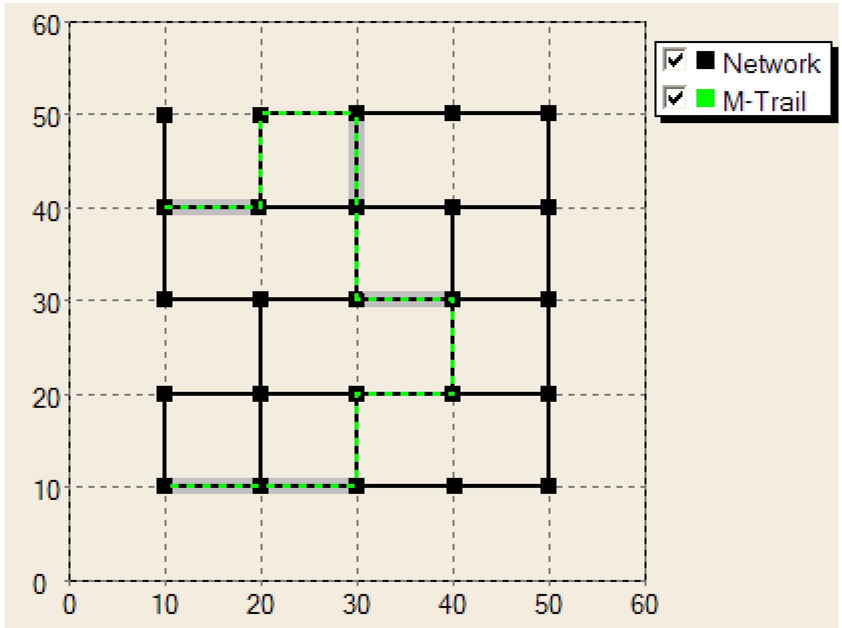

Fig. 5.6: Optimized Solution for the 5x5 Matrix Network

Fig. 5.7 shows the optimized solution for the 6x6 matrix networks given earlier. The trail solution has 13 hops.

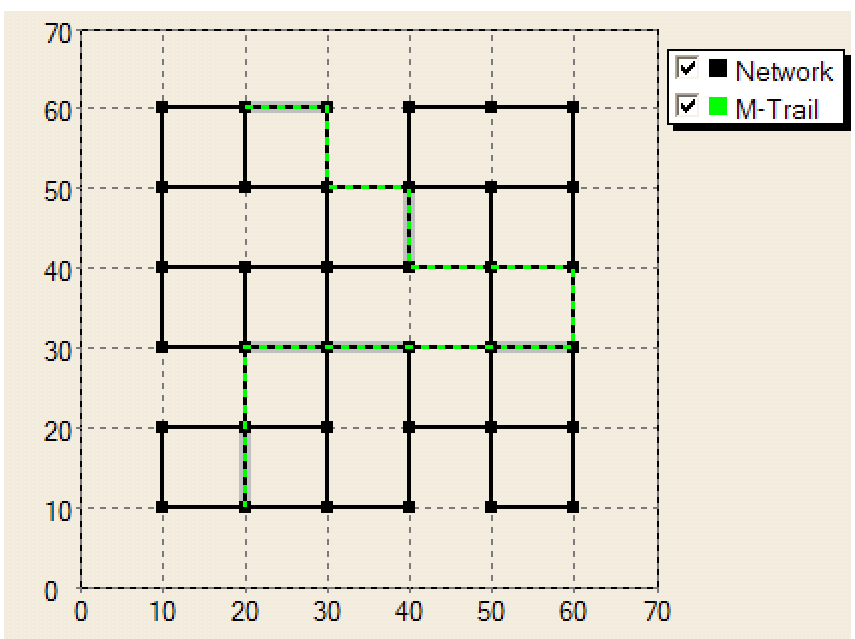

Fig. 5.7: Optimized Solution for the 6x6 Matrix Network

5.2.6 M-Trail Different Solutions

The different solutions described in Chapter 4 for the m-trail construction of a network with lightpaths that are already established are illustrated in Table 5.2 in comparison with the optimized solution. This illustration represents both the adapted TSP and CCP, and the GMP solutions of 4x4, 5x5 and 6x6 matrix networks. The number of hops is calculated for each solution.

Pearson correlation coefficient $\rho = 0.997949$ is obtained between GMP and the optimal solution.

A comparison of these solutions for various matrix networks based on the number of hops is shown in Fig. 5.8.

Table 5.2: Illustration of TSP (adapted), CCP (adapted) and GMP Solutions of 4x4, 5x5 and 6x6 Matrix Networks

Network Topology	GMP	CPP	TSP	Optimal
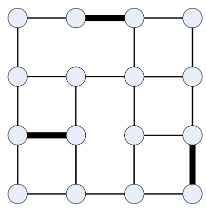 4X4	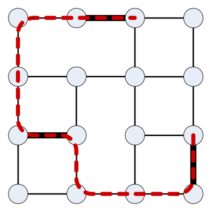 9 hops	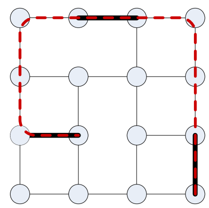 9 hops	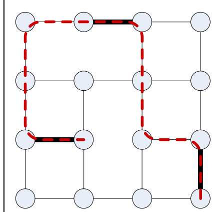 9 hops	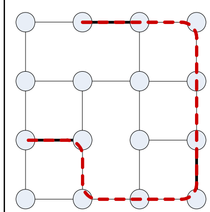 9 hops
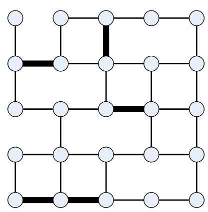 5x5	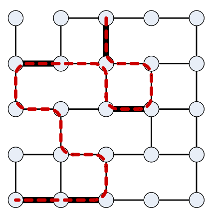 14 hops	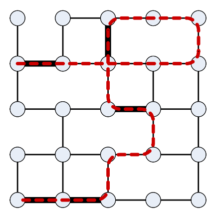 15 hops	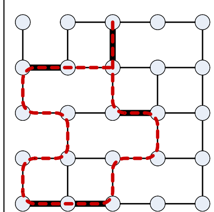 15 hops	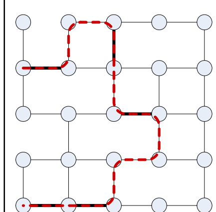 11 hops
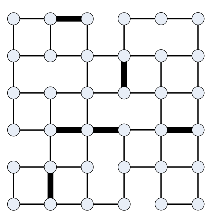 6x6	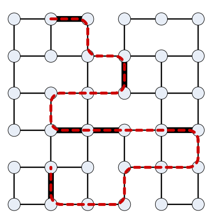 18 hops	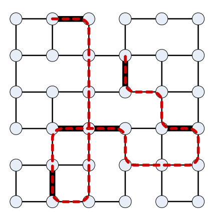 19 hops	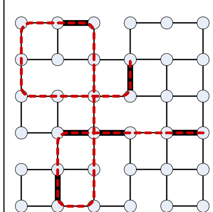 20 hops	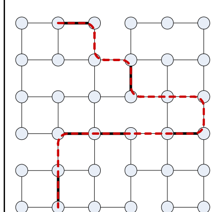 13 hops

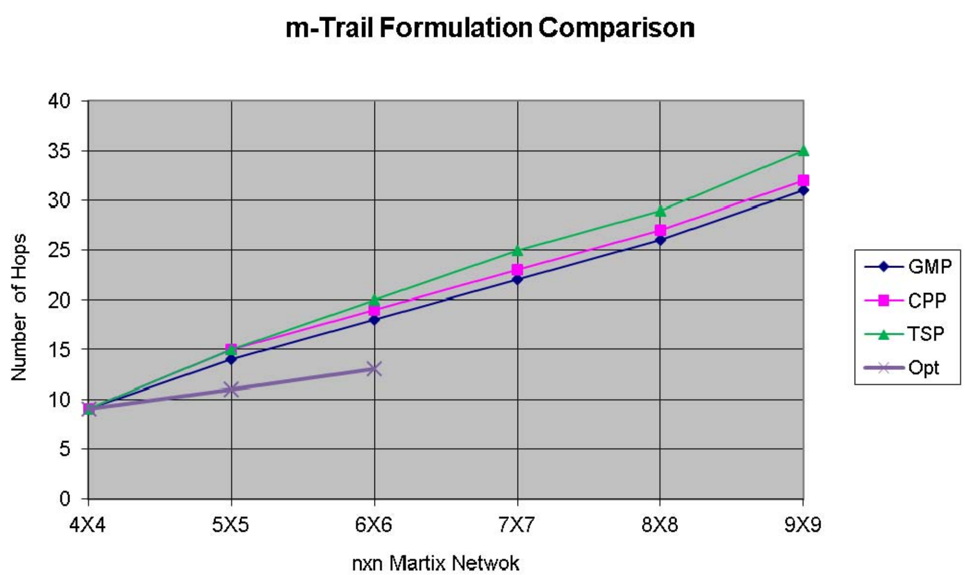

Fig. 5.8: M-Trail Formulation Comparison Between TSP (adapted), CCP (adapted) and GMP

5.3 PON Survivability Function

Assume there is N ONUs in a PON system, and the number of unavailable ONUs after failure is N_u, then S_x can be defined as the following [JIN07]:

$$S_x = (N - N_u)/N \times 100\% \quad (5.23)$$

S_x is a random variable over a discrete sample space Ω, and has a probability function *f(y)*, namely $P(S_x = y)$. y is the normalized event occurrence number and $\sum_{\Omega} y = 1$. So the expected survivability function S can be obtained [ZOL94]:

$$S = E[S_x] = \sum_{y} yP(S_x = y) \quad (5.24)$$

Taking the survivability model shown in Fig. 5.9(a) as an example to calculate S, one needs to specify a disaster which can result in link failures and consider the number of remaining ONUs connected to OLT. This was the first step in the assessment process [MAA11b].

For the analysis, it is assumed that link failures are independent, and the probability of each link failure is the same.

The expected survivability function S for this model is calculated as follows:

$$S = \frac{C_1^{16}}{C_2^{17}} \times \frac{0}{16} + \frac{C_2^{16}}{C_2^{17}} \times \frac{14}{16} = \frac{16}{136} \times \frac{0}{16} + \frac{120}{136} \times \frac{14}{16} = 0.772$$

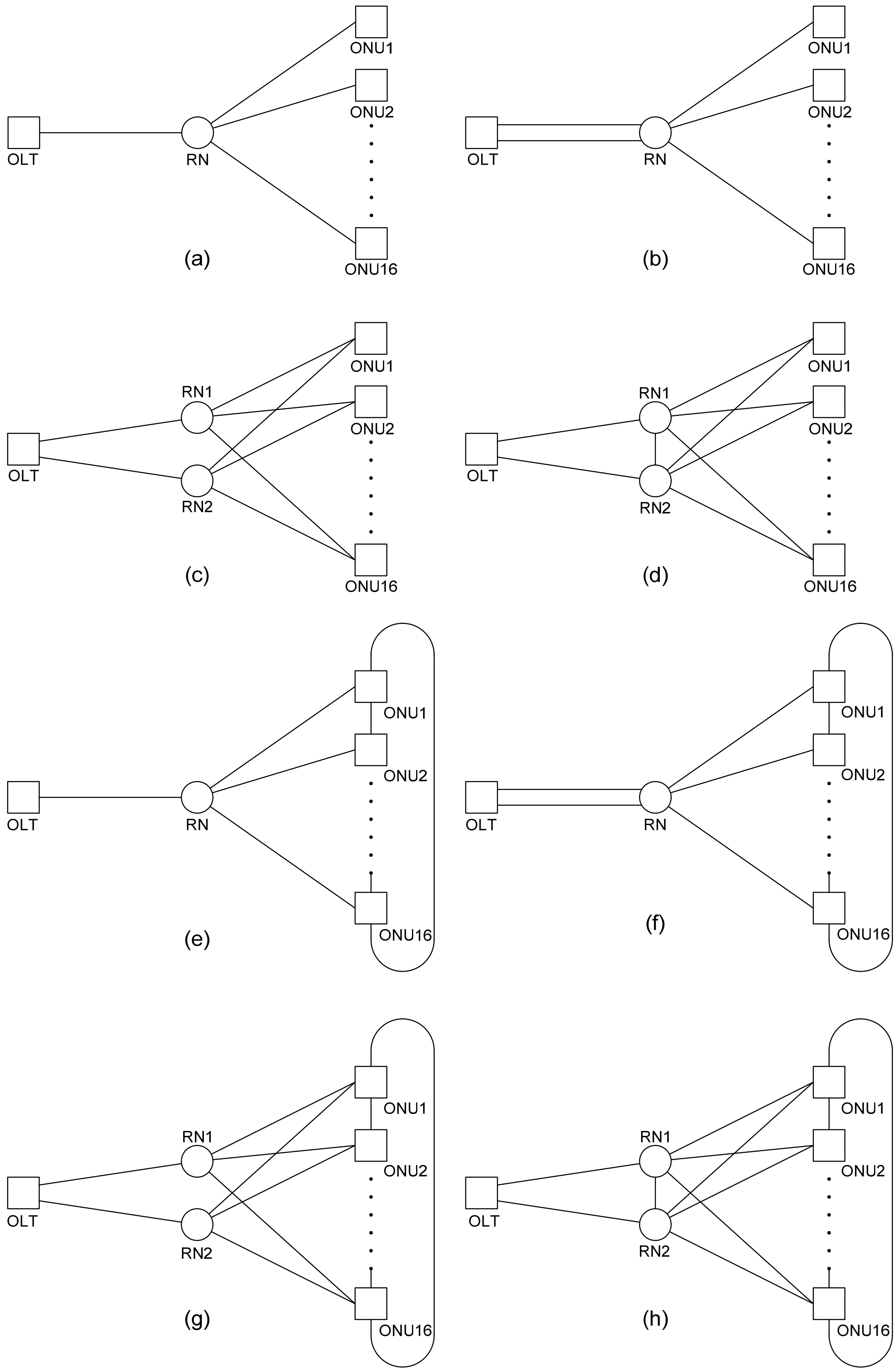

Fig. 5.9: Different PON/ RoF-PON Survivability Models [MAA11b]

Fig. 5.10 and 5.11 illustrate comparisons between these proposed models for their expected survivability function for different number of faults.

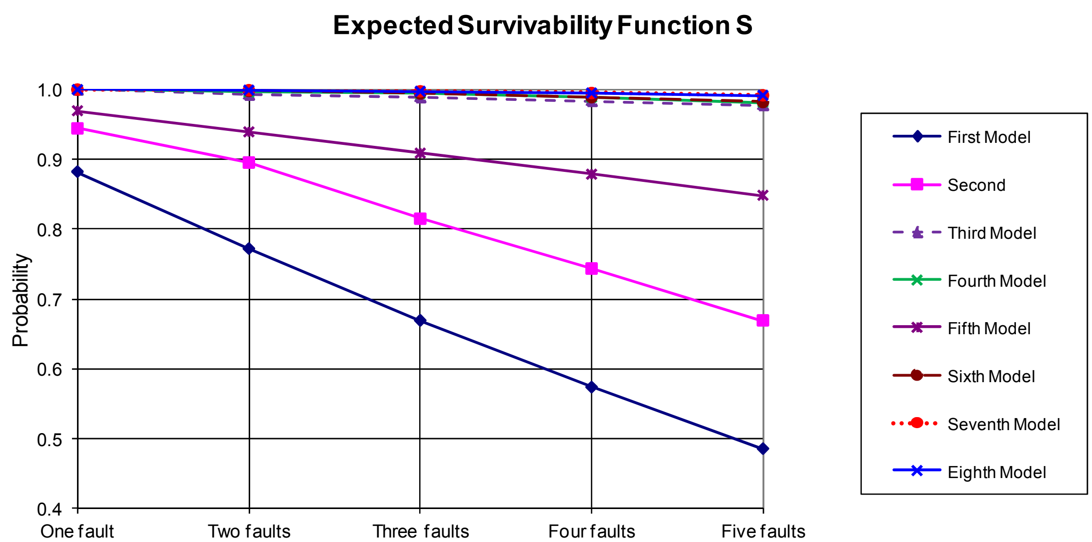

Fig. 5.10: Expected Survivability Function of the Eight Models for Different Number of Faults [MAA11b]

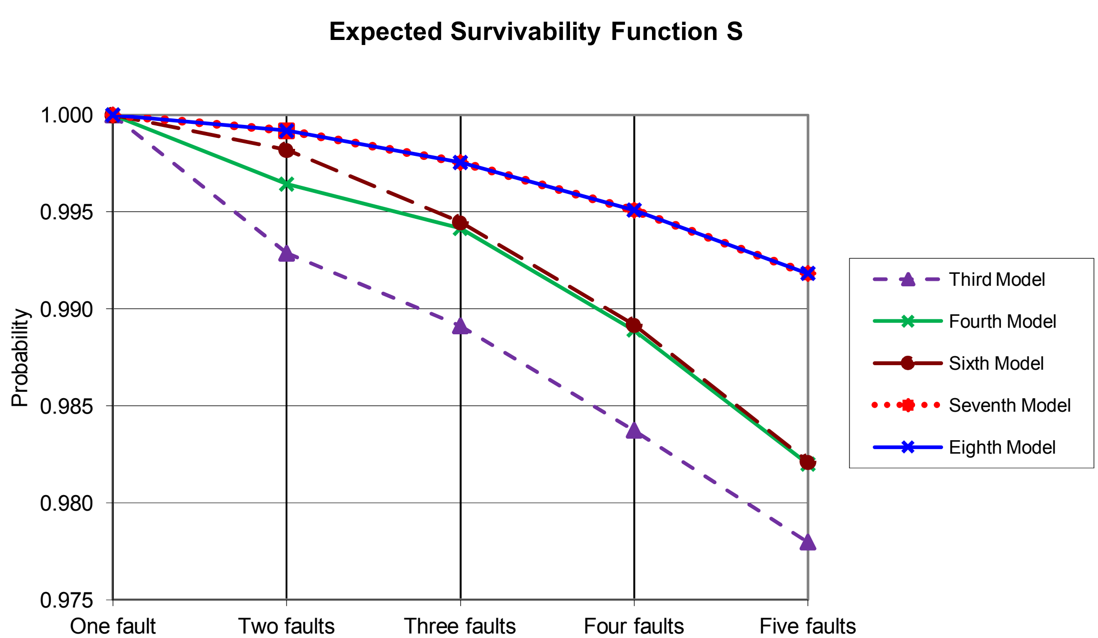

Fig. 5.11: Expected Survivability Function of The Last Five Models for Different Number of Faults [MAA11b]

5.4 M-Trail Possible Solutions for the Proposed PON/ RoF-PON Models

In this section, m-trail possible solutions for the Proposed PON/ RoF-PON models will be presented with the use of the techniques described in Chapter 4.

The results of the deployment methods discussed earlier are introduced in this section along with some possible solutions for the previously defined PON/ RoF-PON models.

Fig. 5.12 shows an m-trail possible solution for the first PON Model. This solution utilizes 32 m-trails employing 32 distinct wavelengths. Fig. 5.13 shows another m-trail possible solution for the same first Model. This solution utilizes 17 m-trails employing only 3 distinct wavelengths.

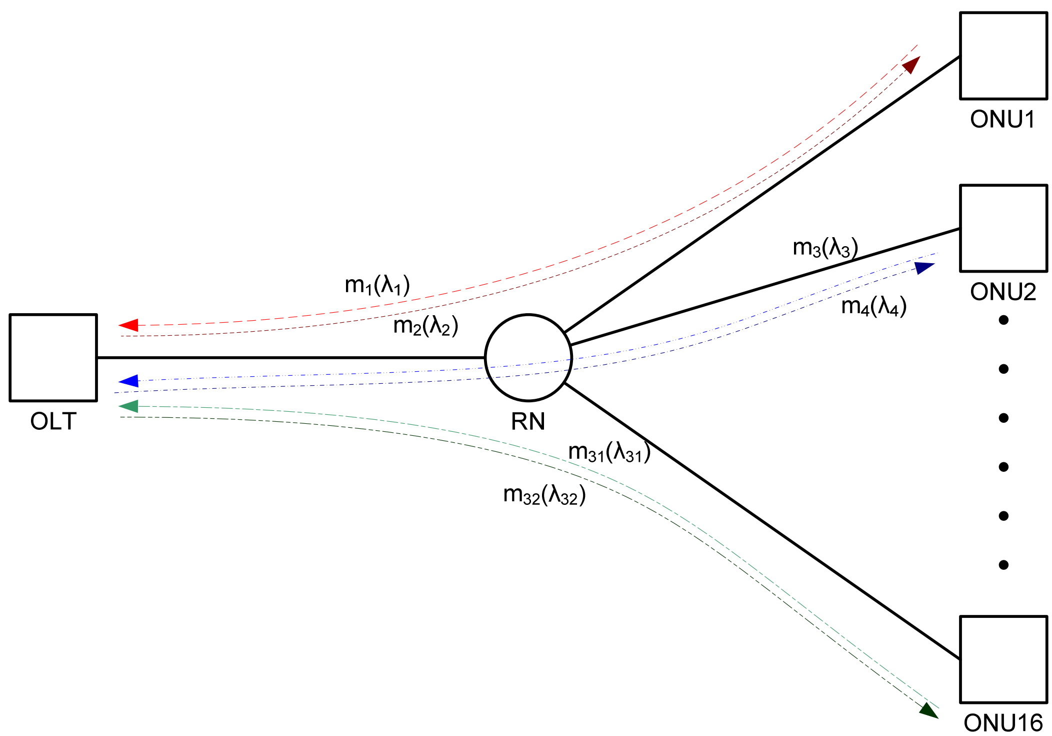

Fig. 5.12: M-Trail Possible Solution for The First PON Model

The comparisons between the two solutions are different and depend on the m-trail design concept. If the design problem is making use of the deployed optical paths for the normal operation of this PON Model, then the first proposed solution is optimal because no more trails are needed as those optical paths will be used for monitoring. The second design is appropriate when the separation between the monitoring and the operation functions is needed.

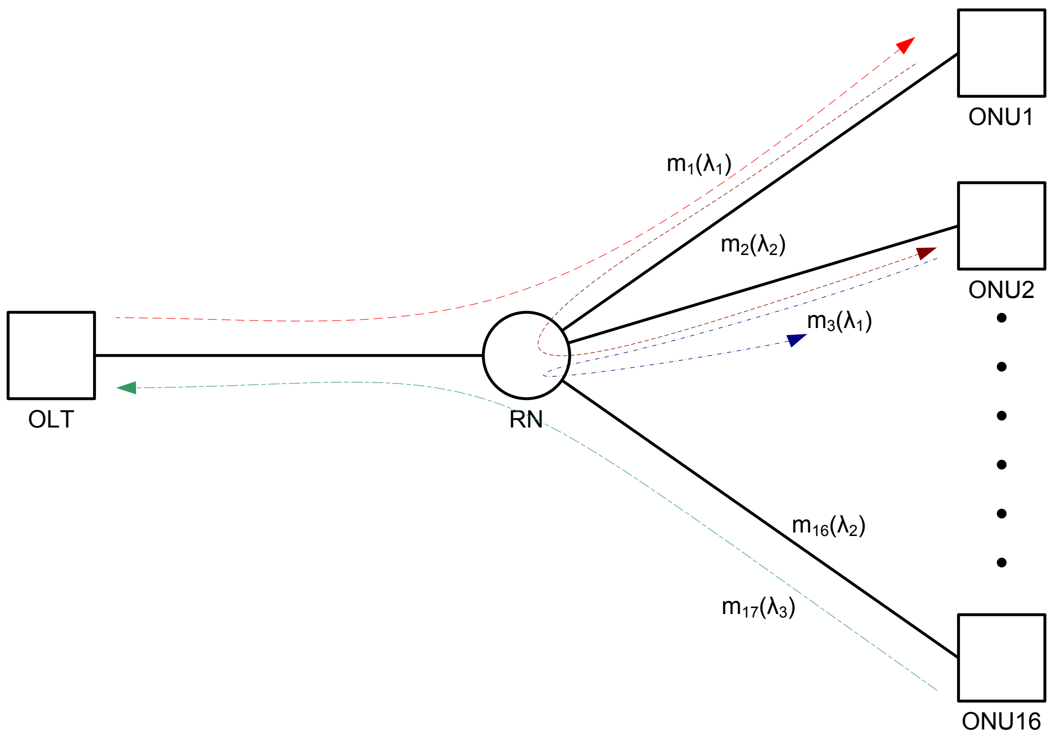

Fig. 5.13: Another M-Trail Possible Solution for The First PON Model

Fig. 5.14 shows an m-trail possible solution for the second PON Model. This solution utilizes 17 m-trails employing 2 distinct wavelengths. Another similar design solution is shown in Fig. 5.15 for the same PON model. This solution utilizes the same number of 17 m-trails that employs same number of 2 distinct wavelengths.

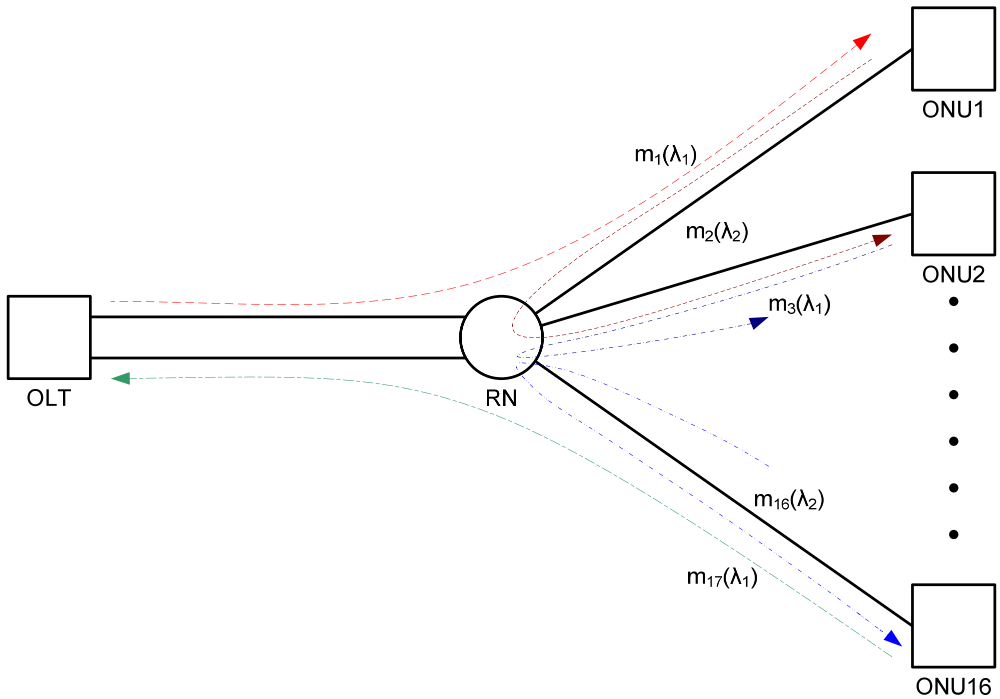

Fig. 5.14: M-Trail Possible Solution for The Second PON Model

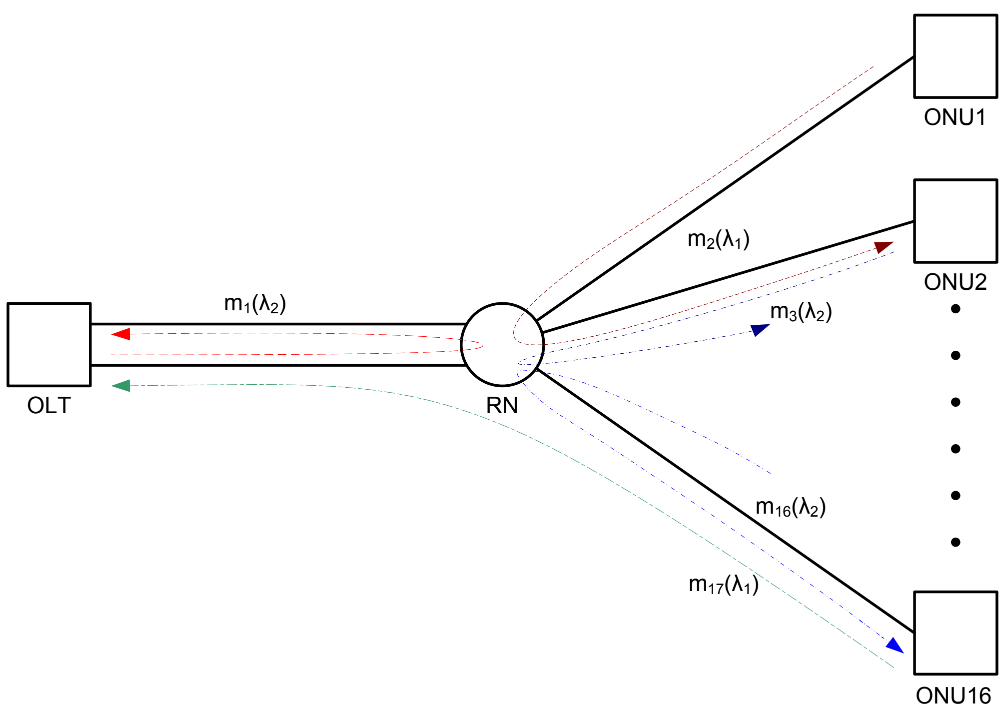

Fig. 5.15: Another M-Trail Possible Solution for The Second PON Model

The last two solutions for the second PON model are for deploying m-trails on the top of the operating optical paths or in the case of separating the monitoring and operation functions.

To solve the design problem and make use of the deployed optical paths for the normal operation of this PON model as monitors, Fig. 5.16 demonstrates a possible solution for 1+1 structure while Fig. 5.17 demonstrates another possible solution for 1:1 protection structure.

The solutions presented in Fig. 5.16 and Fig. 5.17 utilize a single m-trail employing a distinct wavelength from the operating optical paths. It is important to note that a single m-trail is enough to achieve survivability for the whole network as the working optical paths are used for monitoring. This method saves a lot of resources related to increasing the complexity of the network management system, NMS.

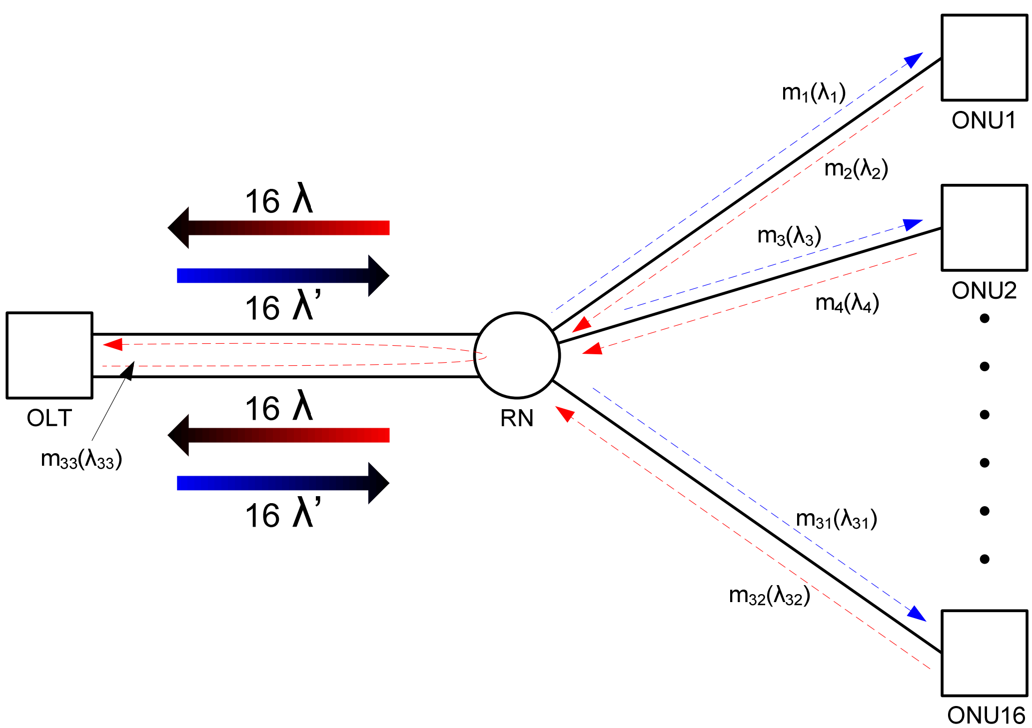

Fig. 5.16: M-Trail Possible Solution for The Second 1+1 PON Model

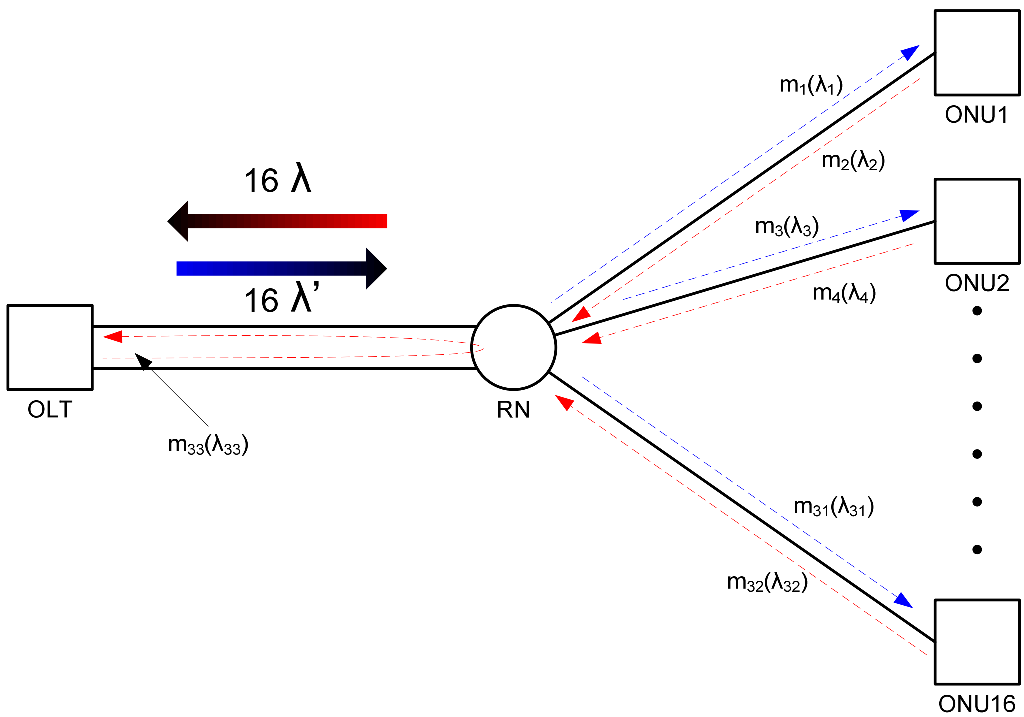

Fig. 5.17: M-Trail Possible Solution for The Second 1:1 PON Model

Fig. 5.18 shows an m-trail possible solution for the third PON Model on the top of the operating optical paths or in the case where a separation between monitoring and operation functions is needed. This solution utilizes 32 m-trails employing 2 distinct wavelengths.

A solution to the design problem which makes use of the deployed optical paths in the normal operation of this PON Model as monitors is the same as the proposed solution for the first model (Fig. 5.12). These solutions are optimal because there is no need for any more trails as those operating optical paths will be used for monitoring.

It should be noted that the third PON Model can be seen as 1+1 protection or 1:1 protection to the first PON Model from the survivability point of view. Every structure has its own pros and cons, which were stated in Chapter 2, which depends on its mode of operation.

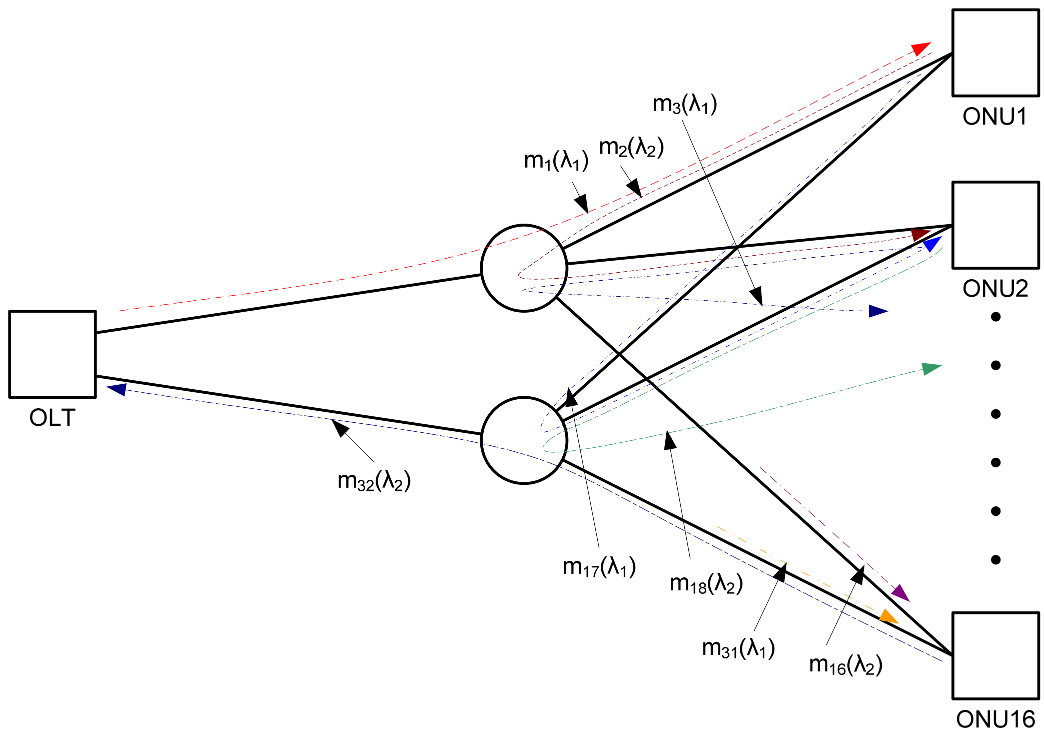

Fig. 5.18: M-Trail Possible Solution for The Third PON Model

Fig. 5.19 shows an m-trail possible solution for the fourth PON Model on the top of the operating optical paths or in the case where a separation between monitoring and operation functions is needed. This solution utilizes 33 m-trails employing 2 distinct wavelengths.

Fig. 5.20 shows another m-trail possible solution for the fourth PON Model on the top of the operating optical paths or in the case of separating monitoring and operation. This solution utilizes the same number of 33 m-trails employing 2 distinct wavelengths.

A solution to the design problem that makes use of the deployed optical paths in the normal operation of this PON Model as monitors is the same as the proposed solution for the first model (Fig. 5.12) with the addition of m_{33} with distinct wavelength λ. That is λ_{33}.

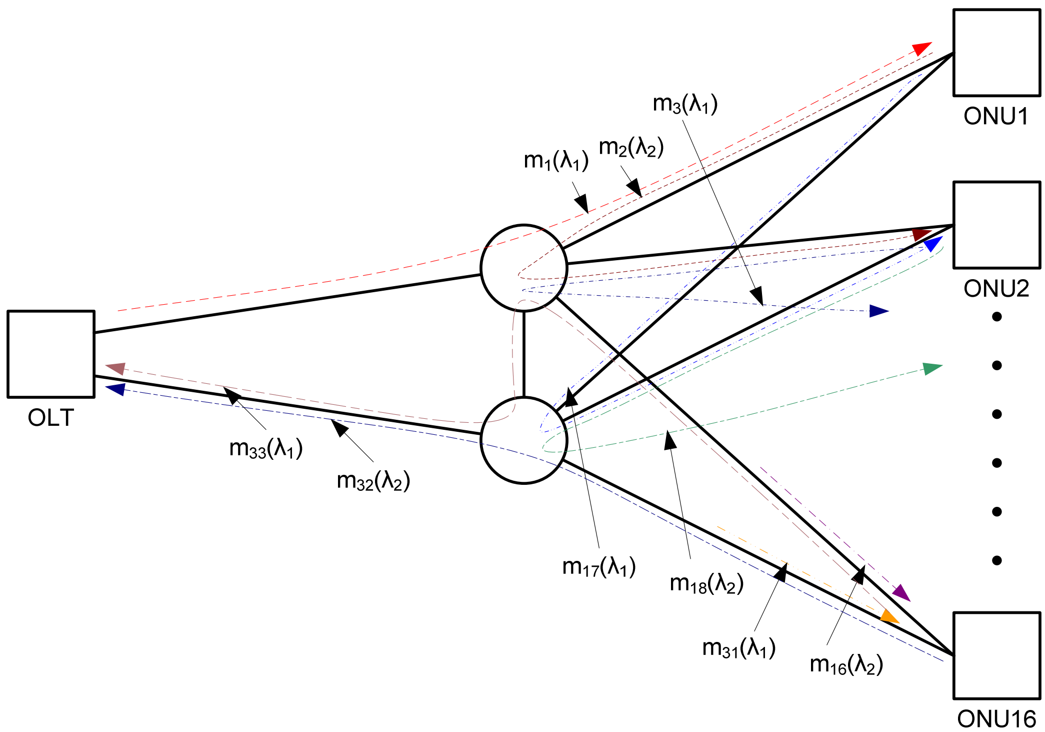

Fig. 5.19: M-Trail Possible Solution for The Fourth PON Model

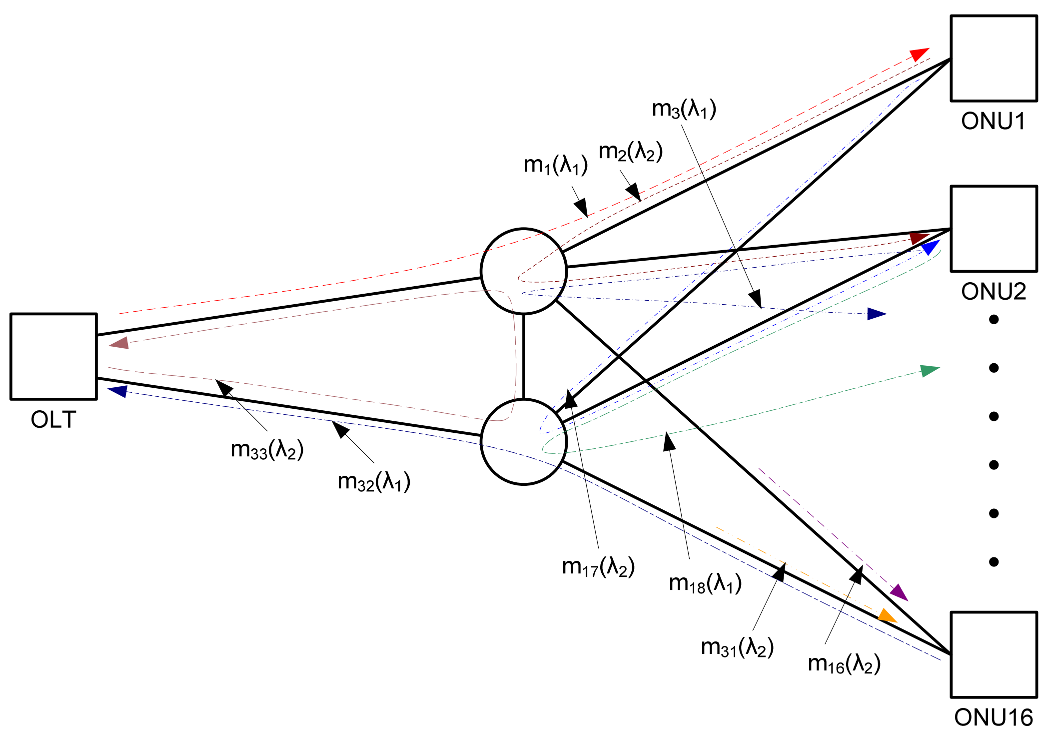

Fig. 5.20: Another M-Trail Possible Solution for The Fourth PON Model

Fig. 5.18 shows an m-trail possible solution for the fifth PON Model on the top of the operating optical paths or in the case where a separation between monitoring and operation functions is needed. This solution utilizes 17 m-trails employing 3 distinct wavelengths.

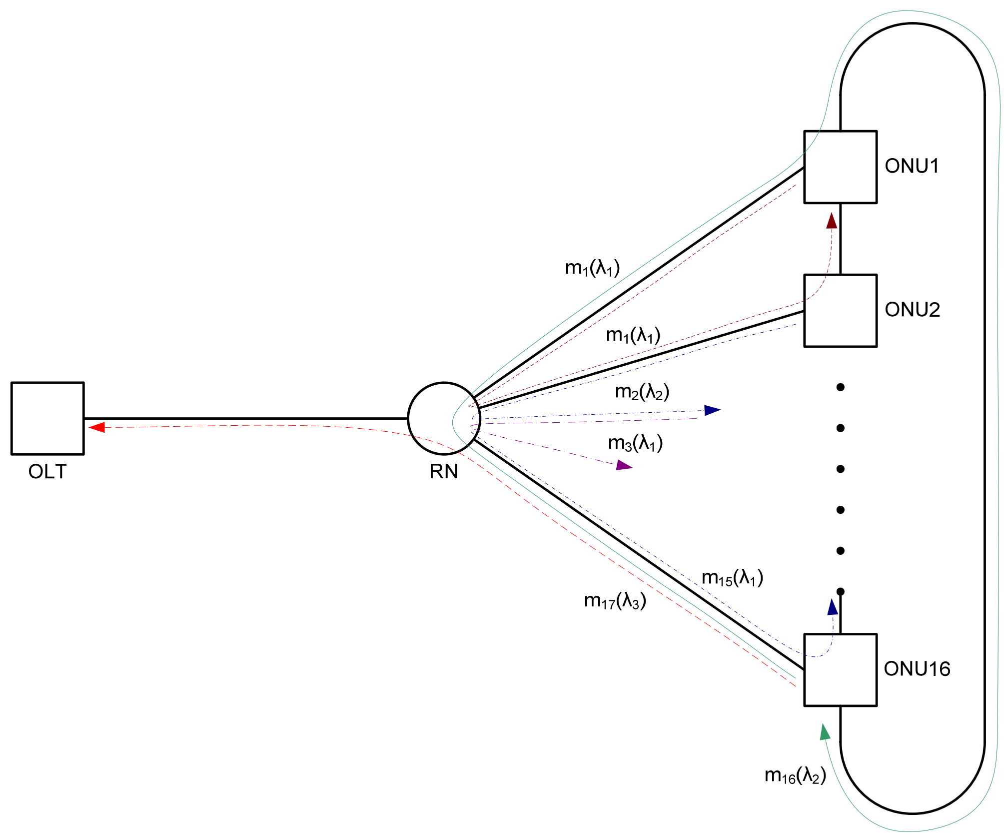

Fig. 5.21: M-Trail Possible Solution for The Fifth PON Model

Fig. 5.22 shows an m-trail possible solution to the design problem which makes use of the deployed optical paths in the normal operation of the fifth PON Model as monitors. This solution utilizes 16 m-trails employing one wavelength.

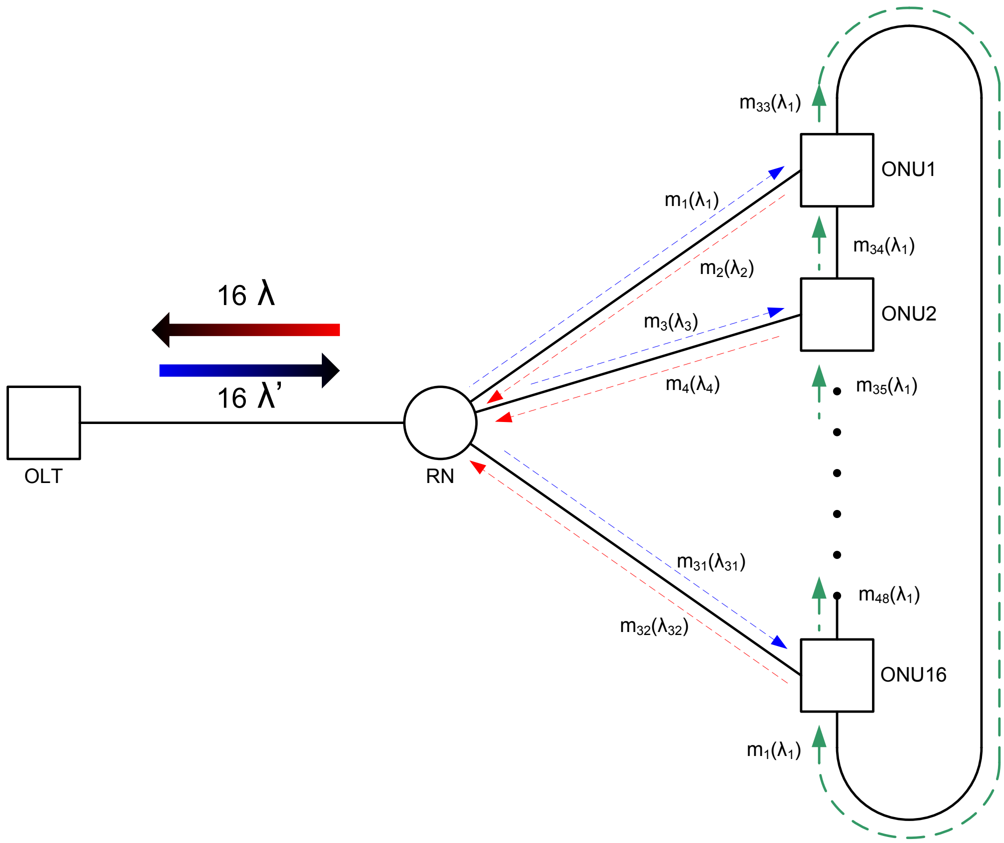

Fig. 5.22: M-Trail Possible Solution for The Fifth PON Model That Makes Use of The Deployed Optical Paths

Fig. 5.23 shows an m-trail possible solution for the sixth PON Model on the top of the operating optical paths or in the case where a separation between monitoring and operation functions is needed. This solution utilizes 33 m-trails employing 2 distinct wavelengths.

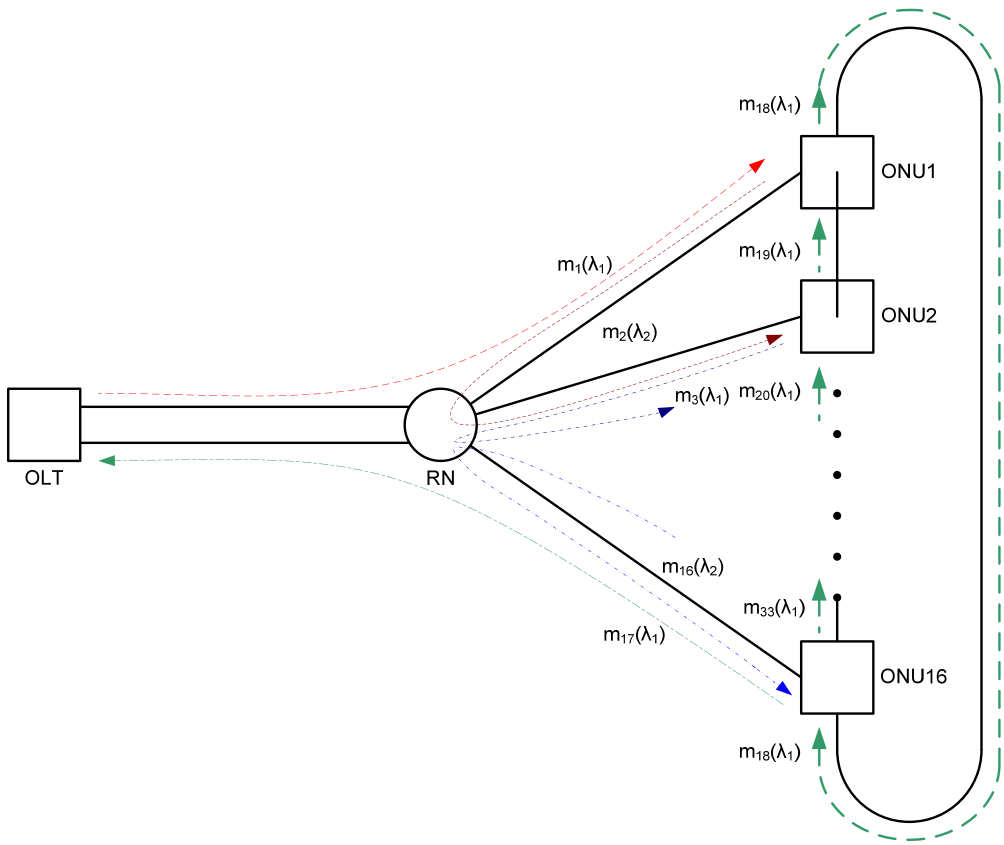

Fig. 5.23: M-Trail Possible Solution for The Sixth PON Model

Fig. 5.24 shows an m-trail possible solution to the design problem which makes use of the deployed optical paths in the normal operation of the sixth PON Model as monitors. This solution utilizes 16 m-trails employing one wavelength.

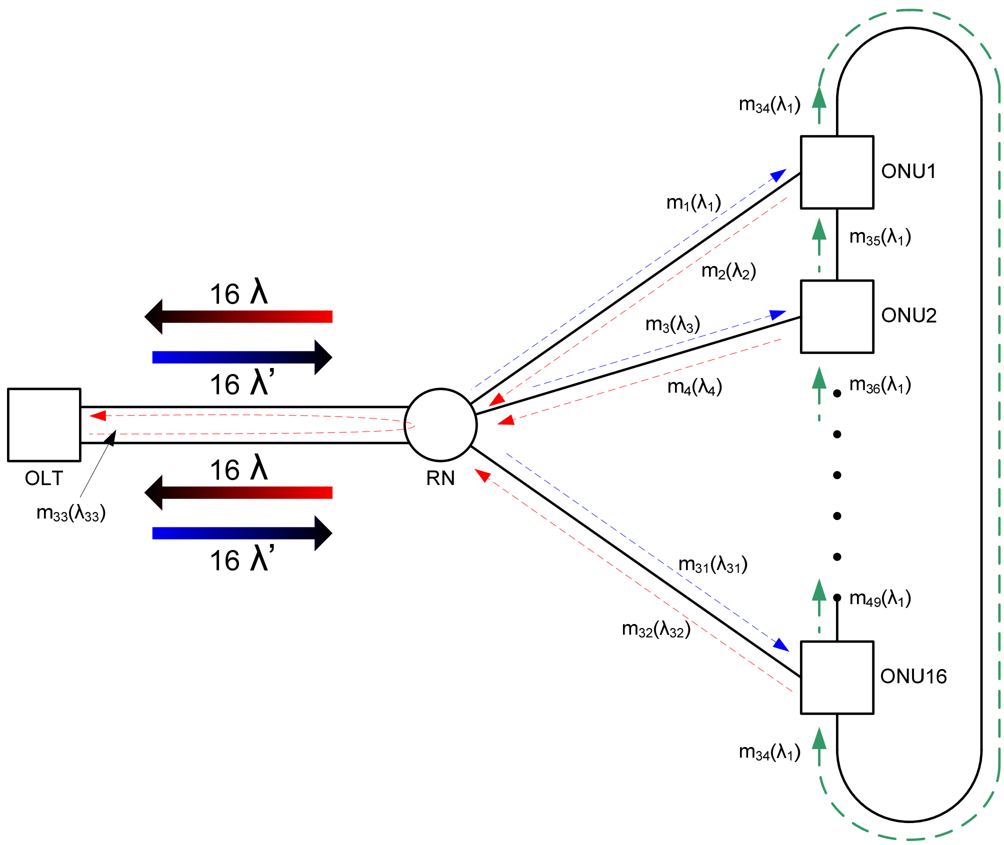

Fig. 5.24: M-Trail Possible Solution for The Sixth PON Model That Makes Use of The Deployed Optical Paths

Fig. 5.25 shows an m-trail possible solution for the seventh PON Model on the top of the operating optical paths or in the case where a separation between monitoring and operation functions is needed. This solution utilizes 48 m-trails employing 2 distinct wavelengths.

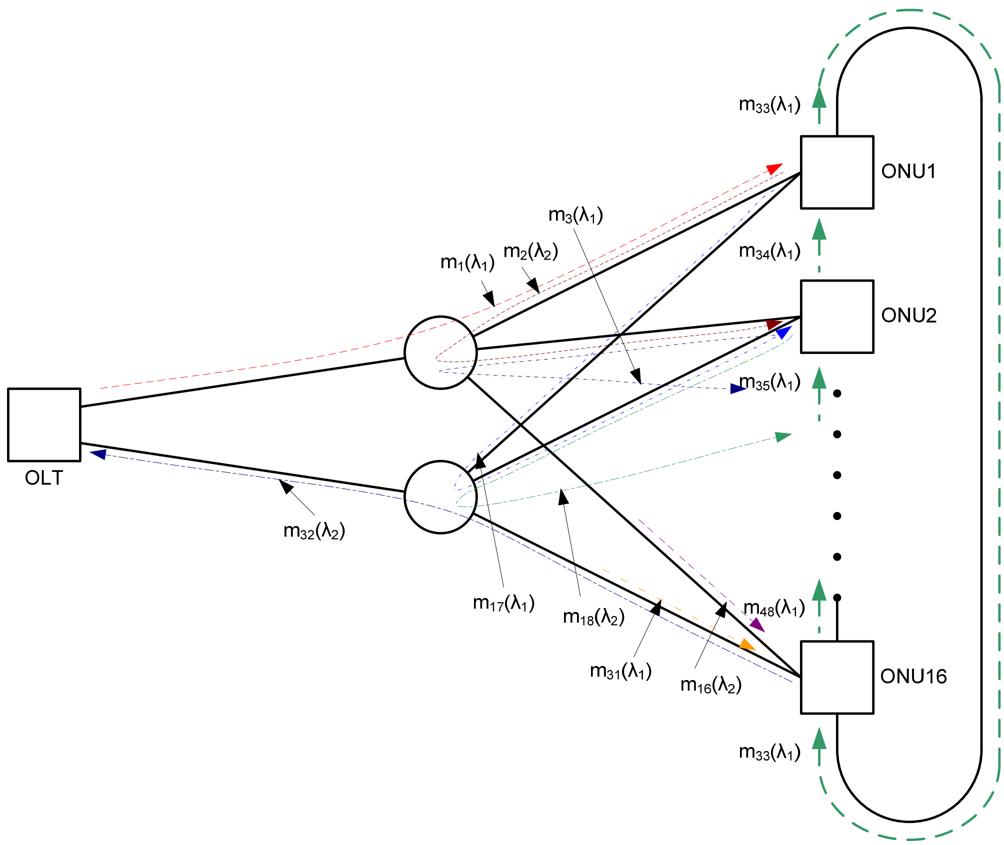

Fig. 5.25: M-Trail Possible Solution for The Seventh PON Model

Fig. 5.23 shows an m-trail possible solution for the eighth PON Model on the top of the operating optical paths or in the case where a separation between monitoring and operation functions is needed. This solution utilizes 49 m-trails employing 2 distinct wavelengths.

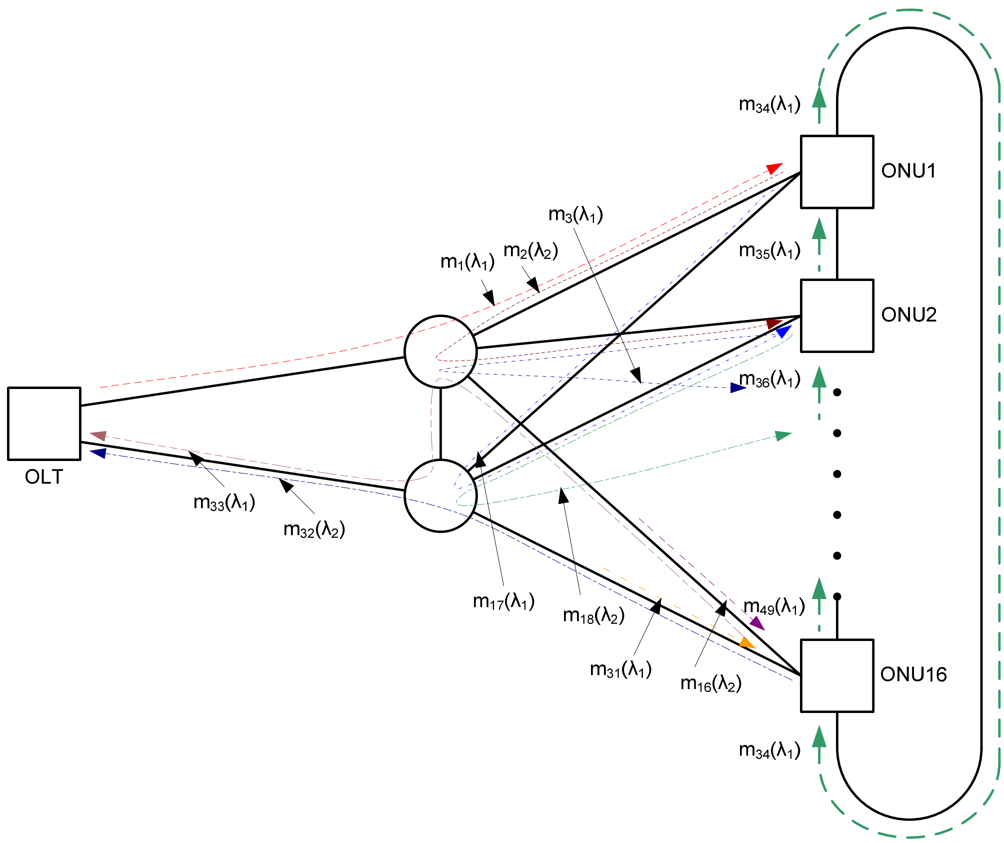

Fig. 5.26: That M-Trail Possible Solution for The Eighth PON Model

Table 5.3 summarizes the m-trail deployment for the different PON models with both cases: on the top of the operating optical paths and with the use of the operating optical paths.

Table 5.3: Summary of m-trail deployment for the different PON models

	On the top of the operating lightpaths				With the use of the operating lightpaths			
Model	Number of m-trails	Number of λ's	Total number of lightpaths	Total number of λ's	Number of m-trails	Number of λ's	Total number of lightpaths	Total number of λ's
1st (a)	32	32	64	64	0	0	32	32
1st (b)	17	3	49	35	0	0	32	32
2nd	17	2	49	34	1	1	32	33
3rd	32	2	64	34	0	0	32	32
4th	33	2	65	34	1	1	33	33
5th	17	3	49	35	16	0	48	32
6th	33	2	65	34	16	1	48	33
7th	48	2	80	34	16	0	48	32
8th	49	2	81	34	17	1	49	33

Table 5.4 summarizes the m-trail deployment for the different RoF-PON models with both cases: on the top of the operating optical paths and with the use of the operating optical paths. Noting that, the RoF-PON needs more 15 lightpaths with 15 distinct wavelengths than the same PON system.

Table 5.4: Summary of m-trail deployment for the different RoF-PON models

	On the top of the operating lightpaths				With the use of the operating lightpaths			
Model	Number of m-trails	Number of λ's	Total number of lightpaths	Total number of λ's	Number of m-trails	Number of λ's	Total number of lightpaths	Total number of λ's
1st (a)	32	32	79	79	0	0	47	47
1st (b)	17	3	64	50	0	0	47	47
2nd	17	2	64	49	1	1	47	48
3rd	32	2	79	49	0	0	47	47
4th	33	2	80	49	1	1	48	48
5th	17	3	64	50	16	0	63	47
6th	33	2	80	49	16	1	63	48
7th	48	2	95	49	16	0	63	47
8th	49	2	96	49	17	1	64	48

5.5 ROF-PON Performance Evaluation

Investigating the behavior and performance simulation of the RoF-PON system is implemented by the high-end optical simulator OptSim releases 5.0 form RSOFT.

The downlink system configuration is almost the same as in Fig. 5.20, with a CS and two ONUs. Three optical carriers with DWDM channel spacing of 12.5 GHz, according to ITU-T (2002) G.694.1 grid, and wavelengths of 1551.41967 nm, 1551.52003 nm and 1551.62041 nm are used in the simulation [MAA09].

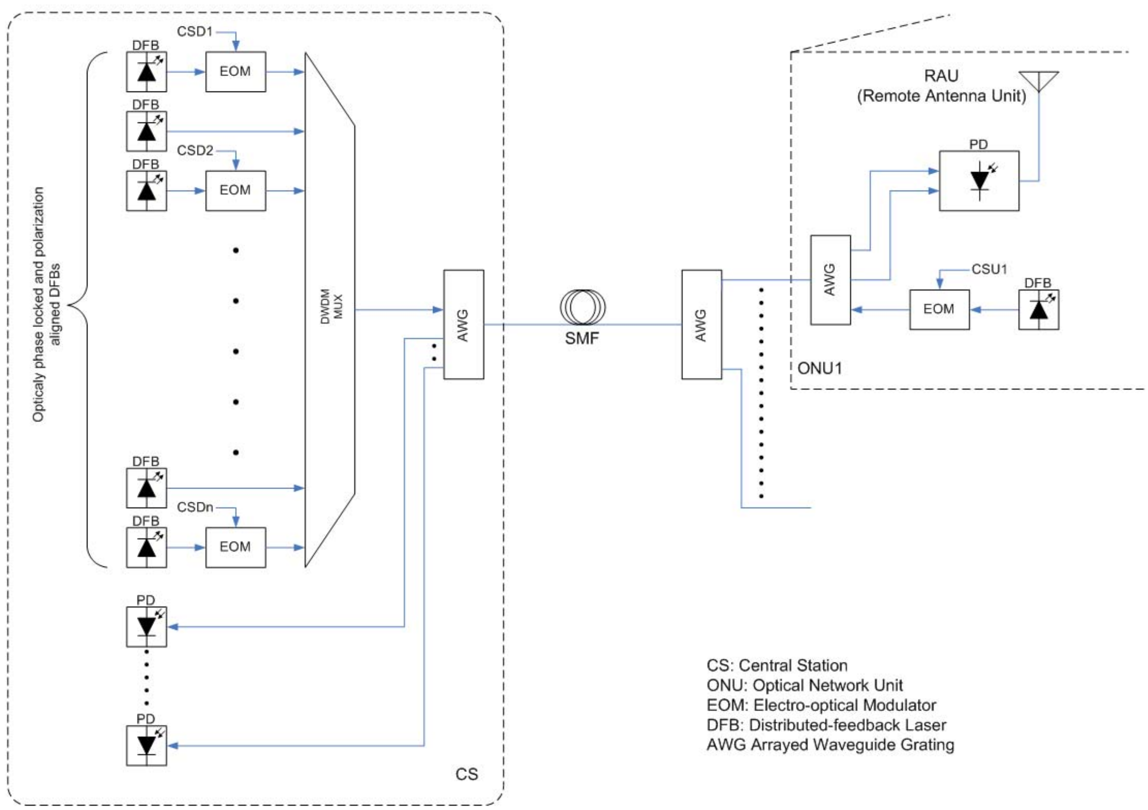

Fig. 5.27: The Proposed Novel RoF-PON Wireless Services System [MAA09]

The optical transmitter at the CS for the optical carriers consists of a CW laser source and an EAM driven by one DPSK modulated signal at 622.08 Mb/s. A DWDM multiplexer combines all the optical carriers and their sub-carriers together resulting an optical spectrum as shown in Fig. 5.21. The optical signal is further sent to ONU 1 via a 10 km downlink SMF link. A DWDM de-multiplexer is used to drop a fraction of optical power to the ONUs which is then passed to the downlink photo detection. At ONU 1, the three adjacent optical carriers and one sub-carrier are extracted by three optical filters with a center wavelength of 1551.41967 nm, 1551.52003 nm and 1551.62041 nm and a bandwidth of 15 GHz. After photo detection, the beat by the optical carrier (1551.41967 nm) with the un-modulated optical carrier (1551.52003 nm) generates an RF current (Fig. 5.22) which is filtered to produce a 12.5 GHz spectrum of Fig. 5.23. The user's device receives the wireless signal transmitted by RAU 1 and recovers the data after DPSK demodulation. The eye diagram for the recovered data is shown in Fig. 5.24.

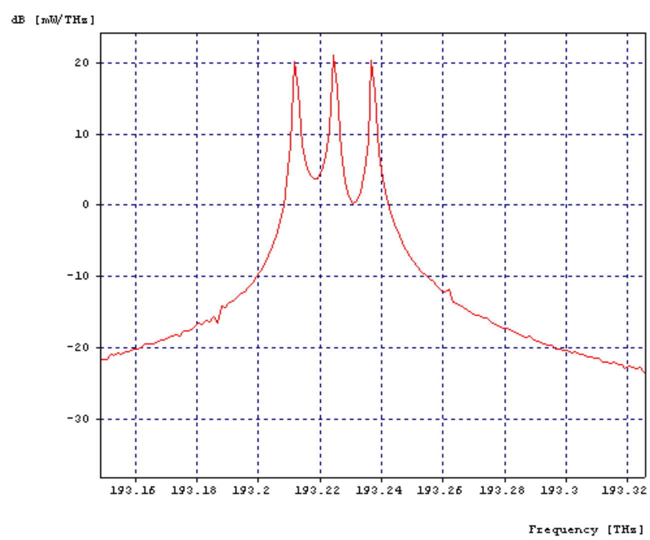

Fig. 5.28: The First Three Optical Carriers at The CS [MAA09]

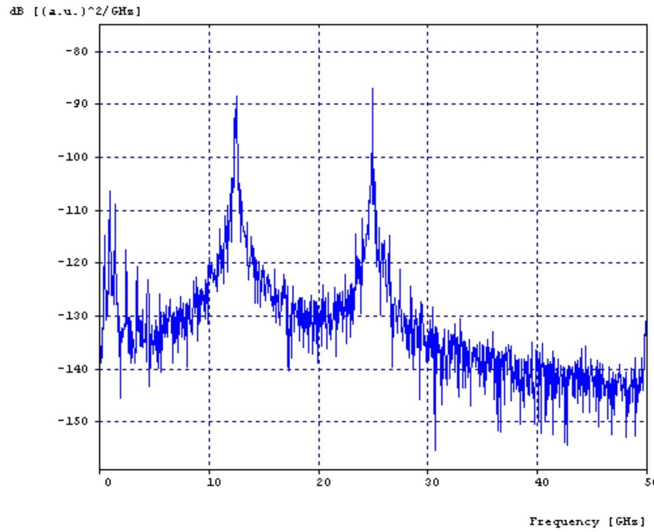

Fig. 5.29: RF Current Generated by The Photo Detector [MAA09]

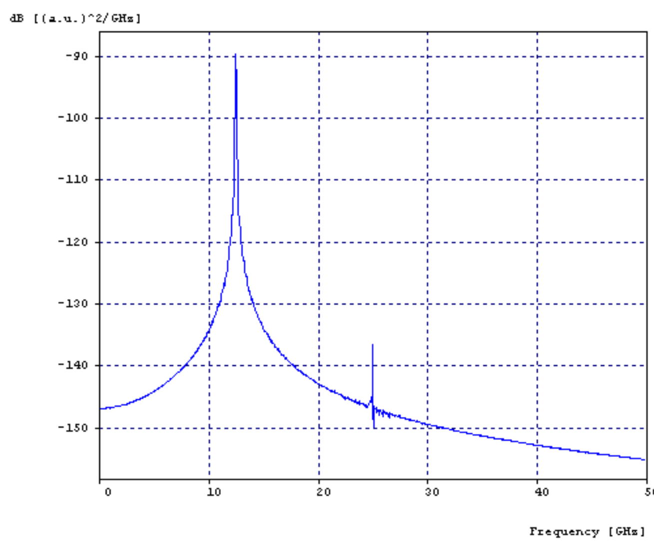

Fig. 5.30: The RF Signal Filtered Around 12.5 GHz Spectrum [MAA09]

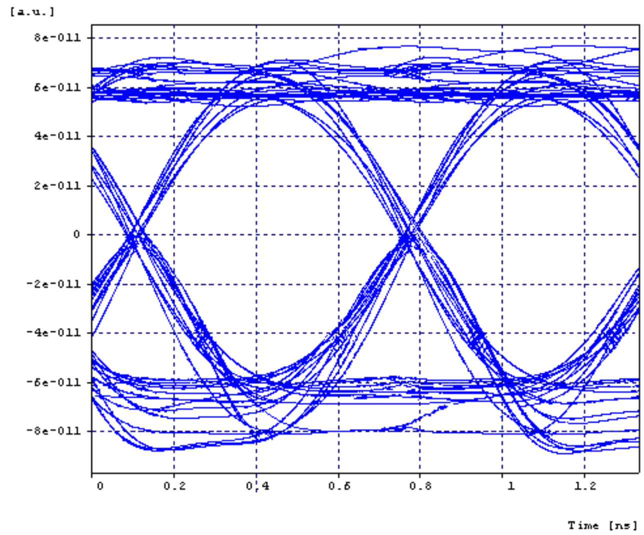

Fig. 5.31: The Eye Diagram of The Recovered User Data [MAA09]

5.6 LVM Performance Evaluation

For simulation, an all-optical mesh network topology (see Fig. 5.25) is used.

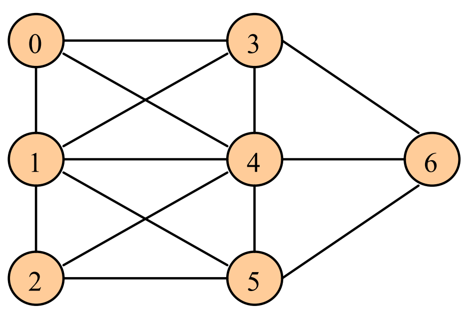

Fig. 5.32: The Simulated Network [JAF09]

This network has 7 nodes where the properties (number of wavelengths per fiber, length of fiber, network traffic type etc.) are changed while simulating different scenarios.

5.6.1 Network Size (Link Length) vs. Fault Localization Time

In this scenario, simulations were conducted with S-D lengths of 100 Km, 500 Km and 1000 Km. In each scenario every fiber has 8 wavelengths maximum capacity and the packet processing time on each node is set to 100 µs. The time to calculate a unicast route is set to 100 µs and the time to calculate a multicast tree is set to 100 µs.

Fig. 5.26 shows the average values of fault localization time and network update time in ms for varying S-D length from 100 Km to 1000 Km. The simulation is run five times for each point in the graph which presents the average with 95% confidence interval.

As seen from Fig. 5.26, once the distance between the links is increased, there is a large increase in the network updating time because it involves each link of the whole network. The fault localization time is not increased in the same manner because fault localization LVM only uses a limited area (the limited perimeter) so an increase in the S-D length does not affect the fault localization time as much as it affects the network updating time where the whole network is to be compiled. LVM is not more sensitive to an increase of size in terms of the S-D length because of its ability to involve only a specific area of network for fault localization instead of transceiving all network nodes [JAF09].

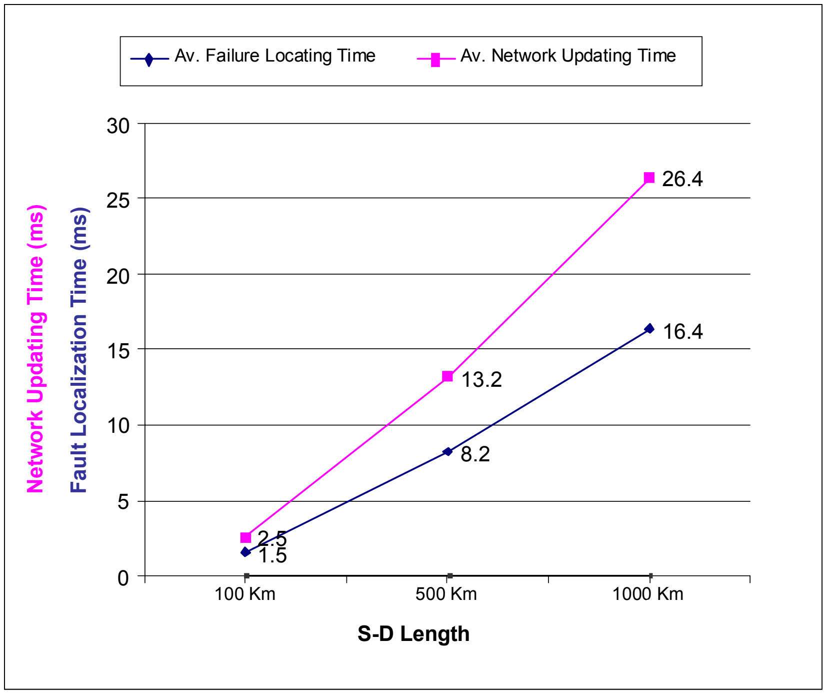

Fig. 5.33: Fault Localization and Network Updating Time in ms with Increasing Link Length per S-D [JAF09]

5.6.2 Network Traffic (Arrival Rate) vs. Blocking Probability

In this scenario, simulations were conducted for different arrival rates with dynamic traffic and Poisson distributions ranging from 50 to 1000 call arrivals per hour. Each fiber spans 100 Km between every fiber has 8 wavelengths maximum capacity. Propagation delay was set to 500 μs while packet processing time and route calculation time were assumed to be constant. Connection holding time was 10 hours and failures were generated after every 5 hours. The simulation is run five times for each point in the graph which presents the average with 95% confidence interval.

Fig. 5.27 shows the average blocking probability for the network with different arrival rates. The blocking probability is increasing at the same time as arrival rate because as traffic is increased, network resources are occupied and the availability of resources goes down. This results in traffic blockage after a specific value. The increase of blocking probability is directly proportional to the increase in the arrival rate [JAF09].

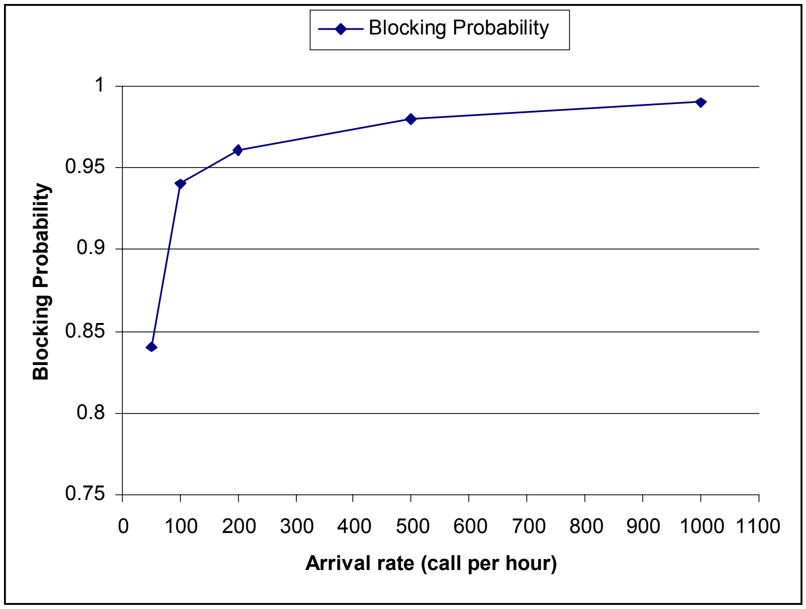

Fig. 5.34: Average Blocking Probability with Increasing Arrival Rate [JAF09]

5.6.3 Network Traffic (Arrival Rate) vs. Fault Localization Time

Fig. 5.28 shows the average fault localization time by LVM with different arrival rates. Each point in the graph presents the average of five times simulation runs with 95% confidence interval. Fault localization time was found to be in the range of 12 to 12.5 ms for arrival rates between 50 and 1000 call arrivals per hour - Poisson distribution. For low arrival rates (50 to 100 call arrivals per hour), there is a nearly constant fault localization time. Whereas, for high arrival rates (500 and 1000 call arrivals per hour- Poisson distribution), the fault localization time is decreasing slowly. This is because the blocking probability is high, network resources are occupied, and there are smooth lightpaths in the network with less regeneration when compared to low traffic and fault localization process. With the arrival rate increase, fault localization process gained from that as there is more traffic in the network, which leads to increase of the information gathered upon failure and/or reduction of the perimeter area. The need to launch supporting lighpaths is also reduced. So, the LVM works even more efficiently when the traffic rate is increased in the network [JAF09].

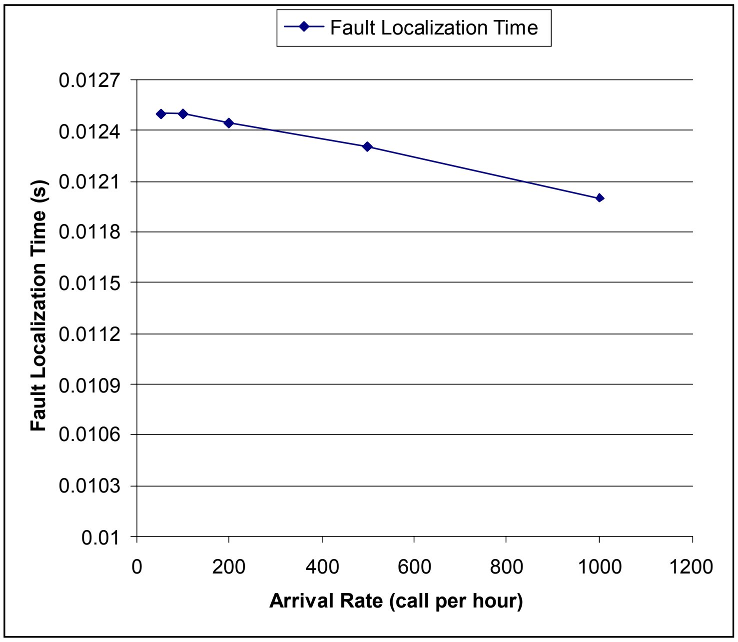

Fig. 5.35: Average Fault Localization Time with Increasing Arrival Rates [JAF09]

5.6.4 Network Size (Number of Nodes) vs. Fault Localization Time

In this scenario, 3 different simulation models were used. All simulation models are ring topology having the same nodal degree (2) and the same link distance (100 Km) but have different number of nodes (5, 8 and 10). The length of each fiber was 100 Km between each node and every fiber has 8 wavelengths maximum capacity. Dynamic traffic with a Poisson distribution was used in this simulation. The traffic arrival rate was 25 arrivals per hour with a connection holding time of 10 hours. Propagation delay was set to 5 μs while packet processing time and route calculation time were assumed to be constant.

Fig. 5.29 shows the graph of the average fault localization times and LOS flooding times from the scenarios discussed above. Each point in the graph presents the average of five times simulation runs with 95% confidence interval. The fault localization process starts as soon as the destination discovers the loss of signal. Loss of signal flooding time is network-dependent, and it increases with an increase in the number of nodes, distance between the nodes, traffic, etc. [JAF09].

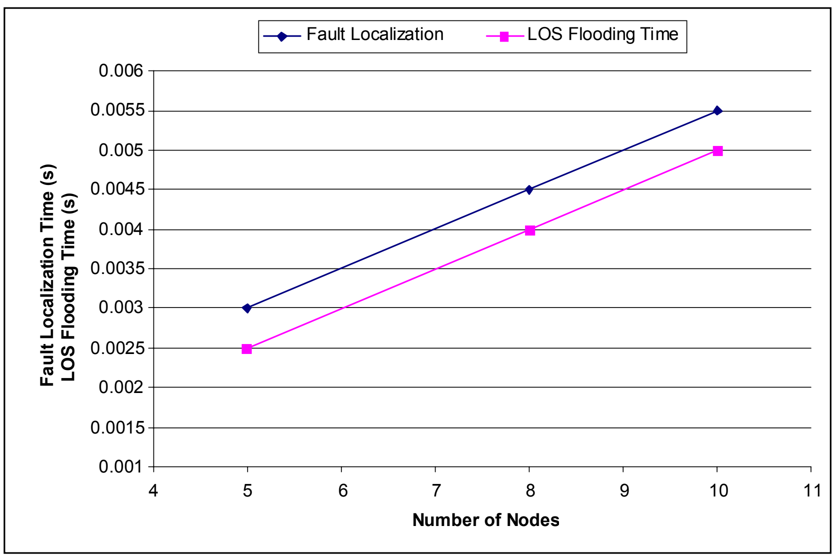

Fig. 5.36: Average Fault Localization Time and LOS Flooding Time with Different Size of Networks [JAF09]

In Fig. 5.29, a steady increase is observed in the LOS flooding time with the increase in the number of nodes in the network. But the processing time to localize failure by LVM is constant on all nodes as shown in Table 5.1. That is because the LVM operates on a limited perimeter area which is almost the same size for both small and large networks.

Table 5.5: Processing Time to Localize Failure by LVM for Different Number of Nodes [JAF09]

Number of nodes	LOS Flooding Time (ms)	Fault Localization Time (ms)	Difference (ms)
5	2.5	3	1.5
8	4	4.5	1.5
10	5	5.5	1.5

5.6.5 Similarities and differences between LVM and M-trail Fault Localization Protocols

The principle of operation of using the LVM and the m-trail in fault localization is the same. They deploy alarm monitor for fault detection and analyze the alarm notification messages that are generated from those monitors to localize the fault. The result obtained from the ALV processing operation in the LVM protocol is similar to m-trail alarm code in the m-trail method.

A comparison between the LVM and m-trail algorithm is illustrated in Table 5.6.

Table 5.6: Comparison between the LVM and M-trail Algorithm

	M-trail Algorithm	LVM Protocol
Network resources used before a failure	Large (lightpaths that are used to deploy the m-trails can be reduced if it the network operating lightpaths are used as m-trails)	None
Network resources used after a failure	Alarm messages only	Alarm and protocol process messages
Processing time	Very small (~µsec) (as soon as the alarm notification messages received, the alarm code is formed and looked up at the ACT)	Large (~ms)
Fulfillment of UFL	Yes	No (There is no guarantee that

		the protocol can localize the fault without a need of deploying extra lightpaths in that perimeter area.
NMS complexity requirement	Low	High

5.7 Summary and Concluding Remarks

Different solutions, which are described in Chapter 4, are demonstrated for the m-trail construction of a network with previously established lightpaths as well as TSP, CCP and GMP solutions of 4x4, 5x5 and 6x6 matrix networks. The number of hops is calculated for each solution.

The optimized solution for the m-trail construction of a network with lightpaths already established is carried out by the student version of FICO Xpress Mosel optimizer version 3.2.3.

A comparison between the proposed PON/ RoF-PON modes for their expected survivability function is illustrated for a different number of faults. M-trail possible solutions for the Proposed PON/ RoF-PON models is also demonstrated which were presented with the use of different techniques described in Chapter 4.

Novel mm-WB RoF system architecture for wireless services with the use of dense wavelength division multiplexing (DWDM) of 12.5 GHz channel spacing (according to ITU-T 2002, G.694.1 grid) is introduced. By using the Remote Heterodyning Detection (RHD) method of RoF, the hardware vendor is benefited by low line losses, resistance to lightning strikes, and electric discharges.

LVM protocol is explored and its performance is evaluated through the simulation results. It is showed that the LVM protocol can achieve excellent performance in terms of fault localization time while maintaining the maximum-level of transparency in all-optical networks. LVM is not too sensitive to an increase of size in terms of the S-D length because of its ability to incorporate only a specific area of network for fault localization instead of transceiving all network nodes. The LVM works more efficiently when traffic rate is increased in the network. LVM processing time to localize failure is constant on all nodes regardless of the increase of the network size (number of nodes).

Chapter 6: Conclusions and Future Research

6.1 Conclusions

In this dissertation, the deployment of the recently introduced m-trails by employing monitoring resources in a form of trails to achieve a fault localization process in all-optical networks is investigated. Novel techniques are introduced and illustrated by examples for using m-trails along with established lightpaths to achieve fault localization.

Summary of Contributions:

(1) A novel technique based on Geographic Midpoint Technique (GMP), an adapted version of the Chinese Postman's Problem (CPP) solution and an adapted version of the Traveling Salesman's Problem (TSP) solution algorithms.

(2) A proposed novel system for delivering future mm-WB RoF systems for wireless services with a use of DWDM architecture.

(3) A number of suggested innovative models for PON/ RoF-PON along with their m-trail design solutions.

In addition to GMP, CPP, and TSP, the manual exercise routine, that is explained in Chapter 4, can be directly applied to the ACT. The simplicity of these new methods provides an added value over the other techniques used for fault localization in all-optical networks. Using m-trails with established lightpaths to achieve fault localization is a superb method as it saves network resources by reducing the number of the m-trails required for fault localization and therefore the number of wavelengths used in the network.

GMP showed a better performance over the other used algorithms in terms of the number of hops that forms the m-trail. The simplicity of the GMP over the other algorithms is an added value to its performance, which shows its ability to be practically implemented at the lower optical layer.

A novel millimeter-waveband (mm-WB) radio-over-fiber (RoF) system architecture for wireless services integrated in a dense wavelength division multiplexing (DWDM) of 12.5 GHz channel spacing was also proposed. The channel spacing follows ITU-T 2002, G.694.1 grid guidance. By using the Remote Heterodyning Detection (RHD) method of RoF, the hardware vendor is benefited by the low line losses, resistance to lightning strikes, and electric discharges. Complexity reduction of the base stations is achieved by attaching a light-weight Optical-to-Electrical (O/E) converter directly to antenna which is known as Fiber to the Antenna FTTA. Another advantage of using such a novel system lies in its ability to provide dynamic capacity allocation based on traffic demands. Today, RoF systems are designed to incorporate added radio-system functionalities in addition to transportation and mobility. Generally, the proposed RoF-PON system is simple, cost-effective and reduces the need for maintenance routines. For the conceptual illustration, a DWDM RoF system with channel spacing of 12.5 GHz is considered. Other frequency spacing may be also chosen e.g. 25 GHz or 50 GHz. These frequency spacing is according to ITU-T G.696.1 spectral grid recommendation. Reducing the frequency spacing can cause undesirable effects like Four Wave Mixing (FWM) and Cross Phase

Modulation (XPM). 12.5 GHz (KU band) may be considered as a future extension to the current 5.8 GHz frequency for home wireless communication.

The LVM protocol is investigated and its performance is evaluated through the simulation results. It is showed that the LVM protocol can achieve excellent performance in terms of fault localization time while maintaining the maximum-level of transparency in all-optical networks. LVM is not too sensitive to an increase of size in terms of the S-D length because of its ability to comprehend only a specific area of network for fault localization instead of transceiving all network nodes. The LVM works more efficiently when the traffic rate is increased in the network. LVM processing time to localize failure is constant on all nodes regardless of the increase of the network size (number of nodes). A comparison between the LVM and m-trail algorithms is provided with their pros and cons.

The use of the expected survivability function to distinguish survivability of different topologies for PON/ RoF-PON is an excellent numerical analysis method: it can provide a comparison between different design problems.

The proposed models of PON/ RoF-PON incorporate some known designs as well some new designs. The comparison between these models uses the expected survivability function which proved that these models are likely to be implemented in the new and existing PON/ RoF-PON systems. A number of solutions for the m-trail design problems for these proposed PON/ RoF-PON models on the top of the working lightpaths are provided. This can be such a case when a separation between monitoring and operation functions is needed.

6.2 Future Research

The m-trail construction analysis with the use of lightpaths that are already established is done by implementing TSP, CCP and GMP algorithms for 4x4, 5x5 and 6x6 matrix networks. More study need to be carried out for another network types showing the advantage of using each method over the others in regards to topology type and size. That study should also discuss the strength and limitations of each algorithm not only in the topology type and size, but also in many other network characteristics and behavior. National Science Foundation Network (NSFNET) and the European Optical Network (EON) should be considered also as real network models in that study.

A comprehensive research to include other TSP and CPP algorithms and their variants like Vehicle Routing Problem (VRP) should also be considered for future research.

The m-trail design problem opens the door to another research area that needs specific edges in the network to be part of the targeted route. This is known as Forced Routing design problem (FR). A study in this area with the use of the novel Geographic Midpoint algorithm needs to be investigated.

Validation of the RoF-PON system performance collected by simulation has to be carried out by experimental tryouts. That proves its operational concept and its capability to be deployed in real life.

The survivability methods of RoF-PON at the ONU area can be extended by applying wireless survivability techniques which will open the doors to the research activities based on the operation principles of this technology.

In the dissertation, it is assumed a single failure can happen to the network. This is the predominant type of problem, but there are still cases of multiple failures, which cannot be neglected. So, m-trail design problems with multiple failures need more study and should have some new optimized and heuristic solutions.

In the calculation of the expected survivability function, it is assumed that the link failures were independent. The framework can accommodate situations that involve dependency among failures; the added complexity for computing the survivability function remains to be studied further.

There is a need to increase the proposed optimization and heuristics models to have the ability to deal with dynamic traffic to achieve fast fault localization.

The use of wavelength conversions in the m-trail design and the extension to a complex trail with multiple monitors needs to be investigated.

[DAM11] has investigated the physical constraints on launching m-trails, mainly focusing on the maximum length each m-trail may have. Other factors such as node hardware complexity and NMS sophistications should be taken into consideration in the m-trail system design.

Bibliography

[ALB06] S. Albarrak and D. Harle, “Pre-Allocated Restoration Technique in a Distributed GMPLS-Based IP/WDM Mesh Network”, Proceedings IEEE Information and Communication Technologies ICTTA '06.2nd, Damascus, Syria, Vol. 2, pp. 2236 – 2241, April 2006.

[ALS90] B. Alspach, J. Bermond, and D. Sotteau, “Decomposition into Cycles 1: Hamilton Decompositions”, Cycles and Rays, Kluwer Academic Publisher, The Netherlands, pp. 9 – 20, 1990.

[ANG12] I. Angelou et al, “Optimized Monitor Placement for Accurate QoT Assessment in Core Optical Networks”, Journal of Optical Communications and Networking, IEEE/OSA, Vol. 4, Issue 1, pp. 15 – 24, 2012.

[BAB11] P. Babarczi, J. Tapolcai, and H. Pin-Han, “Adjacent Link Failure Localization with Monitoring Trails in All-Optical Mesh Networks”, IEEE/ACM Transactions on Networking, Vol. 19, Issue 3, pp. 907 – 920, 2011.

[BAB11] P. Babarczi, J. Tapolcai, and Pin-Han Ho, “SRLG Failure Localization with Monitoring Trails in All-optical Mesh Networks”, 8th International Workshop on the Digital Design of Reliable Communication Networks (DRCN) 2011, pp. 188 – 195, 2011.

[BEN99] Bennett S. et al, "1.8 THz Bandwidth, Zero-Frequency Error, Tunable Optical Comb Generator for DWDM Applications", IEEE Photonics Electronic Letters, Vol. 11, No. 5, pp. 551 – 553, May 1999.

[BHA99] R. Bhandari, “Survivable Networks: Algorithms for Diverse Routing”, Springer; 1st Edition, ISBN-13: 978-0792383819, Jan. 1999.

[BOU94] A.T. Bouloutas, S. Calo, and A. Finkel, “Alarm Correlation and Fault Identification in Communication Networks” IEEE Transactions on Communications, Vol. 42, Issue 234, Part 1, pp. 523 – 533, 1994.

[BOU95] A.T. Bouloutas et al, “Distributed Fault Identification in Telecommunication Networks”, Journal of Network and Systems Management, Vol. 3, No. 3, pp. 295 – 312, 1995.

[BRA01] R. P. Braun and G. Grosskopf, "Optical Feeding of Base Stations in Millimeter-Wave Mobile Communications", Proceedings of the European Conference on Optical Communication 1998 (ECOC'98), Madrid, Spain, pp. 665 – 666, Sept. 2001.

[CAR01] B. Carbon, V. Girod, and G.Maury, "Optical Generation of Microwave Functions", Proceedings of the Workshop on Microwave Photonics for Emission and Detection of Broadband Communication Signals, Graduate School in Electronics and Communications (GSEC), Louvain-la-Nueve, Belgium, April 2001.

[CAS96] J.D. Case et al., "Protocol Operations for Version 2 of the Simple Network Management Protocol (SNMPv2)", IETF Network Working Group, RFC 1905, 1996.

[CHR76] N. Christofides, "Worst-Case Analysis of a New Heuristic for the Travelling Salesman Problem", Carnegie-Mellon University Management Sciences Research Report 388, Pittsburgh, Pa., Feb. 1976.

[DAM11] E. S. Moghaddam et al, "Physical Impairment of Monitoring Trails in All Optical Transparent Networks", 2011 3rd International Congress on Ultra Modern Telecommunications and Control Systems and Workshops (ICUMT), pp. 96 – 102, 2011.

[DEM99] P. Demeester et al., "Resilience in Multilayer Networks," IEEE Communications Magazine, Vol. 37, No. 8, pp. 70 – 76, 1999.

[DEN93] R.H. Deng, A.A. Lazar, and W.Wang, "A Probabilistic Approach to Fault Diagnosis in Linear Lightwave Networks", in H.G. Hegering, Y. Yemini (Eds.), Integrated Network Management III, North-Holland, Amsterdam, pp. 697 – 708, 1993.

[DUP89] A. Dupuy et al, "Network Fault Management: A User's View, in B.Meandzija, J.Westcott (Eds.), Integrated Network Management I, North-Holland, Amsterdam, pp. 101 – 107, 1989.

[FRI02] I. Frigyes, "Basic Microwave Properties of Optical Links: Insertion Loss, Noise Figure, and Modulation Transfer" in H. Al-Raweshidy, and S. Komaki (Eds.), "Radio over Fiber Technologies for Mobile Communications Networks", Artech House Inc, USA, pp. 1 – 61, 2002.

[FTT09] "Fiber Transmission Technologies Short, List Report", Deliverable D12, ReDeSign – 21701430, June 2009.

[FUK01] S. Fukushima et al, "10 to 110 GHz Tunable Opto-Electronic Frequency Synthesis Using Optical Frequency Comb Generator and Uni-Travelling-Carrier Photodiode", IEEE Photonics Electronic Letters, Vol. 37, No. 12, pp. 780 – 781, June 2001.

[FUM00] A. Fumagalli and L. Valcarenghi, “IP Restoration vs. WDM Protection: Is there an optimal choice?”, IEEE Network magazine, Vol. 14 , Issue 6, pp. 34 – 41, Nov.-Dec. 2000.

[GLI987] Gliese U. et al, "Multifunction Fiber-Optic Microwave Links Based on Remote Heterodyne Detection", IEEE Transactions on Microwave Theory and Techniques, Vol. 46, No. 5, 458 – 468, May 1998.

[GOL76] B. L. Golden, "Large-Scale Vehicle Routing and Related Combinatorial Problems", Ph.D. dissertation (unpublished), MIT Operations Research Center, Cambridge, Mass., June 1976.

[HAD10] A. Haddad, E. A. Doumith, and M. Gagnaire, “Meta-heuristic Approach for Monitoring Trail Assignment in WDM Optical Networks, 2010 International Congress on Digital Ultra Modern Telecommunications and Control Systems and Workshops (ICUMT), pp. 601 – 607, 2010.

[HIL01] A. Hills, "Large-Scale Wireless LAN Design", IEEE Communications Magazine, pp. 98 – 104, Nov. 2001.

[HO93] K. P. Ho.and J. M. Kahn, "Optical Frequency Comb Generator Using Phase Modulation in Amplified Circulation Loop", IEEE Photonics Electronic Letters, Vol. 5, No. 6, pp. 721 – 725, June 1993.

[HON03] Q. Honglin, "Research on Survivability and Survivable Networking of BPON", Optical Communication Technology, Vol. 9, pp. 29 – 32, 2003.

[HON91] P. Hong and P. Sen, “Incorporating Non-deterministic Reasoning in Managing Heterogeneous Network Faults”, in I. Krishnan and W. Zimmer (Eds.), Integrated Network Management II, North-Holland, Amsterdam, pp. 481 – 492, 1991.

[HOU95] K. Houck et al., “Towards a Practical Alarm Correlation System”, Integrated Network Management IV, Chapman and Hall, London, pp. 226 – 237, 1995.

[ISO96] ISO, Information Processing Systems-OSI, “ISO Standard 9596-1: Common Management Information Protocol”, Part 1: Specification, 1996.

[ITU02] ITU-T Recommendation G.983.6 (06/2002) ITU-T G.983.6 Telecommunication Standardization Sector of ITU-T, 2002.

[ITU03] ITU-T Recommendation G.709, "Interfaces for the Optical Transport Network", March 2003.

[ITU98] ITU-T Recommendation G.983.1, “Broadband Optical Access Systems Based on Passive Optical Networks (PON)”, 1998.

[JAF09] Z. A. Jaffari, K. M. Maamoun, and H. T. Mouftah, “LVM Fault-Localization Protocol Impact on The Survivability of All-Optical Networks”, Proceedings of 5th International Computer Engineering Conference ICENCO'2009, Faculty of Engineering, Cairo University, Egypt, pp. CCN2.4.1 – 6, Dec. 2009.

[JAK93] G. Jakobson and M.D. Weissman, “Alarm Correlation”, IEEE Network magazine, Vol. 7, No. 6, pp. 52 – 59, 1993.

[JAK95] G. Jakobson and M.D. Weissman, “Real-time Telecommunication Network Management: Extending Event Correlation with Temporal Constraints”, in: A.S. Sethi, F. Faure-Vincent and Y. Raynaud (Eds.), Integrated Network Management IV, Chapman and Hall, London, pp. 290 – 302, 1995.

[JIN07] S Jin, H. Li, and Y. Ji, “Survivability Characterization of PON”, Proceedings of CHINACOM '07, Second International Conference on Communications and Networking, Beijing, China, pp. 484 – 487, 2007.

[JOH006] L. A. Johansson and A. J. Seeds, "Millimeter-Wave Modulated Optical Signal Generation with High Spectral Purity and Wide-Locking Bandwidth Using a Fiber-Integrated Optical Injection Phase-Lock Loop", IEEE Photonics Technology Letters, Vol. 12, No. 6, pp. 690 – 692, June 2000.

[KAT12] B. Kantarci and H. T. Mouftah, “Availability and Cost-Constrained Long-Reach Passive Optical Network Planning”, IEEE Transactions on Reliability, Vol. PP, Issue 99, pp. 113 –124, 2012.

[KAT95a] I. Katzela and M. Schwartz, “Schemes for Fault Identification in Communication Networks”, IEEE/ACM Transactions on Networking, Vol. 3, No. 6, pp. 733 – 764, 1995.

[KAT95b] I. Katzela, A.T. Bouloutas, and S.B. Calo, “Centralized vs Dstributed Fault Localization”, in: A.S. Sethi, F. Faure-Vincent and Y. Raynaud (Eds.), Integrated Network Management IV, Chapman and Hall, London, pp. 250 – 263, 1995.

[KAT96] I. Katzela, “Fault Diagnosis in Telecommunications Networks”, Ph.D. Thesis, School of Arts and Sciences, Columbia University, New York, 1996.

[KAT97] S. Katker and K. Geihs, “A Generic Model for Fault Isolation in Integrated Management Systems”, Journal of Network and Systems Management, Vol. 5, No. 2, pp. 109 – 130, 1997.

[KHA08] M. Khair, J. Zheng and H.T. Mouftah, “Distributed Fault Localization for Multi-Domain All-Optical Networks without Power Monitoring”, Proceedings IEEE Networks‟, Budapest, Hungary, pp. A6.1.1-A6.1.7, September 2008.

[KIM05] H. B. Kim, “Radio over Fiber Based Network Architecture”, Ph.D. Thesis, Technischen Universitat Berlin, 2005.

[KLI95] S. Kliger et al, “A Coding Approach to Event Correlation”, in: A.S. Sethi, F. Faure-Vincent, and Y. Raynaud (Eds.), Integrated Network Management IV, Chapman and Hall, London, pp. 266 – 277, 1995.

[KOO01] Patent No. NL1019047, "Werkwijze en stelsel voor het via een multi-modus optische vezel overdragen van microgolfsignalen", octrooiaanvrage 1019047, indieningsdatum, door A.M.J. Koonen, Sep. 2001.

[KOO02] T. Koonen et al, “Microwave Signal Transport over Multimode Polymer Optical Fiber Networks for Feeding Wireless LAN Access Points”, Proceedings of the European Conference on Optical Communications ECOC’02, pp. 9.2.5.1 – 2, 2002.

[LAG99] Langley L. N. et al, "Packaged Semiconductor Laser Optical Phase-Locked Loop (OPLL) for Photonic Generation; Processing and Transmission of Microwave Signals", IEEE Transactions on Microwave Theory and Techniques, Vol. 47, No. 7, pp. 1257 – 1264, July 1999.

[LAM07] C. F. Lam, “Passive Optical Networks Principles and Practice”, Academic Press, USA, pp. 243 – 266, Oct. 2007.

[LAN99] L. N. Langley et al, “Packaged Semiconductor Laser Optical Phase-Locked Loop (OPLL) for Photonic Generation”, Processing and Transmission of Microwave Signals, IEEE Transactions on Microwave Theory and Techniques, Vol. 47, No. 7, pp. 1257 – 1264, 1999.

[LAR81] R. C. Larson and A. R. Odoni, “Urban Operations Research”, Prentice-Hall, ISBN: 0975914634, New Jersey, March 1981.

[LIE94] S. C.Liew and K. W. Lu, "A Framework for Characterizing Disaster-Based Network Survivability", IEEE Journal on Selected Areas in Communications, Vol. 1, No. 2, pp. 52 – 58, Jan 1994.

[LIM00] C. Lim et al, "Millimeter-Wave Broad-Band Fiber-Wireless System Incorporating Baseband Data Transmission over Fiber and Remote LO Delivery", Journal. of Lightwave Technology, Vol. 18, No. 10, pp. 1355 – 1363, Oct. 2000.

[LIN08] R. Lin, “Next Generation PON in Emerging Networks”, OFC/NFOEC 2008, pp. 1 – 3, 2008.

[LIU12] Y. Liu, L. Guo, and X. Wei, “Optimizing Backup Optical-Network-Units Selection and Backup Fibers Deployment in Survivable Hybrid Wireless-Optical Broadband Access Networks”, Journal of Lightwave Technology, Vol. 30, Issue 10, pp. 1509 – 1523, 2012.

[LIU99] G. Liu et al, “Composite Events for Network Event Correlation in Integrated Network Management”, IEEE Journal of Network and Systems Management VI, pp. 247 – 260, 1999.

[LO99] C. C. Lo and S. H. Chen, “A Scheduling-based Event Correlation Scheme for Fault Identification in Communications Network”, Computer Communications, Elsevier Science B.V., Vol. 22, No. 5, pp. 432 – 438, 1999.

[MAA07] K. Maamoun et al., “Performance Characterization of PON Technologies”, Proceedings of SPIE, Photonics North 2007, 4-7 June, 2007, Ottawa, Ontario, Canada , Vol. 6796, No.2, pp. 67962W.1-67962W.7, 2007.

[MAA09] K. M. Maamoun and H. T. Mouftah, “A Survey and a Novel Scheme for RoF-PON as FTTx Wireless Services”, 6th International Symposium on High-Capacity Optical Networks and Enabling Technologies (HONET), pp. 246 – 253, Dec 2009.

[MAA10a] K. Maamoun and H. Mouftah, “Survivable IP over Optical Transport Networks: Using Multi-layer Survivability Techniques Running in Different Network Layers to Achieve Certain Level of QoS for IP over Optical Transport Networks”, ISBN-10: 3843357072, LAP LAMBERT Academic Publishing, Sep. 2010.

[MAA10b] K. M. Maamoun and H. T. Mouftah, “Using Monitoring Trails (M-Trails) with Established Lightpaths to Perform Fault Localization in All- Optical Networks”, Proceedings of the 6th International Computer Engineering Conference (ICENCO'2010), Cairo, Egypt, pp 68 – 71, Dec 2010.

[MAA10c] K. M. Maamoun and H. T. Mouftah, “Novel Techniques for Deploying Monitoring Trails (M-Trails) for Fault Localization in All-Optical Networks”, Proceedings of the 7th International Symposium of High-capacity Optical Networks & Enabling Technologies’ (HONET'2010), Cairo, Egypt10, pp 26 – 32, Dec. 20.

[MAA11a] K. M. Maamoun and H. T. Mouftah, “Using Geographic Midpoint, the M-Trails Fault Localization Technique, as a Forced Routing Algorithm in All-Optical Networks, High Capacity Optical Networks and Enabling Technologies (HONET) 2011, pp. 305 – 310, 2011.

[MAA11b] K. M. Maamoun and H. T. Mouftah, “Survivability Models for Radio-over-Fiber Passive Optical Networks (RoF-PON)/PON”, Seventh International Computer Engineering Conference (ICENCO) 2011, pp. 13 – 18, 2011.

[MAE98] M. Maeda, “Management and Control of Transparent Optical Networks”, IEEE Journal on Selected Areas in Communications, Vol. 16, No. 7, pp. 1008 – 1023, 1998.

[MAI02] G. Maier, A. Pattavina, and S. De Patre, “Optical Network Survivability: Protection Techniques in the WDM Layer”, Photonic Network Communications, Vol. 4, Issues 3 – 4, pp. 251 – 269, July 2002.

[MAL99] A. Malis, “PPP over SONET/SDH”, RFC 2615, IEFT Network Working Group, June 1999.

[MAU97]. G. Maury et al, “Microwave Frequency Conversion Methods by Optical Interferometer and Photodiode”, IEEE Transactions on Microwave Theory and Techniques, Vol. 45, No. 8, pp. 1481 – 1485, 1997.

[MOR01] Morgado J. A. P. and Cartaxo A. V. T., "Dispersion Supported Transmission Technique: Comparison of Performance in Anomalous and Normal Propagation Regimes", IEEE Proceedings of Optoelectron, Vol. 148, No. 2, pp. 107 – 116, April 2001.

[MYN01] D. K. Mynbaev and L. L. Scheiner, “Fiber Optic Communications Technology”, ISBN-13: 978-0139620690, Prentice Hall, New Jersey, 2001.

[NGO02] A. Ng’oma, “Design of a Radio-over-Fiber System for Wireless LANs”, MTD. Report, Eindhoven University of Technology, Eindhoven, 2002.

[NOV04] D. Novak, “Fiber Optics in Wireless Applications”, OFC 2004, Short Course 217, 2004.

[OPA09] D.Opatic, “Radio over Fiber Technology for Wireless Access”, 32nd International Convention on Information and Communication Technology, Electronics and Microelectronics MIPRO 2009, pp. 202-227, 2009.

[ORE94] J. O’Reilly and P. Lane, "Remote Delivery of Video Services Using mm-Waves and Optics", Journal of Lightwave Technology, Vol. 12, No. 2, pp. 369 – 375, Feb. 1994.

[ORE95] J. O’Reilly, P. M. Lane, and M. H. Capstick , “Optical Generation and Delivery of Modulated mm-waves for Mobile Communications”, in B. Wilson, Z. Ghassemlooy, and I. Darwazeh (Eds.), “Analogue Optical Fiber Communications”, The Institute of Electrical Engineers, London, pp. 229 – 256, 1995.

[PAP76] C. H. Papadimitrio, "On the Complexity of Edge Traversing", Journal of ACM, Vol. 23, No. 3, pp. 544 – 554, 1976.

[SCH96] P.H. Schow, “The Alarm Information Base: A repository for Enterprise Management”, Proceedings of the. Second IEEE Internet Workshop on Systems Management, Los Alamitos, CA, pp. 142 – 147, 1996.

[SCH98] C. G. Schaffer et al, "Microwave Multichannel System with a Sideband Injection Locking Scheme in the 60 GHz Band"; Int Topical Meeting On Microwave Photonics, 1998 Tech Dig., pp. 67 – 69, 1998.

[SHA05] J. S. Shaik and N R Patil, “FTTH Deployment Options for Telecom Operators”, Sterlite Optical Technologies Ltd., White Paper, pp. 1 – 9, 2009.

[SHE03] P. Shen et al, “High-Purity Millimetre-Wave Photonic Local Oscillator Generation and Delivery”, Proceedings of the International Topical Meeting on Microwave Photonics MWP 2003, pp. 189 – 192, 2003.

[SIC06] A. V. Sichani, “Signaling Protocols for Survivable All-optical Networks”, Ph.D. Thesis, School of Information Technology and Engineering SITE, University of Ottawa, 2006.

[SIV05] K. M. Sivalingam and S. Subramaniam, “Emerging Optical Network Technology; Architecture, Protocols, and Performance”, Springer Science & Business Media, Inc., ISBN-13: 978-0387225821, New York, 2005.

[SON05] E. S. Son et al, “Survivable Network Architectures for Wavelength Division Multiplexed Passive Optical Networks”, OSA, Photonic Network Communications, Vol. 12, pp. 111 – 115, 2005.

[STE04] M. Steindera and A. Sethib, “A Survey of Fault Localization Techniques in Computer Networks”, Science of Computer Programming, Vol. 53, pp 165 – 194, July 2004.

[STE95] W. R. Stevens, “TCP/IP Illustrated”, Vol. 1, First Edition, Addison Wesley, ISBN-13: 978-0201633467, MA, 1995.

[SUU74] J. W. Suurballe, "Disjoint Paths in a Network", Networks, Vol. 4, 1974, pp. 125 – 145.

[SUU84] J. W. Suurballe and R. E. Tarjan, "A Quick Method for Finding Shortest Pairs of Disjoint Paths", Networks, Vol. 14, pp. 325 – 336, 1984.

[TAL12] A. Talia et al, “Optimal Selection of p-cycles on WDM Optical Networks with Shared Risk Link Group Independent Restorability using Genetic Algorithm”, Latin America Transactions, IEEE (Revista IEEE America Latina) , Vol. 10 , Issue 1, pp. 1385 – 1390, 2012.

[TAP09] J. Tapolcai, B. Wu, and P. H. Ho, “On Monitoring and Failure Localization in Mesh All-Optical Networks”, IEEE INFOCOM 2009, pp. 1008 – 1016, 2009.

[TAP11] J. Tapolcai et al, “A Novel Approach for Failure Localization in All-Optical Mesh Networks”, IEEE/ACM Transactions on Networking, Vol. 19, Issue 1, pp. 275 – 285, 2011.

[TAP12] J. Tapolcai et al, “Network-Wide Local Unambiguous Failure Localization (NWL-UFL) via Monitoring Trails”, submitted to IEEE/ACM Transactions on Networking, pp. 1 – 12, 2012.

[TRA12] N. Tran et al, “Dynamically Delivering Radio Signals by the Active Routing Optical Access Network”, IEEE Photonics Technology Letters, Vol. 24, Issue 3, pp. 182 – 184, 2012.

[WAK95] D. Wake, "Optoelectronics for Millimetre-wave Radio over Fiber Systems", in Wilson B., Ghassemlooy Z. and Darwazeh I. (Eds.), “Analogue Optical Fiber Communications”, The Institution of Electrical Engineers, London, pp. 202 – 227, 1995.

[WAL92] N. G. Walker, D. Wake, and I. C. Smith, "Efficient Millimetre-Wave Signal Generation Through FM-IM Conversion in Dispersive Optical Fiber Links", IEEE Electronic Letters, Vol. 28, No. 21, pp. 2027 – 2028, Oct. 1992.

[WAN09] X. Wang et al., “A Novel Highly Reliable WDM-PON System”, Asia Communications and Photonics Conference and Exhibition (ACP), Vol. 2009-Supplement, pp. 7633.1V.1 – 10, 2009.

[WAN12] K. Wang et al, ”Experimental Demonstration of a Full-Duplex Indoor Optical Wireless Communication System”, IEEE Photonics Technology Letters, Vol. 24, Issue 3, pp. 188 – 190, 2012.

[WAN89] Z. Wang, “Model of Network Faults”, in: B. Meandzija and J. Westcott (Eds.), Integrated Network Management I, North-Holland, Amsterdam, pp. 345 – 352, 1989.

[WAN89] Z. Wang, B. Meandzija and J. Westcott, “Model of Network Faults”, in “Integrated Network Management”, North Holland: Elsevier Science Publishers B.V., Amsterdam, pp. 345 – 352, 1989.

[WEI11a] H. Wei et al, “Monitoring Trail Allocation for Fast Link Failure Localization without Electronic Alarm Dissemination”, 2011 15th International Conference on Optical Network Design and Modeling (ONDM), pp. 84 – 89, 2011.

[WEI11b] H. Wei et al, “Monitoring Trail Allocation for SRLG Failure Localization”, 2011 IEEE Global Telecommunications Conference (GLOBECOM 2011), pp. 2692 – 2696, 2011.

[WEN00] Wen Y. J., Liu H. F., Novak D. and Ogawa Y., "Millimeter-Wave Signal Generation From a Monolithic Semiconductor Laser via Sub-harmonic Optical Injection", IEEE Photonics Tech. Letters; Vol. 12, No. 8, pp. 1058 – 1060, 2000.

[WU07] B. Wu, K. L. Yeung, “Monitoring Cycle Design for Fast Link Failure Detection in All-Optical Networks”, IEEE GLOBECOM ’07, pp. 2315 – 2319, 2007.

[WU08] B. Wu, P. H. Ho and K. Yeung, “Monitoring Tail: a New Paradigm for Fast Link Failure Localization in WDM Mesh Networks”, IEEE GLOBECOM ’08, pp. 1 – 5, 2008.

[WU09] B. Wu, P. H. Ho, and K. L. Yeung, “Monitoring Trail: On Fast Link Failure Localization in All-Optical WDM Mesh Networks”, Journal of Lightwave Technology, Vol.27, Issue 18, pp. 4175 – 4185, 2009.

[WU10a] B. Wu et al, “A Novel Framework of Fast and Unambiguous Link Failure Localization via Monitoring Trails, 2010 IEEE Conference on Computer Communications Workshops INFOCOM, pp. 1 – 5, 2010.

[WU10b] B. Wu et al, “Optimal Allocation of Monitoring Trails for Fast SRLG Failure Localization in All-Optical Networks”, 2010 IEEE Global Telecommunications Conference (GLOBECOM 2010), pp. 1 – 5, 2010.

[WU11a] B. Wu and K. Yeung, “M2-CYCLE: an Optical Layer Algorithm for Fast Link Failure Detection in All-Optical Mesh Networks”, Computer Networks, Vol. 55, Issue 3, pp. 748 – 758, 2011.

[WU11b] B. Wu et al, “Optical Layer Monitoring Schemes for Fast Link Failure Localization in All-Optical Networks”, IEEE Communications Surveys & Tutorials, Vol. 13, Issue 1, pp. 114 – 125, 2011.

[YEM96] S.A. Yemini et al., “High Speed and Robust Event Correlation”, IEEE Communications Magazine, Vol. 34, No. 5, pp 82 – 90, 1996.

[ZAH10] Y. Zhao et al, “A New Heuristic for Monitoring Trail Allocation in All-Optical WDM Networks”, 2010 IEEE Global Telecommunications Conference (GLOBECOM 2010), pp. ONS0.1.1 – 5, 2010.

[ZEN06] H. Zeng, C. Huang and A. Vukovic, “A Novel Fault Detection and Localization Scheme for Mesh All-optical Networks Based on Monitoring cycles”, Photonic Network Communications, Vol. 11, No. 3, pp 277 – 286, 2006.

[ZEN07] H. Zeng and A. Vukovic, “The Variant Cycle-cover Problem in Fault Detection and Localization for Mesh All-optical Networks”, Photonic Network Communications, Vol. 14, No. 2, pp. 111 – 122, 2007.

[ZHE04] J. Zheng and H. T. Mouftah, “Optical WDM Networks: Concepts and Design Principles”, Wiley-IEEE Press, ISBN: 0471671703, Hoboken, New Jersey, July 2004.

[ZHO00] D. Zhou and S. Subramaniam, “Survivability in Optical Networks”, IEEE Network Magazine, Vol. 14, Issue 6, pp.16 – 23, Nov.- Dec. 2000.

[ZOL94] A. Zolfaghari and F. J. Kaudel, "Framework for Network Survivability Performance", IEEE Journal on Selected Areas in Communications, Vol. 12, No.1, pp. 46 – 51, Jan. 1994.

Appendix A: Fault localization Process Difficulties

Fault localization is subject to complications resulting from complexity, unreliability, and non-determinism of communication systems. The following present common problems that have to be addressed by a fault localization technique:

- Fault evidence may be ambiguous, inconsistent, and incomplete [DUP89, HON91 and KAT95a].
- Ambiguity in the observed set of alarms stems from the fact that the same alarm may be generated as an indication of many different faults. Inconsistency results from a disagreement among devices with regard to the facts related to network operation; one device may have perception that a component is operating correctly, while another may consider the component faulty [SUU84]. Incompleteness is a consequence of alarm loss or delay [HON91]. It is essential that a fault management system be able to create a consistent view of network operation even in the presence of ambiguous, inconsistent, or incomplete information [SUU84].
- A fault management system should provide means to represent and interpret uncertain data within the system knowledge and fault evidence [DEN93, DUP89, HON91, and KLI95].
- A set of alarms generated by a fault may depend on many factors such as dependencies among network devices, current configurations, services in use

since fault occurrence, presence of other faults, values of other network parameters, etc. Due to this non determinism the system knowledge may be subject to inaccuracy and inconsistency. Fault evidence may also be inaccurate because of spurious alarms, which are generated by transient problems or as a result of overly sensitive fault detection mechanisms. When spurious symptoms may occur, the management system may not be sure which observed alarms should be taken into account in the fault localization process.

- An event management system should be able to isolate multiple simultaneous related or unrelated root causes [SUU84].
- The additional complication of fault localization results from the fact that different related and unrelated faults may happen within a short time period. The event management system should be able to isolate such problems even if they happen within a short time of one another and generate overlapping sets of alarms.

A fault localization process should try to find the optimal solution according to some accepted optimality criteria [KAT96].

Given that a single alarm may indicate different types of faults that occurred in different communication devices, fault localization may be unable to give a definite answer. Some approaches discussed here combine fault localization with testing to enable resolving these ambiguities. These approaches are usually tailored to locating specific network faults. In the general case, the lack of automated testing techniques makes it impossible to verify a possible answer in real-time [SUU84]. Therefore, some existing techniques try to isolate a set of probable fault hypotheses that may be later verified on- or off-line depending on the available testing techniques. Preferably, a confidence measure should be associated with each formulated hypothesis based on some measure of goodness [KAT96]. This measure may be a probability that a hypothesis is valid, its information cost, etc. The optimality criteria may include the minimum size of the hypotheses set, the lowest cost solution, the lowest error probability, etc.

Fault localization process in large networks should be performed in a distributed fashion [BOU95, KAT95b, and YEM96].

Communication networks become more and more advanced in terms of their size, complexity, speed, and the level of heterogeneity. Processing large volumes of information necessary to perform fault localization in such systems would be computationally prohibiting. It is also impractical to assume that the fault localization process has access to the information on the entire system. Many researchers [BOU95, KAT95b, and YEM96] have concluded that the fault localization process in large networks should be performed in a distributed fashion by a group of event management nodes with data and processing complexity divided among them. Each of the managers governs a subset of network hardware and/or software components within boundaries marked by protocol layers or network domains. Errors propagate horizontally—between peer associated devices within the same layer—and/or vertically—from upper layers to lower layers and vice versa between related services [WAN89].

They may cross boundaries of management domains. As a result, the fault management system may be provided with indications of faults that did not happen in its management domain and/or be unable to detect all symptoms of faults existing in its management domain [KAT95b and WAN89]. Therefore, distributed fault localization schemes are necessary that would allow the management nodes to reach the solution collectively.

A fault localization process has to take into account temporal relationships among events [JAK95, KAT96, and LIU99].

An important aspect related to fault localization is the representation of time. Events are related not only causally but also temporally. Therefore, the fault localization process has to provide means to represent and interpret the time associated with an event occurrence as well as a technique for correlating events related with respect to the time of their occurrence and duration.

Appendix B: Techniques for Transporting RF Signals over Optical Fiber

Several techniques for distributing and generating microwave signals via optical fiber exist. The techniques may be classified into two main categories namely Intensity Modulation - Direct Detection (IM-DD) and Remote Heterodyne Detection (RHD) techniques [GLI98]. The electrical signal at the head-end of the optical link can be one of three kinds that is: baseband, modulated IF, or the modulated RF signal itself. Doesn't matter what the kind is, the plan is to produce proper RF signals at the remote station, which meet the specifications of the wireless application. The RoF system may also perform modulation function in addition to transporting and frequency up-conversion of the data.

There are other factors than functionality, such as performance, complexity and power issues to be considered when selecting an appropriate RoF system to deploy. In general, the RoF system must be cost-effective for the particular application. This chapter reviews some of RoF techniques available. It covers the principle of operation as well as the pros and cons of the different techniques.

B.1 RF Generation by Intensity Modulation and Direct Detection [MAU97]

The simplest method for RoF is just directly modulating the intensity of the light source with the RF signal itself and then to use direct detection at the photo detector to get back the RF signal. This method falls under the IM-DD technique. There are two ways of modulating the light source. The laser diode can itself be modulated directly by using the appropriate RF signal to drive the laser bias current. The second option is to operate the laser in continuous wave (CW) mode and then use an external modulator such as the Mach-Zehnder Modulator (MZM), to modulate the intensity of the light. The two options are shown in Fig. B.1. In both cases, the modulating signal is the actual RF signal to be distributed. The RF signal must be appropriately pre-modulated with data.

After transmission through the fiber and direct detection on a PIN photodiode the photocurrent will be a replica of the modulating RF signal applied either directly to the laser or to the external modulator at the transmitter. The photocurrent undergoes trans-impedance amplification to yield a voltage that is in turn used to excite the antenna. If the RF signal used to modulate the transmitter is itself modulated with data, then the generated RF signal will be carrying the same data. The modulation format of the data is preserved. This is exactly how the pioneer 900 MHz RoF system given in Fig. 3.2 operates. Since the RF signal itself must be present at the head-end, this technique can be used for distribution purposes only as it provides no other radio-system functions.

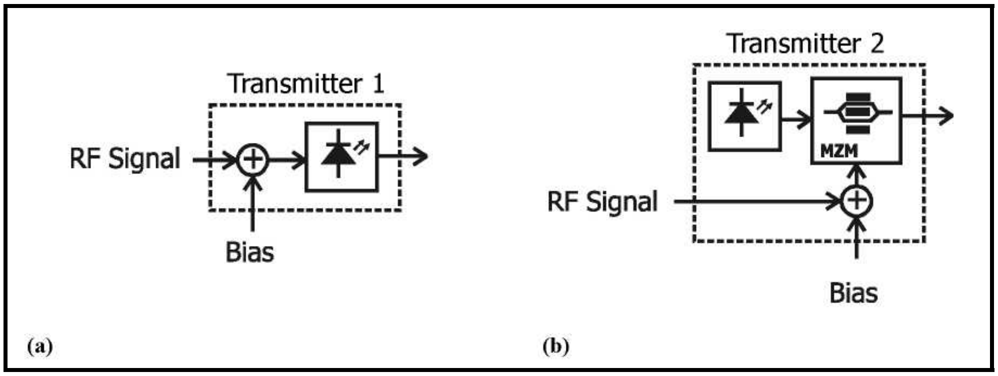

Fig. B.1: Generating RF Signals by Direct Intensity Modulation (a) of the Laser, (b) Using an External Modulator [MAU97]

B.1.1 Advantages of IM-DD

The advantage of this method is that it is simple. Secondly, if low dispersion fiber is used together with a (Linearized) external modulator, the system becomes linear. Consequently, the optical link acts only as an amplifier or attenuator and is therefore transparent to the modulation format of the RF signal [GLI98]. That is to say that both Amplitude Modulation (AM) based schemes and constant envelop based modulation schemes such as Phase Modulation (PM / QPSK) can be used. Such a system needs little or no upgrade whenever changes in the modulation format of the RF signal occur. Sub-Carrier Multiplexing (SCM) can also be used on such a system. Furthermore, unlike direct laser bias modulation, external modulators such as the Mach Zehnder Modulator (MZM) can be modulated with mm-wave signals approaching 100 GHz, though this comes with a huge cost regarding power requirements [ORE95].

B.1.2 Disadvantages of IM-DD

The disadvantage of this method lays in the fact that only low RF frequency signals can be generated (distributed). This is so because to generate higher frequency signals such as mm-waves, the modulating signal must also be at the same high frequency. For direct laser modulation, this is not possible due to lack of bandwidth, and laser non-linearity, which leads to inter-modulation product terms that cause distortions. On the other hand, external modulators such as the MZM can support high frequency RF signals. However, they require high drive voltages, which in turn lead to very costly drive amplifiers.

A further disadvantage of RFoF is that it is susceptible to chromatic dispersion, which induces frequency- or length-dependent amplitude suppression of the RF power, if Double Side Band modulation of the optical signal is used [NOV04], [FRI02]. The amplitude suppression effect may be modeled by the modulation transfer of the externally-modulated IM-DD system, which is given by the following equation [FRI02]:

$$\frac{i_{RF}}{I_o} = -\sqrt{2}m.\cos\omega_m\tau.\cos\left(\frac{\beta_2 L_f \omega_m^2}{2} - \frac{\pi}{4}\right) \quad \text{(B.1)}$$

Where ωm is the modulation frequency, β_2 is the second derivative of the propagation constant β (i.e. $\beta_2 = d^2\beta/d\omega^2$), Lf is the fiber length, and τ = t - (z/υg) with υg being the group velocity. From this equation, the fiber span of a 60 GHz IM-DD system operating at 1550 nm may be limited to just 1.5 km, when the first null occurs. The amplitude suppression effects may be overcome by using dispersion tolerant techniques such as Optical Single Side Band modulation [NOV04 and FRI02], which eliminates the transmission of a second sideband. This may be achieved by either filtering one of the sidebands off [HO93 and BEN99] or by using dual drive intensity modulators [NOV04]. All of this makes the OSSB IM-DD RoF system more complex.

B.2 The Principle of Photo detector-based Optical Heterodyning [MAU97]

Most RoF techniques rely on the principle of coherent mixing in the photodiode. These techniques are generally referred to as Remote Heterodyning Detection (RHD) techniques. While performing O/E conversion, the photodiode also acts as a mixer thereby making it a key component in RHD based RoF systems. However, this does not necessarily make it the most complex or expensive component in the entire system. Since most methods utilize coherent mixing, the principle is discussed first.

Two optical fields of angular frequencies ω_1 and ω_2 can be represented as:

$$E_1 = E_{01}\cos(\omega_1 t)$$
$$E_2 = E_{02}\cos(\omega_2 t) \quad \text{(B.2)}$$

If both fields impinge on a PIN photo detector, the resulting photocurrent on the surface will be proportional to the square of the sum of the optical fields. That is the normalized photocurrent will be:

$$i_{PIN} = (E_1 + E_2)^2 = E_{01}E_{02}\cos(\omega_1 - \omega_2)t + E_{01}E_{02}\cos(\omega_1 + \omega_2)t + \text{other terms} \quad \text{(B.3)}$$

The term of interest is $E_{01}E_{02}\cos(\omega_1 - \omega_2)t$ which shows that by controlling the difference in frequency between the two optical fields, radio signals of any frequency can be generated. The only limit to the level of frequencies that can be generated by this method is the bandwidth limitation of the photodiode itself [ORE95]. If we consider optical power signals instead of optical fields, then the generated photocurrent is given by:

$$i_{PIN} = 2R\sqrt{p_1(t)p_2(t)}\cos\left[\left(\omega_1(t) - \omega_2(t)\right)t + \phi_1(t) - \phi_2(t)\right] + \text{other terms} \quad \text{(B.4)}$$

Where R is the responsivity of the photo detector, t is the time, $p_1(t)$ and $p_2(t)$ are the two instantaneous optical power signals with instantaneous frequencies, $\omega_1(t)$ and $\omega_2(t)$ respectively. The instantaneous phases of the signals are given by $\varphi_1(t)$ and $\varphi_2(t)$ respectively.

Two laser diodes are made to emit light at frequencies (wavelengths) separated by the required microwave frequency. The two electric fields will then mix on the photodiode to yield an electrical signal as described above. However, since the relative offset between the two optical carriers is so small compared to the absolute frequencies of the carriers, any small frequency drift in either of the carriers translates into a major shift in the generated microwave frequency. This implies that, to keep a stable microwave signal at the output of the photodiode the relative offset between the emission frequencies must be kept constant. In other words, absolute shifts in emission frequencies are not important, but the relative offset only. Normally, only one of the two optical carriers is modulated with data.

Given that the laser emission frequency is highly sensitive to temperature variations, phase noise and other effects, techniques to maintain the required frequency offset have to be used. There are several methods for controlling the relative frequency offset between the two lasers. These include:

- Optical Frequency-Locked Loop (OFLL)
- Optical Phase-Locked Loop (OPLL)
- Optical Injection Locking (OIL) and

- Optical Injection Phase-Locked Loop (OIPLL)

B.2.1 Advantages of Optical Heterodyning

Using optical heterodyning, very high frequencies can be generated, limited only by the photo detector bandwidth. Furthermore, heterodyning yields high-detected power (higher link gain) and higher carrier-to-noise ratio (CNR). This is so because all the optical powers of the two optical fields contribute to the power of the generated microwave signal.

Remote heterodyning has an inherent advantage concerning chromatic dispersion. If only one of the two optical carriers is modulated with data, system sensitivity to chromatic dispersion can be reduced greatly. This is not possible in direct intensity modulation based methods, where the two optical sidebands end up both being modulated with data. Reducing chromatic dispersion effects is very important in phase noise sensitive applications such as Orthogonal Frequency Division Multiplexing (OFDM) and systems carrying phase modulated data such as QPSK.

An important attribute of RHD is that it permits low frequency data modulation at the switching centre since the high frequency microwave is not generated there but at the remote station. Therefore, in contrast to IMDD, the RHD modulator at the switching centre may be driven either with baseband data or by a low frequency RF signal. Low frequency modulators generally have low $V\pi$ and therefore require lower drive levels.

Consequently, low frequency modulators are easier to linearize. Furthermore, linear drive amplifiers are more readily available and less costly for baseband or low frequency modulation applications. At the remote side, the need for mm-wave frequency filters is eliminated when baseband data is used.

A further advantage of optical heterodyning is that it is capable of producing signals with 100% intensity modulation depth [ORE95]. Other benefits of RHD include photonic signal processing and radio system function capabilities such as phase control, filtering, frequency conversion [GLI98 and CAR01].

B.2.2 Disadvantages of Optical Heterodyning

The major drawback of this method is the requirement for the two optical carriers to be phase correlated. In other words, the phase noise in the laser sources directly translates into phase noise of the generated RF. Therefore, the generated RF signal is very sensitive to phase noise occurring in the optical link. Since semiconductor lasers are prone to phase noise, extra measures to minimize the noise have to be taken. These measures often lead to more complex systems. Techniques used to reduce phase noise sensitivity include Optical Phase Locked Loops (OPLL) and Optical Injection Locking (OIL), which are discussed in the sections that follow below.

B.3 Optical Frequency/Phase Locked-Loops (OFLL/OPLL)

The basic configuration of OFLL and OPLL techniques is shown in Fig.B.2. It consists of a free running master laser, a PIN photodiode, a microwave amplifier, a frequency or phase detector, a loop filter, a slave laser and a microwave reference oscillator. The combined outputs of the master and slave lasers are split into two parts. Part of the optical signal is used in the OP/FLL at the head-end while the other part is transmitted to the remote station. The optical signal at the head-end is heterodyned on a photodiode generating a microwave signal. The generated microwave signal is compared to the reference signal. A phase error signal in the case of OPLL (and a frequency error signal in the case of the OFLL) is fed back to the slave laser. In this way, the slave laser is forced to track the master laser at a frequency offset corresponding to the frequency of the microwave reference oscillator.

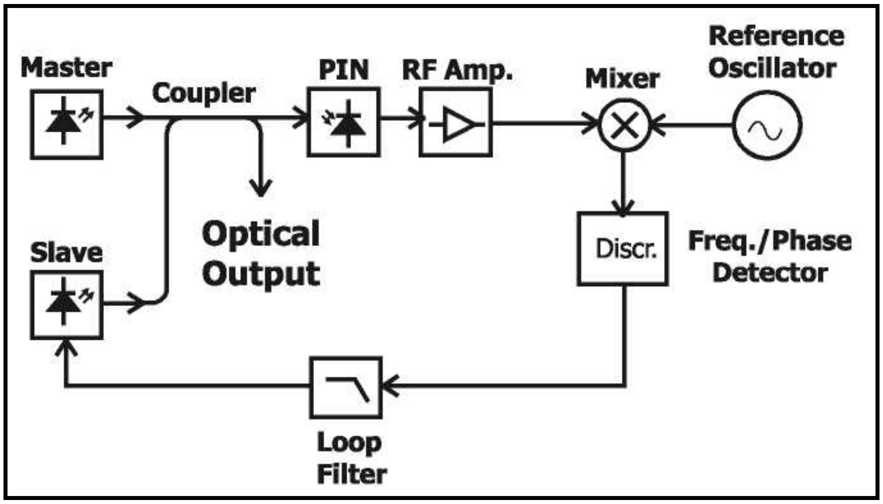

Fig. B.2: Principle of Optical Frequency-/Phase-Locked Loop [LAG99]

As the names suggests, OFLL strives to maintain the required mean frequency offset. It ignores small-scale frequency variations caused by phase noise. On the other hand, OPLL is able to track small scale phase perturbations as well. A packaged OPLL system based on semiconductor lasers capable of producing very narrow line-width microwave signals up to 14 GHz is reported in [LAG99].

B.3.1 Advantages of OFLL/OPLL

Because OPLL techniques track small phase variations they are capable of producing high quality RF signals with narrow line-width. OPLLs also have good temperature tracking capabilities. In addition, OPLLs exhibit a wide locking range. On the other hand, OFLL techniques have the advantage that they can be realized with standard and fairly inexpensive DFB lasers [ORE95].

B.3.2 Disadvantages of OFLL/OPLL

The disadvantage of OFLL techniques is that they generate microwave signals with broad line-widths. The line-width of the signal generated by the OFLL system is roughly the sum of the line-widths of the lasers. This is a consequence of the fact that OFLLs maintain only the mean frequency offset. In addition to this, the instantaneous frequency of the generated microwave signal is equal to the instantaneous frequency difference between the two beating optical fields. Therefore, in order to produce narrow line-width microwave signals using OFLL, lasers with narrow line-widths are necessary. However reducing the source line-width reduces the maximum power that can be transmitted in the fiber without experiencing severe attenuation due to Stimulated Brillouin Scattering (SBS) [ORE95]. Therefore, there is a practical limit to the narrowness of the laser line-width.

The major drawback of OPLLs is that they require far more complex laser structures such as 3-contact DFBs. This requirement is a direct consequence of the fact that to track the frequency perturbations of the master laser, the tuning rate of the slave laser must be sufficiently high. This also implies that sufficient feedback bandwidth must be available. The required feedback bandwidth is determined by the summed laser line-width, the requirements for loop stability, and phase noise requirements placed on the optical microwave signal by the system in which the OPLL is to be applied. A wide feedback bandwidth is necessary if semiconductor lasers are used, because they have a large amount of phase noise. In order to achieve the wide feedback bandwidth, the loop-propagation delay must be small. In addition to this, the response bandwidths of the microwave components, together with the slave laser FM response, must be wide and uniform in both magnitude and phase [LAG99]. These requirements are not easy to fulfill. They make the design and construction of OPLL components challenging.

B.4 Optical Injection Locking

Optical Injection Locking (OIL) is a technique that involves modulating the master laser with a low frequency signal, f_{Ref}, which is a sub-harmonic of the cavity round trip of the slave laser. The spectrum of the master laser therefore comprises several sidebands separated by the sub-harmonic frequency, f_{Ref}. The modulating signal of the master is the reference signal. Part of the output of the master laser is fed into the slave laser. Since f_{Ref} is a sub-harmonic of the slave laser's resonant frequency, there will be an nth sideband of the modulated master laser's output that will coincide with the slave laser's frequency as shown in Fig.B.3. This will cause the slave laser to lock onto the master's sideband frequency and resonate there. The offset of the slave's emission frequency from the master's will therefore vary with both the master central frequency and the reference signal f_{Ref}. If f_{Ref} is kept constant, the slave's emission frequency will be able to track variations in the master's emission frequency, keeping the emitted mm-wave signal frequency constant. Using this technique, the generation of a 35 GHz mm-wave signal with a detuning frequency range larger than 300MHz has been demonstrated [WEN00]. And a system-wide set-up based on the OIL technique and used to generate a 63 GHz mm-wave signal carrying 155 Mbps data is reported in [SCH98].

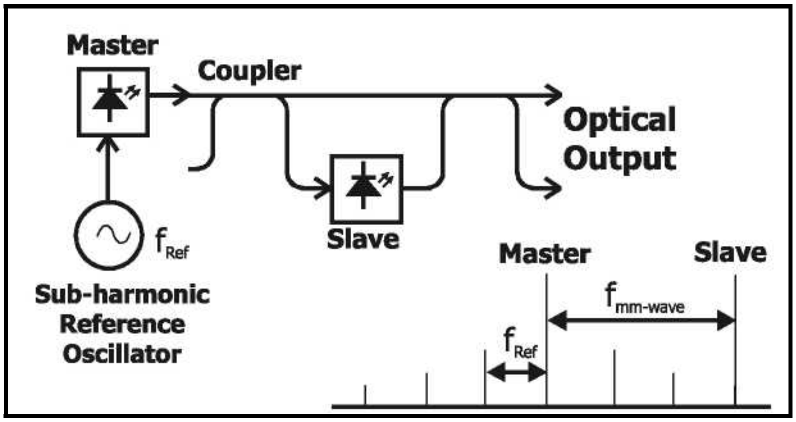

Fig. B.3: Optical Injection Locking [WEN00]

B.4.1 Advantages of OIL

One advantage of using OIL is that cheaper broad-line-width lasers can still be used to generate stable narrow electrical line-width signals. Secondly, OIL exhibits good phase noise suppression. Thirdly, because the slave laser locks on to a sub-harmonic of its resonance frequency, low frequency reference signals are used. These are simpler and easier to achieve.

B.4.2 Disadvantages of OIL

The major disadvantage of OIL is that it has a small frequency detuning range. Optimum phase noise suppression occurs only at one point of slave laser detuning relative to the free-running frequency.

B.5 Optical Injection Phase Locked Loop (OIPLL)

The Optical Injection Phase Locked Loop (OIPLL) technique combines both OPLL and OIL principles. The objective is to combine the benefits of both techniques and to complement their weaknesses. The principle of OIPLL is shown in the schematic of Figure B.4.

In the OIPLL system, the master laser is modulated at a sub-harmonic frequency of the desired mm-wave just like in OIL. A small part of the master's output is then injected into the slave laser diode through the optical circulator. The slave laser is then tuned to lock to the nth harmonic sideband of the injected master laser's light. The outputs of both the master and the slave lasers are combined and made available at the output as shown. Just as it is in OIL the required mm-wave frequency is the offset between the two optical frequencies. A small part of the combined optical signals is sent to the OPLL. At the photo detector heterodyning takes place. The generated microwave signal at the photo detector is amplified and then compared with reference signal. This comparison takes place in a balanced mixer, which is sub-harmonically pumped. The output is then passed through the loop filter. The filtered signal is converted to a current signal and then added to the injection current of the slave laser. In this way, two-phase control mechanisms - OIL and OPLL are combined.

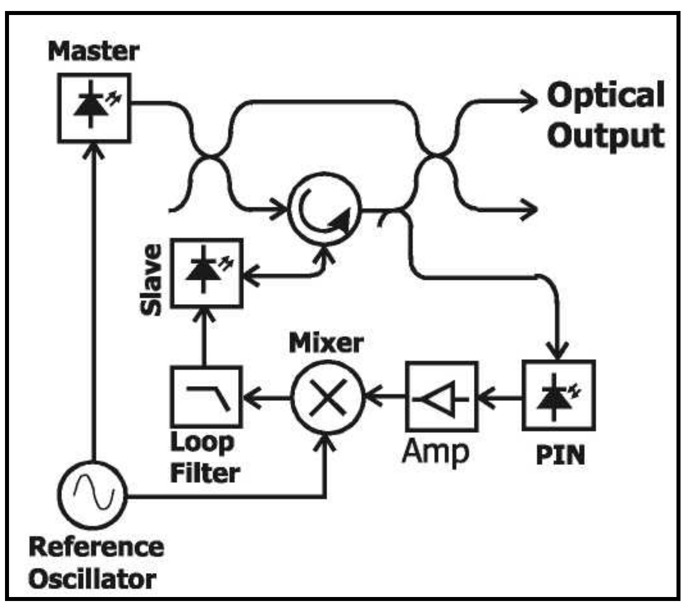

Fig. B.4: The Principle of Operation of the Optical Injection Phase Locked Loop (OIPLL) Technique [ORE95]

This technique has been used to generate 36 GHz mm-waves of very narrow line-width of a few kHz only. OIPLL has been shown to have the ability to increase the locking range of an OIL system from 2 GHz to 30 GHz when OPLL is activated [JOH00]. A Radio-over-Fiber system employing the OIPLL technique to generate a 36 GHz microwave signal modulated with 140 Mbps is reported in [ORE95].

Another way to generate the sidebands is to use an amplified fiber loop Optical Frequency Comb Generator (OFCG) as shown in Fig.B.5 [FUK01]. The OFCG generates a wide comb of optical frequencies. Two sidebands with the desired frequency difference are selected and subsequently heterodyned to generate the desired microwave signal. The filtering is achieved by using two slave lasers mode-locked on two different frequencies separated by the required microwave. This technique is therefore a combination of OFCG and OIL techniques. With the OFCG system, mm-waves at extremely high frequencies may be generated. For example the technique was used to generate precise signals of high spectral purity from 10 to 110 GHz [FUK01]. A high speed Uni-Travelling-Carrier Photodiode (UTC-PD) was used in the experiments.

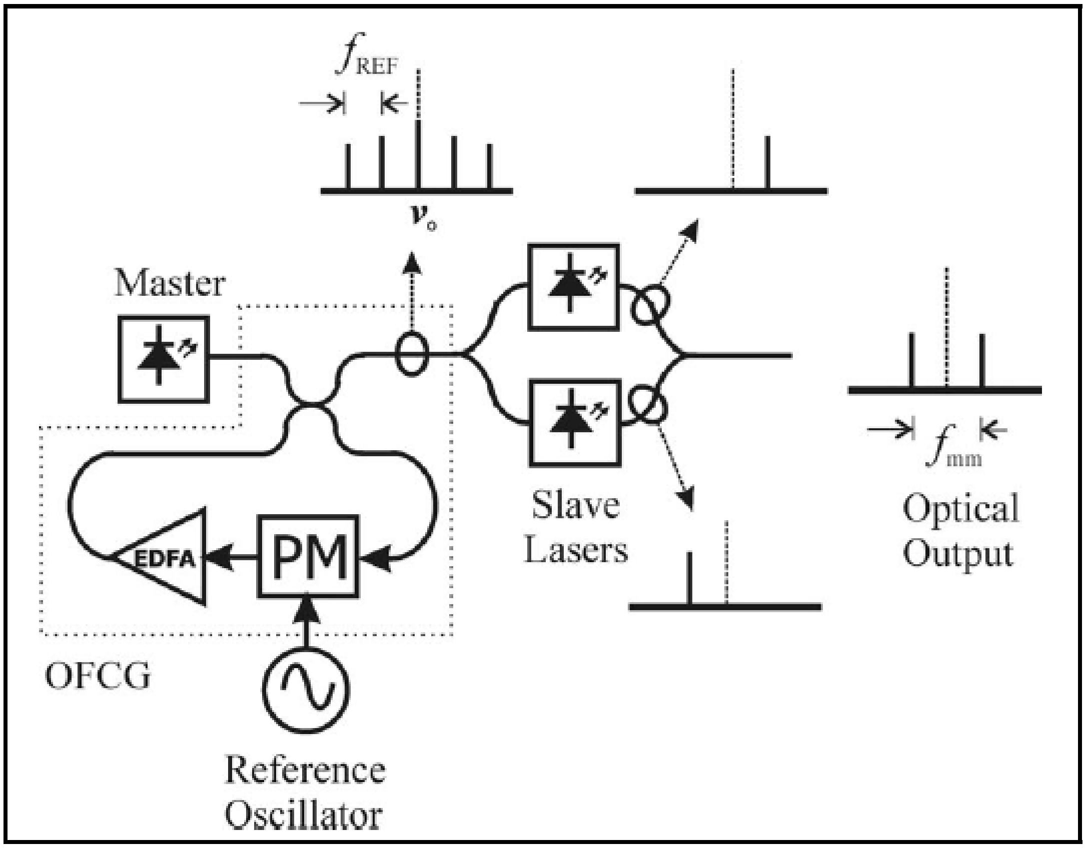

Fig. B.5: Optical Frequency Comb Generator for Carrier Generation Through Heterodyning [FUK01]

B.5.1 Advantages of OIPLL

As stated earlier, OIPLL seeks to combine the benefits OIL and OPLL techniques thereby complementing their weaknesses. Therefore OIPLL benefits from the low phase noise exhibited by OIL while having an extended locking range provided by the OPLL part of the system. In addition, the short loop propagation delay required in OPLL becomes less important. Furthermore, OIPLL does not require narrow line-width lasers but performs well with ordinary broad line-width lasers, which are cheaper.

B.5.2 Disadvantages of OIPLL

The disadvantage of OIPLL lies in the complexity of the technique itself being a hybrid of two complex techniques.

B.6 Dual Mode Lasers

The major drawback of optical heterodyning based techniques is the sensitivity to phase noise, and the dependence of the two heterodyning signals on their respective states of polarization. There are several techniques used to improve beat signal phase noise. They range from reducing laser line-width by use of external cavities to the use of electrical or optical feedback techniques to control and lock the frequency or phase. The later techniques have been discussed above. They employ two lasers and some kind of external feedback control loop to enable the slave to track the master frequency. A different approach to reducing beat signal phase noise is to ensure that the optical modes are correlated. When this happens, the beat noise cancels out. Correlation of optical modes can be achieved by having both optical modes in the same cavity. One way to do so is to remove the phase shift in the DFB laser so that no oscillation occurs at the Bragg frequency. What results is referred to as a dual mode laser as it supports two modes, one on either side of the Bragg frequency. The required mode separation is obtained by tuning the grating strength coefficient.

A dual mode laser designed to test the viability of this technique showed that direct electrical injection at a sub-harmonic of the beat frequency was still needed in order to generate a pure mm-wave [ORE95]. In the reported experiment, a 57 GHz mm-wave was generated using a 6.3 GHz (9th harmonic) injected reference signal.

.

B.7 Optical FM-Filter System

The Optical FM-Filter technique is a single-laser technique that involves modulating the optical frequency by applying an electrical signal to one of the laser's terminals. This generates a series of optical spectral lines (sidebands) all spaced by the drive frequency as shown in Fig. B.6. Two sidebands are then selected. The sidebands must be separated by the required RF frequency, which is normally in the mm-wave range of frequencies. The selected sidebands subsequently impinge on the surface of the photodiode and mix coherently to generate the desired RF signal as discussed earlier.

There are three commonly used methods for selecting the required sidebands. These are:

- Simple optical filtering
- Semiconductor Optical Amplifier (SOA) and
- Injection-locked lasers

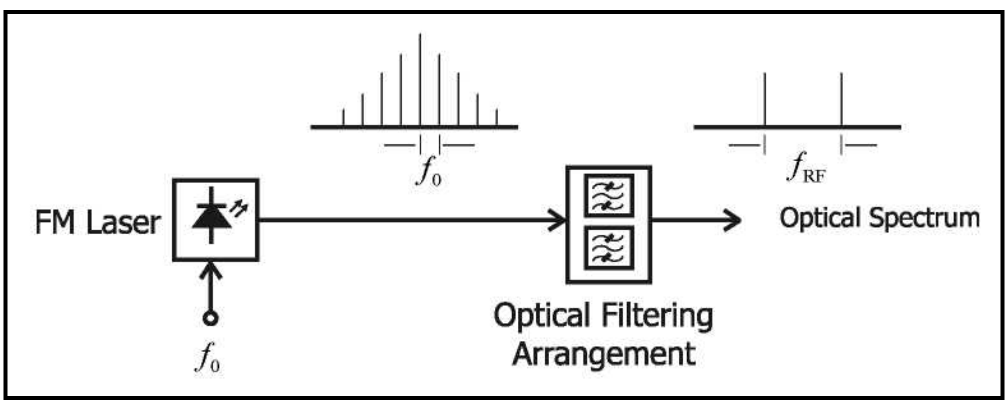

Fig. B.6: Optical Coherent Mixing Based on The FM Laser [ORE95]

Using an optical filter, the required sidebands are selected while the rest are rejected as shown in Fig. B.7. This approach was used to remotely deliver mm-wave signals at 54 GHz, 90 GHz and 126 GHz to a RAU fed by a 9 km SMF link [SHE03]. An optical phase modulator was driven by an IF signal at either 13.5 GHz or 22.5 GHz, to generate a series of sidebands. A tunable Fiber Fabry Perot Interferometer (FFPI) was used to select two sidebands separated by the desired mm-wave frequency. The FFPI had a Free Spectral Range (FSR) of 17.963 GHz, and a Finesse of 100. The filtered optical signal was transmitted over the length of the fiber link, amplified, and detected with a waveguide based photo mixer. The power of the detected mm-wave signal at 90 GHz was -8 dBm. The measured phase noise of the 90 GHz signal at 100 kHz offset was -95 dBc/Hz, which was 13 dB higher than that of the 22.5 GHz reference signal. Two problems with this scheme were highlighted – namely polarization sensitivity attributed to the photo mixer, and the severely limited tuning range, which was just 360 MHz (6 dB) [SHE03]. On the other hand, the SOA selects and amplifies the desired sidebands above the rest.

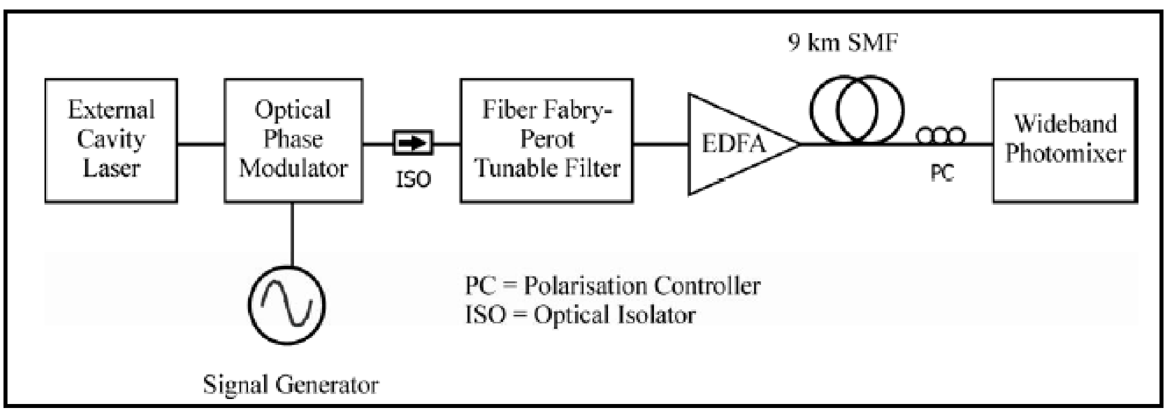

Fig. B.7: Remote Heterodyning by Using a Filter to Select the Mixing Sidebands [SHE03]

B.7.1 Advantages of FM-Filter System

Using this technique high frequency RF signals with very narrow line-width can be generated. Generation of signals with frequencies of up to 35 GHz with a 10 Hz line-width has been reported in [ORE95].

B.7.2 Disadvantages of FM-Filter System

The major disadvantage lies in the fact that the sideband selection system must accurately track any shifts in the position of the sidebands. In addition to this, very selective optical filtering is required. These issues sometimes lead to very complex circuitry

B.8 Techniques Based on Harmonics Generation

B.8.1 The FM - IM Conversion Technique

The FM - IM conversion technique is interesting in that it thrives on the otherwise undesired fiber chromatic dispersion to work. The conversion from an FM modulated signal to an Intensity Modulated one is performed by the fiber's chromatic dispersion itself. Here is how the technique works. An FM laser is FM modulated by applying a drive signal to one of its terminals. This produces an optical spectrum that consists of spectral lines spaced by the drive frequency. The FM optical signal is then propagated over dispersive fiber. Due to chromatic dispersion effects, the relative phasing of the optical sidebands is altered leading to intensity fluctuations of light at harmonics of the drive frequency. This technique of generating microwaves has been analyzed theoretically and demonstrated experimentally in [ORE95 and MYN01]. For the case of an FM modulated optical signal and standard SMF with chromatic dispersion, the instantaneous optical intensity received after propagating through the fiber is given by

$$i(t) = I_o + \sum_{p=1} 2\left|I_p\right| \cos\left(p\omega t + \xi_p\right) \quad \text{(B.5)}$$

Where I_p is the pth harmonic component of intensity variation, with I0 being the dc photocurrent. The parameter ω is the modulating angular frequency, and ξ_p is the phase of the pth harmonic. The pth harmonic component I_p is given by:

$$I_p = J_p\left(2\beta \sin(p\phi)\right) \quad \text{(B.6)}$$

Where $J_p(x)$ is the Bessel function of the first kind, β is the FM modulating index (or phase modulation index) and φ is an angle characterizing the fiber dispersion given by:

$$\phi = -\frac{w^2}{4\pi}\frac{D\lambda^2}{c} z \quad \text{(B.7)}$$

Where λ is the free space wavelength of the laser, c is the speed of light, z is the fiber length, and D is the fiber group dispersion parameter.

If the modulation depth M_p of the pth harmonic is defined as the ratio of the amplitude of the alternating photocurrent at the pth harmonic to the dc photocurrent, then M_p will be given by:

$$M_p = \left|2J_p\left(2\beta \sin(p\phi)\right)\right| \quad \text{(B.8)}$$

In demonstration experiments, the FM-IM technique was used to generate mm-waves up to 60 GHz (15th harmonic of 4 GHz drive signal). In theory the maximum achievable modulation depth is 60% for the 10th harmonic. However, only 13% modulation depth was achieved in practice. This was attributed to inherent intensity modulation present in the laser output (i.e. optical signal was not pure FM) [MYN01]. The FM-IM modulation technique has also been used to overcome the chromatic dispersion limit of SMF in digital transmission systems where it is referred to as Dispersion Supported Transmission (DST) [MOR01].

B.8.1.1 Advantages of FM - IM

FM - IM conversion technique can be used to generate mm-waves at very high frequencies efficiently. It is a simple technique to implement, which exploits the undesirable fiber chromatic dispersion to operate.

B.8.1.2 Disadvantages of FM - IM

The obvious drawback of this technique is that the modulation depth varies with the fiber length. However, it can be argued that varying the FM index can compensate for the effect of length dependency of the modulation depth. Unfortunately, lasers with good broadband FM response are not readily available. The FM laser must be capable of wide optical frequency deviation at microwave rates. In general the peak-to-peak frequency deviation must at least be equal to the millimeter-wave frequency desired [ORE95]. To solve the problem of intensity modulation inherent in the directly modulated FM laser, an external phase modulator in combination with a CW laser could be used. Using this approach, theoretical modulation depths are realizable in practice.

B.8.2 Modulation Sideband Techniques

There are two modulation side band techniques dubbed *2f* and *4f* methods. Unlike the FM-IM technique, these techniques generate high order harmonics without recourse to dispersive fiber by relying on the non-linear transfer characteristic of the Mach Zehnder amplitude modulator (MZM). The output of the MZM in terms of the E-field can be described by:

$$E_{out}(t) = E_{in}(t)\cos\left(\frac{\pi}{2}\frac{V_{\mathrm{mod}}(t)}{V_\pi}\right) \quad \text{(B.9)}$$

Where $E_{in}(t)$ is the optical field applied to the input of the modulator, $V_{mod}(t)$ is the modulating voltage applied to the modulator, and V_π is the modulating voltage required to totally suppress the output. If the modulating voltage $V_{mod}(t)$ is sinusoidal, it can be shown that the output field may be written in the form [ORE95]:

$$\begin{aligned} E_{out}(t) = &\frac{1}{2}J_0\left(\alpha\frac{\pi}{2}\right)\cos\left(\frac{\pi}{2}(1+\varepsilon)\right)\cos(\Omega t) \\ &-\frac{1}{2}J_1\left(\alpha\frac{\pi}{2}\right)\sin\left(\frac{\pi}{2}(1+\varepsilon)\right)\cos(\Omega t \pm \omega t) \\ &+\frac{1}{2}J_2\left(\alpha\frac{\pi}{2}\right)\cos\left(\frac{\pi}{2}(1+\varepsilon)\right)\cos(\Omega t \pm 2\omega t) \\ &-\frac{1}{2}J_3\left(\alpha\frac{\pi}{2}\right)\sin\left(\frac{\pi}{2}(1+\varepsilon)\right)\cos(\Omega t \pm 3\omega t) \\ &+\ldots \end{aligned} \quad \text{(B.10)}$$

Where J_i is the ith Bessel function of the first kind, ε is the normalized bias, and α is the drive level. The equation shows that by adjusting the bias to appropriate levels $\varepsilon=0$, or $\varepsilon=1$, the 2nd or 4th order harmonics of the drive signal may be generated.

B.8.2.1 The *2f* Method

To realize this method, the MZM is biased at V_π, which means that $\varepsilon = 0$. This will suppress the component at the optical central frequency, Ω as well as all other even components at $\Omega \pm 2\omega$, $\Omega \pm 4\omega$, etc. What remains are two strong components separated by 2ω and centered on Ω as shown in Fig.B.6, and higher order odd terms. The higher order terms have lower amplitudes and can be reduced to 15dB below the two major components by careful control of the bias point [ORE94]. The modulated optical signal is transported across the fiber length up to the remote station. When the two strong components separated by 2ω impinge on the photodiode, they are heterodyned to generate a microwave signal with angular frequency equal to 2ω. In other words, the generated microwave signal has a frequency that is double the frequency of the modulating signal $f_{mm} = 2f_{mod}$. This doubling in frequency is what leads to the name *2f* method. Adding data modulation is achieved by filtering one of the optical sideband components and then modulating it with the data before combining and transmitting both components, as shown in Fig. B.8.

B.8.2.2 *4f* Method

The *4f* method is an extension to the frequency doubling *2f* method discussed above. In this case the bias level is chosen such that $\varepsilon = 1$. This leads to the suppression of all odd harmonics. The optical spectrum then consists of spectral lines located at the central optical angular frequency, ω and on each side of the central frequency separated by 2ω. By carefully choosing the drive voltage α such that $J_0 (\alpha \pi/2) = 0$ the central component at Ω can be suppressed. This happens when $\alpha\pi/2 \sim 2.4$ or $\alpha \sim 1.53$. The resulting optical spectrum now consists of two main components separated by four times the drive frequency of the modulator. Heterodyning at the photodiode produces a high frequency electrical signal $f_{mm} = 4f_{mod}$ at four times the drive frequency, hence the term *4f* method. Data modulation is added in a similar fashion to the *2f* method.

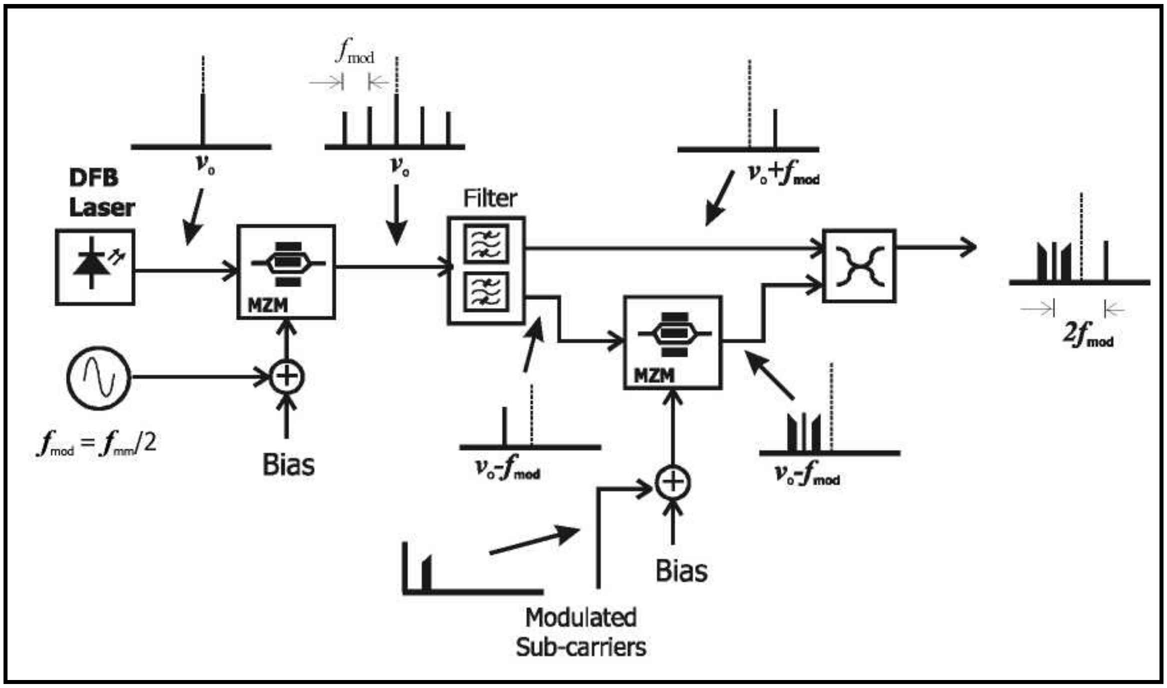

Fig. B.8: The 2f Technique for Generating Millimeter –Wave [LIM00]

A modified *2f* method is reported in [LIM00]. In this technique, baseband data is transmitted as such, up to the remote station where it is up-converted. The Local Oscillator required for up-conversion is also transmitted over the fiber. This is achieved by using a dual electrode Mach Zehnder modulator to modulate the output of a DFB laser. One of the two electrodes is driven with baseband data while the other one is driven with an RF signal at half the required LO frequency (i.e. $1f_{LO}$). Both electrodes are biased at the quadrature points. The resulting optical spectrum comprises the optical carrier modulated with baseband data and two sidebands spaced at $1f_{LO}$ from the carrier.

The modulated optical signal is transported over the fiber to the remote base station where both direct detection and heterodyning take place on a high-speed photodiode. The baseband data is recovered from the optical carrier through direct detection. In addition, the beating of the two side bands with the modulated carrier generates an RF signal (Modulated with data) at the frequency $1f_{LO}$. A third signal is generated at f_{LO} due to the beating of the two sidebands with each other. The modulated electrical signal at $1f_{LO}$ is discarded while the generated electrical signal at f_{LO} is used as the LO for up-converting the recovered baseband data as shown in Fig. B.9. The figure shows the use of the modified *2f* technique to generate 34 GHz mm-waves in a 37.5 / 34.8 GHz experimental set-up of a full duplex broadband wireless system with simultaneous bi-directional data transmission (155 / 622 Mbps) [LIM00].

An alternative approach for the *4f* method is discussed in [ORE94]. The method uses two Mach Zehnder Interferometer (MZI) filters and two MZMs. One of the MZM is modulated with the 4^{th} sub-harmonic while the other with data modulated sub-carriers. This approach is more complex and requires modulators that allow access to both arms.

B.8.2.3 Advantages of the *2f* and *4f* methods

Both the *2f* and *4f* methods rely on optical heterodyning. Therefore, they are capable of generating high frequency mm-waves. Since the same laser generates both optical fields, the phase noise is highly correlated resulting in very narrow line-width mm-waves. In fact, the performance of these methods in terms of phase noise is comparable to the OPLL system. The modulation depths achievable with these techniques in practice are larger than in FM-IM techniques. A comparison between the theoretical and the practically achievable modulation depths is reported in [ORE95].

B.8.2.4 Disadvantage of the *2f* and *4f* methods

The main disadvantage of these techniques is the need for filtering one of the sidebands for data modulation. Temperature control is very important in order to keep the filter aligned with the optical side band to be filtered

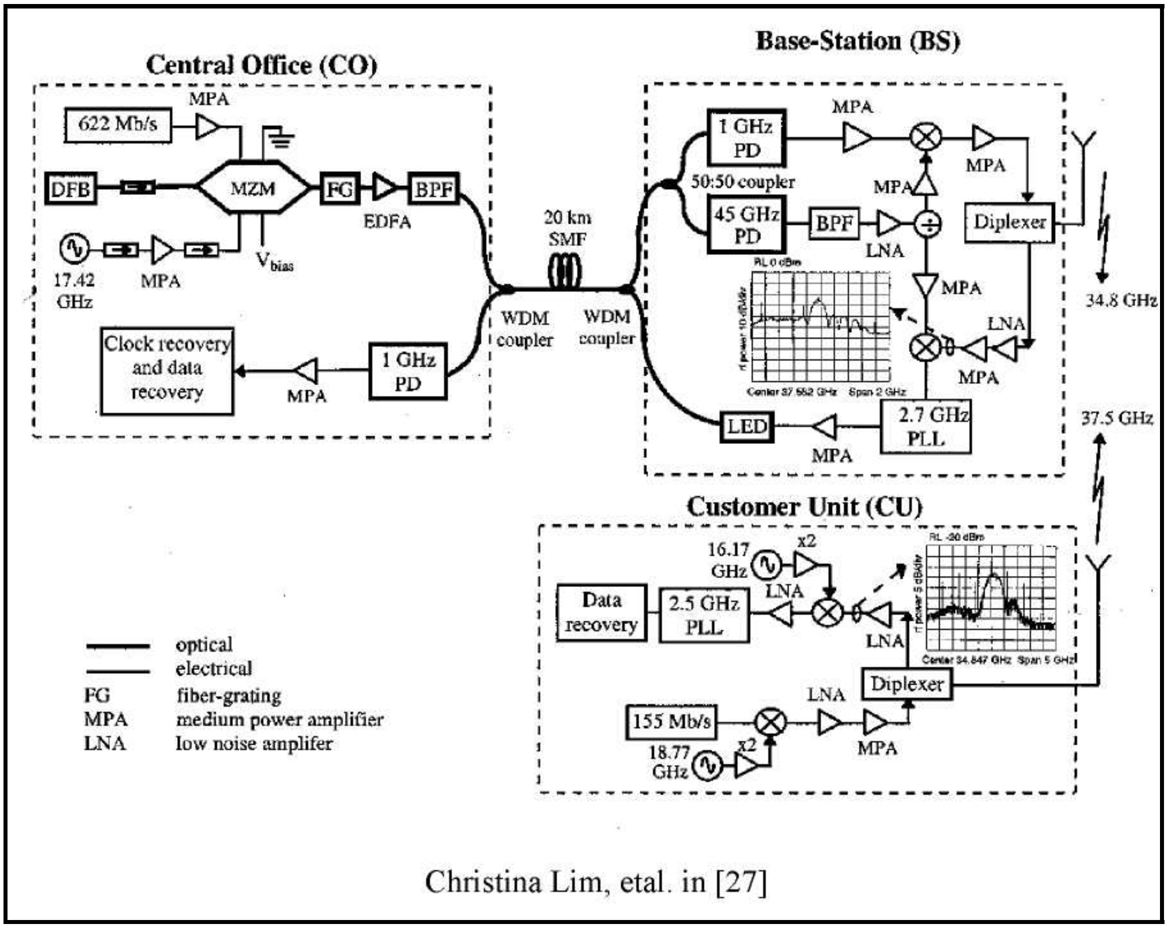

Fig. B.9: Using the 2f Method to Remotely Deliver Baseband Data and LO For Up Conversion at The Base Station [LIM00]

B.8.3 Heterodyning based on Mode-Locked Comb Generation

This approach uses an amplified fiber loop Optical Frequency Comb Generator (OFCG) to generate a wide comb of optical frequencies (about 100). Two frequencies are selected and subsequently heterodyned to generate the desired microwave. The filtering is achieved by using two slave lasers mode locked on two different frequencies separated by the required microwave. This technique is therefore a combination of OFCG and OIL techniques. The selected comb lines are combined to form the two-sideband optical signal as shown in Fig. B.10.

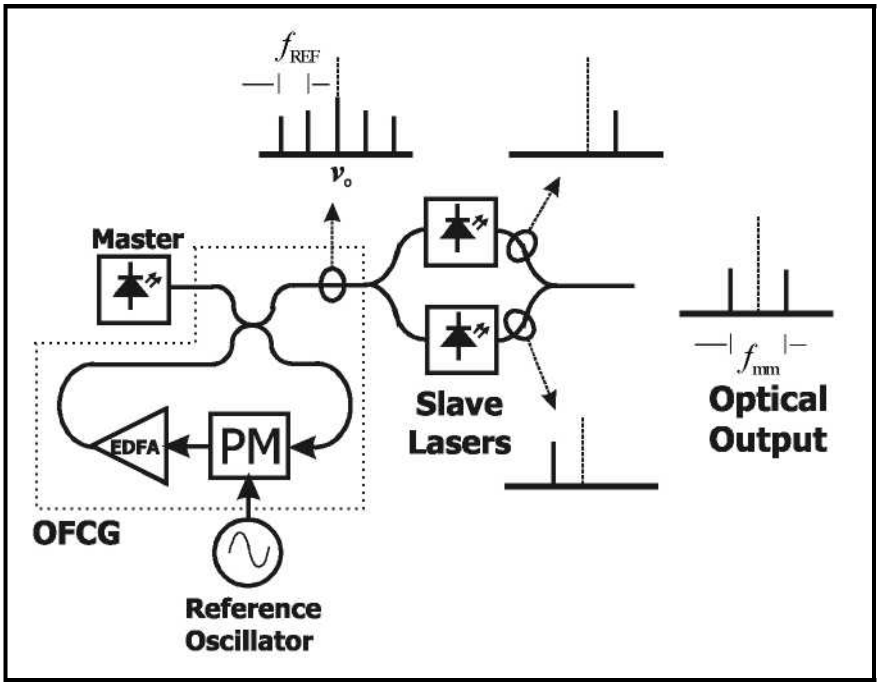

Fig. B.10: Optical Heterodyning Based on Optical Frequency Comb Generator (OFCG) Using Phase Modulation in an Amplified Circulation Loop [FUK01]

The OFCG based technique shows a potential to generate extremely high frequency mm-waves. The technique was used to generate precise signals of high spectral purity from 10 to 110 GHz [FUK01]. A high speed Uni-Travelling-Carrier Photodiode (UTC-PD) was used in the experiments. All the benefits found in OIL systems apply to this technique as well because the selected pair of comb lines is highly correlated. In addition, the mode-locked OFCG technique provides rapid frequency hoping (<1 ns) and an ultra-wide frequency tuning range. These features are very important in DWDM systems [HO93 and BEN99].

B.8.4 Interferometer based Mixing

Another harmonic up-conversion method that uses an interferometer to achieve mixing is illustrated in Fig. B.11 [ORE94, MAU97, and HIL01]. In this method a LO signal and an RF signal are used to modulate a laser diode, and then mixed in a MZI/photodiode configuration. The FSR of the MZI is chosen so as to maximize the mixing product.

The challenge in this approach regards the fact that both the laser wavelength and filter response must be stabilized against environmental disturbances. In addition, the system performance is very sensitive to polarization perturbations.

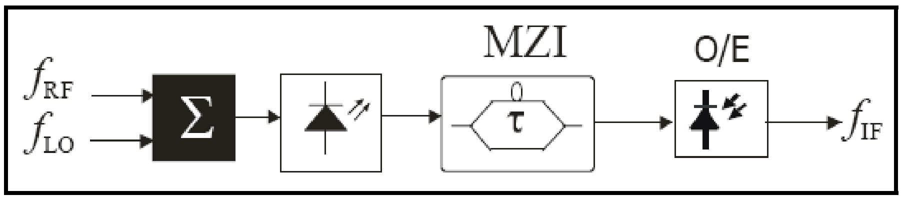

Fig. B.11: Frequency Conversion through Mixing by a Mach Zehnder Interferometer [MAU97]

B.9 Principle of Optical Frequency Multiplication

OFM is a method by which a low-frequency RF signal is up-converted to a much higher microwave frequency through optical signal processing. This is achieved by periodic filtering and photo-detection of an optical signal whose wavelength is continuously swept by the low-frequency RF signal, fsw, as shown in Fig. B.12. The desired microwave signal is selected by the band-pass filter [JOH00, KOO01, and HIL01]. The OFM system is split into two main parts, namely the head-end and the Radio Access Unit (RAU). The RAU may be remoted from the head-end by an optical fiber link. In that case, the radio access unit is also referred to as a Remote Antenna Unit (also RAU).

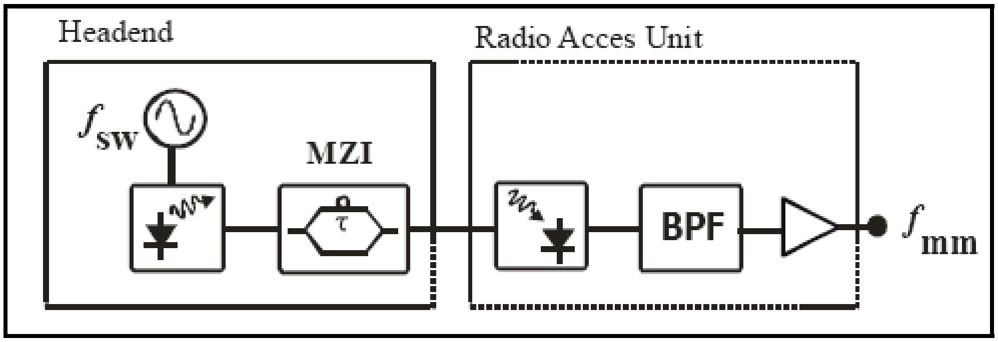

Fig. B.12: Principle of Optical Frequency Multiplication [JOH00]

Periodic filtering is achieved by using an interferometer whose response is characterized by multi-pass-band transmission characteristics. The Mach-Zehnder Interferometer (MZI), and Fabry Perot Interferometer (FPI) are some of the common filters that may be used. A wavelength-swept optical signal may be achieved by driving a tunable laser with the sweep signal [JOH00] or by using the combination of a CW laser diode followed by an Optical Phase Modulator [NGO02].

Tuning of the laser diode wavelength may be achieved through temperature tuning, the use of a movable external cavity diffraction grating, or by changing the carrier density (and so the resonant conditions) inside an active region of the laser diode. Tuning speeds of temperature-tuned lasers and external cavity tunable lasers are limited to a few milliseconds. Three section lasers such as the Distributed Bragg Reflector (DBR) tunable lasers have faster tuning speeds, but they are still limited to just several tens of nanoseconds [WAL92]. This means that in general the tunable laser option is only available for limited sweeping rates of a few hundred MHz at best. For faster tuning speeds of laser wavelength, the use of commercially-available phase modulators is a more practical option.

Fig. B.13 illustrates what happens when a wavelength-swept optical signal passes through an interferometer, followed by detection by a photo-receiver. For simplicity's sake, a linear wavelength sweep is used here. Beginning at time t0, the wavelength is swept to produce the peak-to-peak optical frequency deviation of $\Delta\lambda_{pp}$ in nanometers (equivalent to Δf_{pp}, in Hz) at t_1. The wavelength returns to its initial value at t_2, completing one cycle. The period of this cycle is determined by the low-frequency sweep signal, f_{sw} and equals $T_{sw} = 1/f_{SW} = t_2 - t_0$.

If Δf_{pp} is chosen such that it is N multiple times the Free Spectral Range (FSR) of the periodic filter, then $2N$ transmission peaks of the filter are traversed during a single wavelength swing cycle resulting in the production of 2□N intensity bursts of photocurrent at the output of the photodiode as shown in Fig. B.13. Therefore, the generated electrical signal exhibits a smaller period of $T_{mm} = T_{sw}/2N$. This implies an increased signal frequency of $f_{mm} = 2N \cdot f_{sw}$, signifying a base frequency up-conversion factor of $2N$, where $N = \Delta f_{pp}/FSR$ [NGO02 and KOO02].

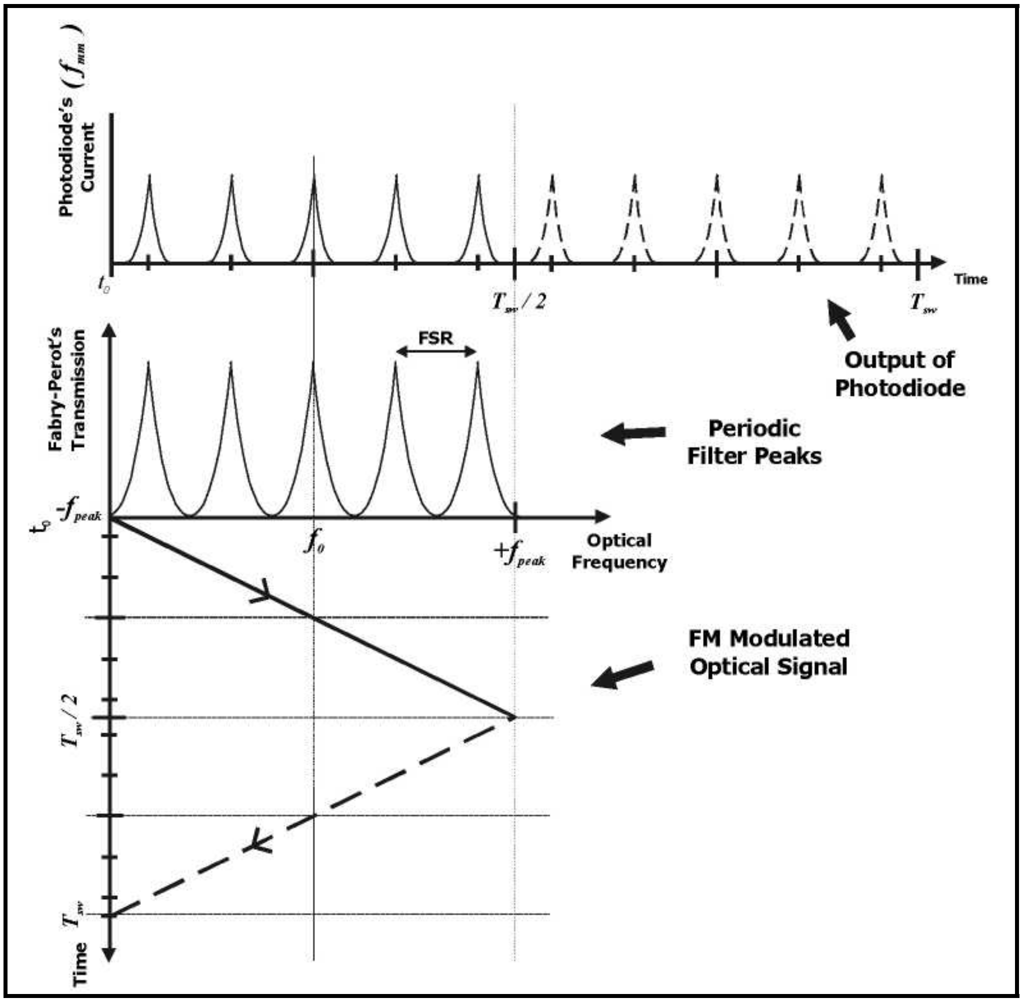

Fig. B.13: Illustration of Optical Frequency Multiplication - Generating the Fundamental Frequency [NGO02]

B.10 Sub-Carrier Multiplexing

The Sub-carrier Multiplexing (SCM) technique is a maturing simple and cost effective approach for exploiting optical fiber bandwidth in analogue optical communication systems in general and in RoF systems in particular. In SCM, an RF or microwave signal (the sub-carrier) is used to modulate an optical carrier at the transmitter's side. This result in an optical spectrum consisting of the original optical carrier f_0, plus two side-tones located at f_o-f_{sc} and f_o+f_{SC} where f_{SC} is the sub-carrier frequency. If the sub-carrier itself is modulated with data (analogue or digital), then sidebands centered on $f_o - f_{sc}$ and $f_o + f_{SC}$ are produced as shown in Fig. B.14.

To multiplex multiple channels on to one optical carrier, multiple sub-carriers are first combined and then used to modulate the optical carrier as shown in Fig.B.14. At the receiver's side the sub-carriers are recovered through direct detection and then radiated. The mobile station is tuned to select and receive the desired sub-carrier(s), which may then undergo down conversion and appropriate demodulation. Different modulation schemes may be used on the different sub-carriers. In addition, the data used to modulate the sub-carriers need not be of the same kind. One sub-carrier may carry digital data, while another may be modulated with an analogue signal such as video or telephone traffic. In this way, SCM supports the multiplexing of various kinds of mixed mode broadband data. Modulation of the optical carrier may be achieved by either directly modulating the laser (as shown in the figure), or by using external modulators such as the MZM discussed above

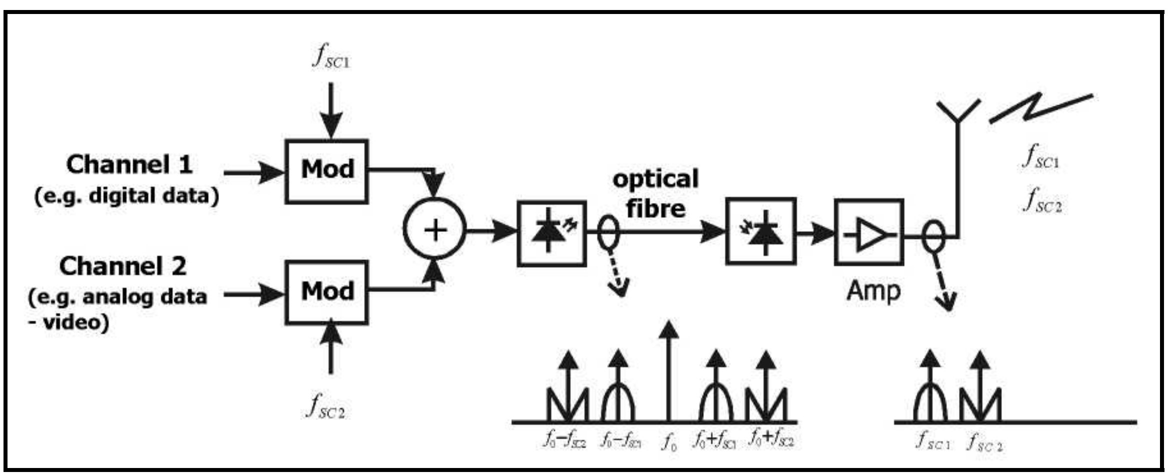

Fig. B.14: Sub-Carrier Multiplexing of Broadband Mixed Mode Data in RoF Systems [BRA01]

A practical application of SCM in a 60 GHz RHD-based RoF communication system is reported in [BRA01]. Two sub-carriers were used to multiplex two data streams. Since the setup was based on OIL, each of the sub-carriers (1.27 GHz and 1.79 GHz) was first OQPSK modulated with 155 Mbps data and then used to modulate one of the two slave lasers. The two resulting phase modulated optical carriers were transmitted through the fiber together with a third reference optical carrier. After heterodyning at the photodiode, the two sub-carriers are up-converted to 62.07 GHz and 62.21 GHz respectively, and radiated. BER measurements on the data recovered at the mobile station confirmed the cost effectiveness of the SCM based RoF system.

B.10.1 Advantages and Disadvantages of Sub-Carrier Multiplexing

One of the main advantages of SCM is that it supports mixed mode data traffic. Therefore, it can be used for a wide range of applications such as CATV, wireless LANs and mm-wave applications to name but a few. This is a consequence of the fact that the modulation technique used and data carried on each sub-carrier are independent of what happens on other sub-carriers. Furthermore, because the sub-carriers are of low frequencies, components required for SCM-based systems are readily available. Modulators, mixers and amplifiers employed in cable (or community) TV (CATV) and other satellite systems can still be used in SCM systems leading to low system costs.

The disadvantage of SCM is that being an analogue communication technique, it is more sensitive to noise effects and distortions. This places stringent linearity requirements on the performance of components especially for applications such video, were a Carrier-to-Noise-Ratio (CNR) > 55 dB may be required. The light source's

Relative Intensity Noise (RIN) is the major source of noise and should be kept as low as possible [SHE03].

B.11 Wavelength Division Multiplexing in RoF Systems

Wavelength Division Multiplexing (WDM) is also used to exploit fiber bandwidth in RoF systems. A practical demonstration of WDM in an mm-wave RoF system is reported in [LAN99]. Carriers modulated with mm-waves are dropped from and added to a fiber ring using Optical Add-Drop Multiplexers (OADM). The OADM are placed at base stations and tuned to select the desired optical carriers to drop.

Appendix C: Confidence Interval Estimation

Let X be an unknown parameter to be estimated based on a random sample $X_1, X_2, \cdots, X_n$, from a distribution with that parameter X. We want an interval [L, U], where L and U are two statistics calculated from $X_1, X_2, \cdots, X_n$, such that the interval includes X with a pre-assigned probability, 1 - α. Specifically, we want to have $P\{L \le X \le U\} \ge 1 - \alpha$ regardless of the true value of X. Note that L and U are random variables, being functions of $X_1, X_2, \cdots, X_n$, so [L, U] is a random interval. It is called a 100(1 - α) % Confidence Interval (CI), 1 - α is called confidence level, and L and U are confidence limits.

Consider a random sample $X_1, X_2, \cdots, X_n$ with $N(\mu, \delta^2)$ distribution, where the variance δ^2 is assumed to be known and μ is the sample mean $\overline{X}$.

$$\overline{X} = \frac{1}{n}\sum_{i=1}^{n} X_i \quad \text{(C.1)}$$

$$\delta^2 = \frac{1}{n-1}\sum_{i=1}^{n} X_i - \overline{X} \quad \text{(C.2)}$$

From the properties of the normal distribution, it follows that there is 95% probability that X falls within a distance of $1.96\, \delta/\sqrt{N}$ from

$$\mu : p\left[\mu - 1.96\, \delta/\sqrt{N} \le \overline{X} \le \mu + 1.96\, \delta/\sqrt{N}\right]$$

$\overline{X}$ is within a distance of $1.96\,\delta/\sqrt{N}$ from μ if and only if μ is within a distance of $1.96\,\delta/\sqrt{N}$ from $\overline{X}$.

Therefore, we have, $p\left[L=\overline{X}-1.96\,\delta/\sqrt{N} \le \mu \le \overline{X}+1.96\,\delta/\sqrt{N}=U\right]=0.95$.

For 90% and 99% confidence interval, $\overline{X}$ is within a distance of $1.65\,\delta/\sqrt{N}$ and $2.58\,\delta/\sqrt{N}$ respectively.

For example if we consider a group of data for 10 independent runs per simulation experiment: $X_1, X_2, \bullet\bullet\bullet, X_n$ = 85, 89, 98, 83, 88, 77, 94, 92, 80, and 89; then, we can calculate our parameters including $\overline{X}$ = 87.5, δ = 6.4261, and $1.96\,\delta/\sqrt{N}$ = 3.9768. As a result, confidence limits would be [L=83.5232, U=91.4768].